research report

Effect of Anchorage and Sheathing Configuration on the Cyclic Response of Long Steel-Frame Shear Walls

RESEARCH REPORT RP00-6

2000
REVISION 2007

American Iron and Steel Institute

Steel Framing Alliance™
Steel. The Better Builder.

DISCLAIMER

The material contained herein has been developed by researchers based on their research findings and is for general information only. The information in it should not be used without first securing competent advice with respect to its suitability for any given application. The publication of the information is not intended as a representation or warranty on the part of the American Iron and Steel Institute, Steel Framing Alliance, or of any other person named herein, that the information is suitable for any general or particular use or of freedom from infringement of any patent or patents. Anyone making use of the information assumes all liability arising from such use.

PREFACE

This report presents the results of cyclic tests of seventeen full-size, cold-formed steel-framed shear walls sheathed with oriented strand board, with and without openings.

The findings provided a basis for continued research and development efforts, leading to the establishment of provisions for cold-formed steel-framed Type II shear walls.

Research Team
Steel Framing Alliance

Effect of Anchorage and Sheathing configuration on the Cyclic Response of Long Steel-Frame Shear Walls

Virginia Polytechnic Institute and State University
Department of Wood Science and Forests Products
Brooks Forest Products Research Center
Timber Engineering Center
1650 Ramble Road
Blacksburg, Virginia 24061-0503

Report No. TE-2000-002

by:

Shabbir Vagh
Research Assistant

J.D. Dolan
Associate Professor of Wood Engineering

And

W. S. Easterling
Associate Professor of Civil Engineering

Submitted to:
The American Iron & Steel Institute
Washington, DC

October, 2000

Abstract

Presented are results of cyclic tests of seventeen full-size, cold-formed steel-frame shear walls sheathed with oriented strandboard, with and without openings. Walls of four configurations with sheathing area ratio ranging from 0.48 to 1.0 were tested. The specimens were 12-m (40-ft.) long and 2.4-m (8-ft.) high with 11-mm (7/16-in.) OSB sheathing. One wall had additional 13-mm (0.5-in.) gypsum wallboard sheathing. All specimens were tested in horizontal position with no dead load applied in the plane of the wall. Resistance of walls was compared with predictions of the perforated shear wall design method (already developed for wood-framed walls and validated for cold-framed steel walls by Salenikovich, et al., 1999) in order to validate that the perforated shear wall method is valid for cold-formed steel walls with various anchorage arrangements. Also, comparisons were made to the tests performed by Salenikovich, et al. (1999) to determine whether sheathing orientation, sheathing end wall size, gusseting of sheathing around openings, presence of a Tie-down anchors, and using either bolts or screws to attach the top and bottom tracks to the test frame effected the load capacity of the walls.

Results of the study revealed that these steel-framed walls had a similar performance to the walls tested by Salenikovich, et al. [1999]. In steel framing, bending of framing elements and head pull-through of sheathing screws was the predominant failure mode. Gypsum sheathing added 30% to stiffness and strength of fully-sheathed walls in monotonic tests, however contribution of gypsum wallboard in cyclic loading circumstances remains questionable. Predictions of the perforated shear wall method were conservative for configurations using mechanical tie-down anchors at the end of the wall specimens.

AKNOWLEDGEMENTS

The Authors would like to acknowledge the financial and technical support provided for this project by the American Iron and Steel Institute through Research Contract CC-8184.

TABLE OF CONTENTS

LIST OF TABLES

LIST OF FIGURES

Introduction

Light-frame shear walls are a primary element in the lateral force-resisting system in residential construction. Both prescriptive and engineering methods have been developed for cold-formed steel construction. Shear wall design values for segmented walls of cold-formed steel construction have been included in the three model building codes for the United States as well as the *2000 International Building Code* and *2000 International Residential Code*. If similar sheathing materials and connections are used for wood- and steel- frame shear walls, it is reasonable to assume similar performance for both types of framing. This study validates that the perforated shear wall method for design of shear walls is also valid for cold-formed steel shear walls when mechanical tie-down anchors are used at the end of the walls and when tie-down anchors are not used if the capacity of the fully-sheathed equivalent anchored configuration is known.

Traditional segmented shear wall design for steel framing requires fully sheathed wall sections to be restrained against overturning. Their behavior is often considered analogous to a deep cantilever beam with the end framing members acting as "flanges" or "chords" to resist overturning moment forces and the panels acting as a "web" to resist shear. This analogy is generally considered appropriate for wind and seismic design. Overturning, shear restraint, and chord forces are calculated using principles of engineering mechanics. While shear resistance can be calculated using engineering mechanics as well, tabulated shear resistance values for varying fastener schedules have been introduced in the codes and are typically used.

Traditional segmented design of shear walls containing openings, for windows and doors, involves the use of multiple shear wall segments. Each full-height shear wall segment is required to have overturning restraint supplied by structure weight and/or mechanical tie-down anchors. The shear capacity of a wall is equal to the sum of the individual full-height segment shear

capacities. Sheathing above and below openings is not considered to contribute to the overall performance of the wall.

An alternate empirical-based approach to the design of wood-framed shear walls with openings is the perforated shear wall method which appears in Chapter 23 of the *Standard Building Code 1996 Revised Edition* (SBC) (1996), the *International Building Code* (2000), and the *Wood Frame Construction Manual for One- and Two- Family Dwellings - 1995 High Wind Edition* (WFCM) (1995). The perforated shear wall method consists of a combination of prescriptive provisions and empirical adjustments to design values in shear wall selection tables for the design of shear wall segments containing openings. Shear walls designed using this method, must be anchored to resist overturning forces only at the wall ends, not each wall segment.

Japanese researchers performed a number of monotonic tests on one-third scale models of wood-frame shear walls and proposed a basis for the perforated shear wall method (Yasumura and Sugiyama 1984, and Sugiyama and Matsumoto 1994). A number of monotonic and reverse-cyclic tests on 12.2-m (40-ft.) long wood-frame walls performed by Johnson (1997) and Heine (1997) demonstrated conservative nature of the proposed method. A recent study by Salenikovich, et al. (1999) on long steel-frame shear walls with openings also predicted the conservative nature of the proposed method. This study provides information about the performance of long, full-sized, perforated shear walls with cold-formed steel framing tested under monotonic and reverse-cyclic loads with various tie-down anchorage and sheathing configurations. Monotonic tests serve as a basis for establishing design values in wind design. Cyclic tests are performed to establish conservative estimates of performance during a seismic event.

Objectives

Results of cyclic tests of full-size cold-formed steel-frame shear walls are reported. The objectives of this study were to determine the effects of anchorage, cyclic loading, sheathing corners gusseted at openings, orientation of the sheathing, and reduced size of end wall segments, on the shear wall performance. Results were also used to compare the strength of walls with predictions of the perforated shear wall method.

Background

Design values for cold-formed steel-framed shear walls are based on monotonic and cyclic tests of shear walls. The tests were traditionally conducted on 2.4 x 2.4 m (8 x 8 ft.) and 1.2 x 2.4 m (4 x 8 ft.) wall specimens, similar to those used for wood-framed shear walls. Seismic and wind design values are based on testing conducted by Serrette, et al. (1996) and Serrette (1997), which included monotonic and cyclic tests of walls sheathed with plywood, oriented strandboard, and gypsum wallboard on both 1.2 × 2.4 m (4 × 8 ft.) and 2.4 × 2.4 m (8 × 8 ft.) wall specimens.

The perforated shear wall design method for wood-frame shear walls appearing in the SBC, IBC, and WFCM is based on an empirical equation, which relates the strength of a shear wall segment with openings to one without openings. Adjustment factors in Table 2313.2.2 in the SBC and Supplement Table 3B in the WFCM are used to reduce the strength or increase the required length of a fully sheathed shear wall segments to account for the presence of openings.

In accordance with SBC and WFCM, and for the purposes of this study, a perforated shear wall must include the following components:

1) Structural sheathing, including areas above and below window and door openings;
2) Mechanical shear restraint capable of resisting the shear capacity of each segment;
3) Tie-down anchors at the ends of the wall to provide overturning restraint and maintain a continuous load path to the foundation where any plan discontinuities occur in the wall line;

4) Minimum length of full-height sheathing at each end of the wall (based on height-to-length ratios for blocked shear wall segments as prescribed by the applicable building code).

Prescriptive provisions and empirical adjustments are based on results of various studies conducted on shear walls with openings. Many of the prescriptive provisions are necessary to meet conditions for which walls in previous studies were tested. Empirically derived adjustment factors, or shear capacity ratios, for the perforated shear wall method take roots in works of Sugiyama and Matsumoto (1993,1994). To determine the shear capacity ratio, Sugiyama and Matsumoto (1993) defined the sheathing area ratio:

$$r = \frac{1}{1 + \frac{A_0}{H \sum L_i}} \tag{1}$$

where: $A_0 = \sum A_i$, total area of openings, H = height of wall, and $\sum L_i$ = sum of the lengths of full-height sheathing as shown in Figure 1.

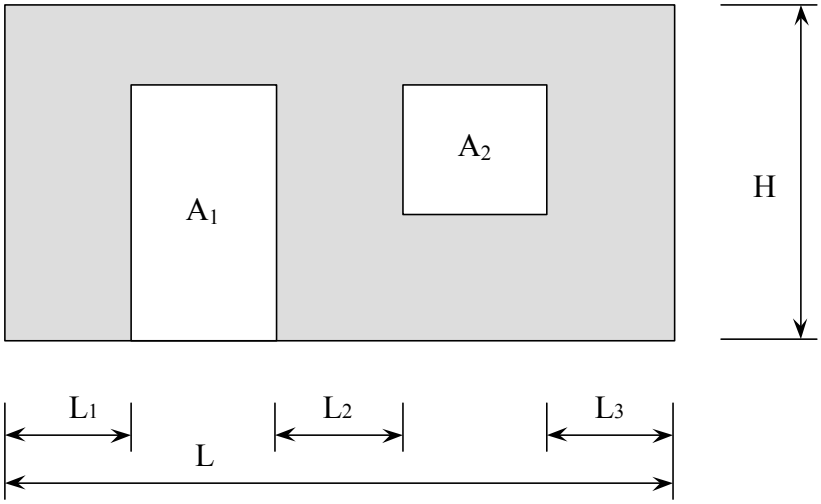

Figure 1 - Sheathing area ratio.

Initially, Yasumura and Sugiyama (1984) proposed the following equation for the shear capacity ratio, or the ratio of the strength of a shear wall segment with openings to the strength of a fully sheathed shear wall segment without openings:

$$F = \frac{r}{3 - 2r} \tag{2}$$

The relationship was derived based on results of monotonic racking tests on 1/3-scale walls and was considered applicable for the apparent shear deformation angle of 1/100 radian and for ultimate load. Later, Sugiyama and Matsumoto (1994) published two more equations based on tests of longer wall models and suggested for use in North-American light-frame construction:

$$F = \frac{3r}{8 - 5r} \tag{3}$$

for the shear deformation angle γ = 1/300 radian, and

$$F = \frac{r}{2 - r} \tag{4}$$

for γ = 1/100 and 1/60 radian.

Sugiyaiama and Matsumoto (1994) suggest two limitations on the use of Equations (3) and (4):

1) The depth-to-width ratio in the wall space above and/or below an opening is not less than 1/8;
2) The sheathing area ratio is not less than 30%.

Studies have proven Equation (2) to be conservative in predicting both monotonic and cyclic capacities of long shear walls. Resent tests conducted by Salenikovich, et al. (1999) on long steel-frame shear walls with the same wall configurations as Johnson (1997) also suggested Equations (2) and (3) to be conservative at all levels of deflection under monotonic and cyclic loading for steel-framed shear walls.

Test Program

The wall configurations tested by Salenikovich, et al. (1999) were used as appropriate configurations in the construction of wall specimens for this study. Also, results of Salenikovich, et al. (1999) tests were used for comparison of results generated from these tests. The test

involved different variations of the five configurations originally tested by Johnson (1997) (summarized by Dolan and Johnson 1996a and b) and Heine (1997) for wood-framed walls. The variations are as explained below along with the other wall constructional and testing protocols applied.

1) The sheathing was connected to the wall framing in three configurations: a) sheathing joints at the edge of each opening, b) sheathing joints arranged so that the opening corners were gussetted (and potentially strengthened) by the sheathing, and c) the sheathing attached with the long dimension oriented horizontally.
2) 11-mm (7/16-in.) OSB sheathing instead of 12-mm (15/32-in.) plywood was used for exterior sheathing, similar to the wood-frame configurations tested by Heine (1997) and Salenikovich, et al. (1999).
3) 13-mm (1/2-in.) gypsum drywall interior sheathing was omitted except for one cyclic test of a fully sheathed wall (Configuration **A** in Table 1).
4) Instrumented bolts were used to measure uplift forces transferred through tie-down anchors at the ends of walls.
5) Specimens were a mirror image of walls tested by Salenikovich, et al. (1999) (i.e., load was applied to the upper left-hand end of the specimens, where Salenikovich, et al. applied to load to the upper right-hand end of the walls).
6) Maintaining the same sheathing area ratios as the walls tested by Salenikovich, et al. (1999) comparisons were made to the performance of the walls under cyclic loading for the following wall configurations:
    a) Gussetted sheathing around the openings.
    b) Reducing the width of the sheathing of the end wall segments from 4 feet to 2 feet.
    c) Replacing the shear transfer bolts with screws.
    d) Removing the mechanical tie-down anchors from the wall ends.
    e) Changing the orientation of the sheathing from vertical to horizontal.

A combination of one or more of the above variations was incorporated into each wall specimen for the purpose of comparison. Also, direct comparisons were made with the results obtained from the tests carried out by Salenikovich, et al. (1999).

Cyclic tests were conducted on walls of each configuration shown in Table 1 size and placement of openings were selected to cover the range of sheathing area ratios encountered in light-frame construction. With the exception of one test (Configuration **A**), gypsum sheathing was omitted to provide correlation with design code values (UBC, SBCCI, BOCA, and IBC), test the weakest conditions, and minimize variables in the tests. All specimens were built in accordance with the *Builder's Steel-Stud Guide* (AISI, 1996) and framed to provide the weakest framing condition that still conformed to the design and construction requirements. For instance, headers over openings were framed as shown in Figure 2 rather than using methods to increase fixity such as extended strapping or blocking.

Specimen Configuration

All specimens were 12.2-m (40-ft.) long and 2.4-m (8-ft.) tall with the same type of framing, sheathing, fasteners, and fastener schedules. For reference, the opening dimensions and opening locations for each wall configuration tested by Salenikovich, et al. (1999) are given in Table 1. Wall Configuration **A** ($r = 1.0$) had no openings and was included in the investigation for determining the capacity of the fully-sheathed wall. The strength ratios of Walls **B** through **E** to Wall **A** were compared directly to the shear capacity ratio, F, calculated using Equations (2), (3), and (4) to investigate the conservative nature of the perforated shear wall method.

a) b)

Figure 2 - Typical Header Details.a) door opening, b) window opening

Table 1 - Wall configurations and opening sizes of tests carried out by Salenikovich, et al.(1999).

Wall configuration [1, 4, 5]	Wall type	Sheathing area ratio, (r)	Opening size	
			Door	Window [2]
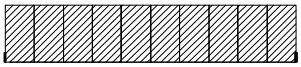	**A**	1.0	-	-
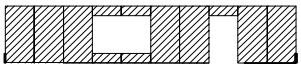	**B**	0.76	6'-8" × 4'-0"	5'-8" × 7'-10½"
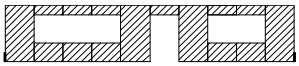	**C**	0.56	6'-8" × 4'-0"	4'-0" × 11'-10½" 4'-0" × 7'-10½"
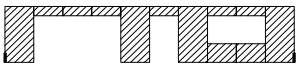	**D**	0.48	6'-8" × 4'-0" 6'-8" × 12'-0"	4'-0" × 7'-10½"
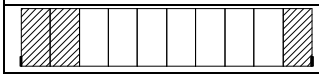	**E**	0.30	(Sheathed at ends) [3] 8'-0" × 28'-0"	-

1: All walls are framed with studs spaced at 24 inches on center. Shaded areas represent sheathing.
2: The top of each window is located 16 inches from the top of the wall.
3: Wall E has studs along the full length of wall but is sheathed only at the ends of the wall.
4: Load was applied to the top left-hand corner of the specimens in either monotonic racking (compression) or reversed cyclic racking.
5: 5/8 inch anchor bolts with 1-1/2 inch round washers were located at 24 inches o.c. along the top and bottom of the specimen except for pedestrian and garage door openings.
Note: 1ft. = 304.8 mm, 1in. = 25.4 mm

The wall configurations tested in this study, with all the variations are shown in Table 2. Opening sizes for doors and windows, and sheathing ratios for various configurations were maintained as described in Table 1, to comply with the tests carried out by Salenikovich, et al. (1999). A nomenclature method was developed as described in Table 2 for easy identification of the different variations incorporated in the wall specimen.

Materials and Fabrication Details

Material and construction details used for the wall specimens are summarized in Table 3. Included are the sizes of headers and jack studs used around openings. Wall framing consisted of single top and bottom tracks, single intermediate and double end-studs, and double studs around doors and windows. All frame members consisted of cold-formed steel profile. 'C'--shaped members were used for studs and headers, whereas track was used for top and bottom plates. Tracks had 89-mm (3.5-in.) width (web) and intermediate studs were spaced 610 mm (24 in.) on center.

Exterior sheathing was 11-mm (7/16-in.) OSB. All full-height panels were 1.2×2.4-m (4×8 ft.) and oriented vertically except for one wall (Configuration A) where in the orientation was horizontal with staggered joints. To accommodate openings, the panels were cut to fit above and below the doors and windows, and in the gusseted walls the panels were cut such that they wrapped around the opening corners in an attempt to stiffen and strengthen the walls. OSB sheathing was applied with joints located at the ends of headers to simulate the weakest condition possible except when the sheathing gusseted the opening.

Interior sheathing of 13-mm (1/2-in.) gypsum wallboard was applied to wall Configuration A in a staggered horizontal pattern. All joints in the interior sheathing were taped and covered with drywall compound. Compound drying time complied with the manufacturer’s recommendation and was adjusted to ambient temperature and humidity.

Table 2- various wall configurations tested for the study

CONFIGURATIONS			
A	**B**	**C**	**D**
A2hb		**C2ab**	**D2ab**
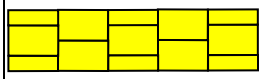			
Horizontal staggered-sheathing with dry wall, Shear bolts at 2 feet, **No Tie-down anchor**		**2** foot end wall , Shear bolts at 2 feet, With tie-down anchor	**2** foot end wall , Shear bolts at 2 feet, With tie-down anchor
	B2gab	**C2gab**	**D2gab**
	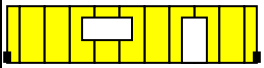	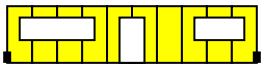	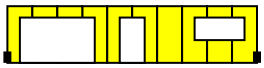
	2 foot end wall , Gusseted sheathing Shear bolts at 2 feet, With tie-down anchor	**2** foot end wall , Gusseted sheathing Shear bolts at 2 feet, With tie-down anchor	2 foot end wall , Gusseted sheathing Shear bolts at 2 feet, With tie-down anchor
SPECIMEN NOMENCLATURE 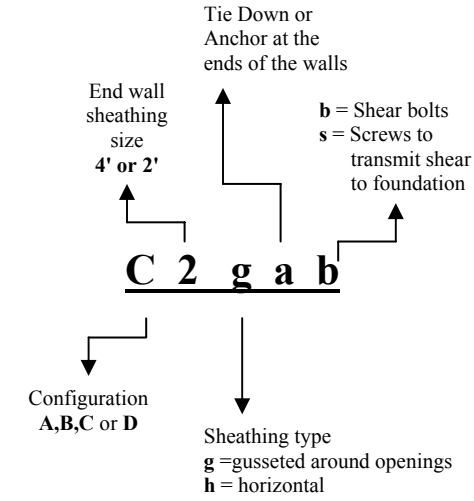 Tie Down or Anchor at the ends of the walls End wall sheathing size **4' or 2'** **b** = Shear bolts **s** = Screws to transmit shear to foundation **C 2 g a b** Configuration **A,B,C** or **D** Sheathing type **g** =gusseted around openings **h** = horizontal		**C2gb**	
		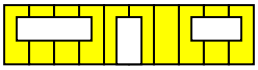	
		2 foot end wall , Gusseted sheathing Shear bolts at 2 feet, **No Tie-down anchor**	
		C4b	**D4b**
			
		4 foot end wall , 2 Shear bolts at 2 feet, **No Tie-down anchor**	**4** foot end wall , 2 Shear bolts at 2 feet, **No Tie-down anchor**
		C4s	**D4s**
			
		4 foot end wall , 2 Screws to transmit shear at every 1 foot **No Tie-down anchor**	**4** foot end wall , 2 Screws to transmit shear at every 1 foot **No Tie-down anchor**

Note: Load was applied to the upper right hand corner of the wall specimen

Table 3 - Wall materials and construction data

Component	Fabrication and Materials
Studs Top and bottom tracks	350S150-33 (2×4 'C'-section cold-formed steel stud, 33 mil) 350T125-33(2×4 cold-formed steel track, 33 mil)
Sheathing: Exterior Interior [1]	 OSB, 7/16 in., 4×8 ft. sheets installed vertically. Gypsum wallboard, ½ in., installed vertically, joints taped
Headers: 4'-0" opening 7'-10½" opening 11' - 10½" opening	 (2) 600S163-43 (2 × 6 steel headers, 43 mil. One jack stud at each end.) (2) 1000S163-54 (2 × 10 steel headers, 54 mil. Two jack studs at each end.) (2) 1000S163-54 (2 × 10 steel headers, 54 mil. Two jack studs at each end.)
Tie-down	Simpson HTT 22, fastened to end studs with 32 #8, self-drilling screws; 5/8-in. diameter A307 bolt to connect to foundation.
Shear Bolts	5/8-in. diameter A307 bolts with 1½-in.round washers; 24 in. on center
Screws to transmit shear to foundation	Grabber #12 x 3/4.hex head self-drilling screws - V12075H *(Note: pilot holes had to be drilled in foundation before using the screws)*

1: If applied. Note: 1ft. = 304.8 mm, 1in. = 25.4 mm

Specimens were attached to 76×127-mm (3×5-in.) steel tubes at the top and the bottom. Shear Bolts (A307 bolts 16 mm (5/8-in.) diameter with 38 mm (1½-in.) round washers; 610 mm (24 in.) on center) for the purpose of anchoring the walls were used in all except 4 walls. The four walls, 2 of each configuration **C** and **D,** were anchored to the foundation at the bottom of the wall with self drilling #12 x 19 mm (3/4 in.) (Grabber V12075H) screws 305 mm (12 in.) on center. A307 bolts were used at the top of the wall placed at 610 mm (24 in.) on center. This test was carried out to study the effect of wall anchoring on performance. The test fixture was narrower than the framing, therefore, both exterior and interior sheathing were able to rotate past the test fixture at the top and bottom **(**Figure 3).

Two tie-down anchors were used to resist overturning force, one at each double stud at the wall ends for the wall configurations specified with tie-down anchors (Table 2). For this purpose, a Simpson Strongtie model HTT22 tie-down anchor was attached to the bottom of the end studs by thirty-two #8 self-drilling framing screws with hex heads. A 16-mm (5/8-in.) diameter instrumented bolt connected the tie-down, through the bottom track, to the structural steel tube test fixture.

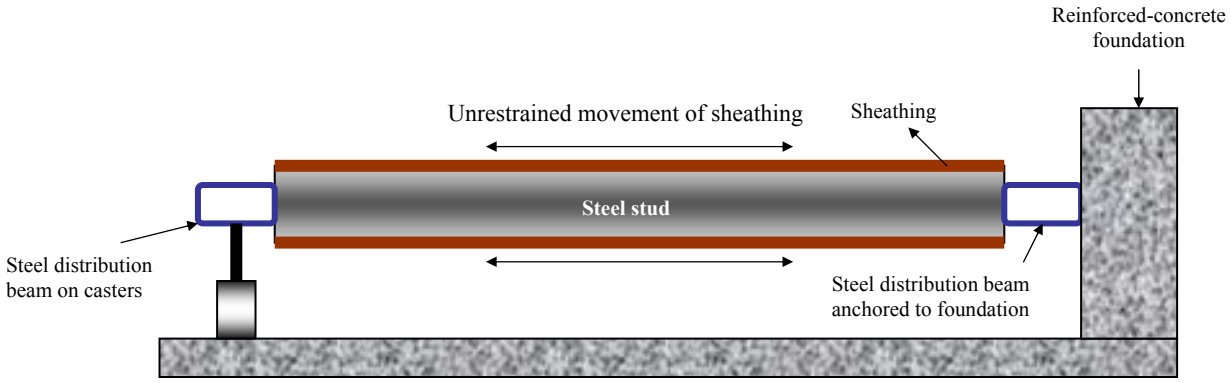

Figure3 - Fixture used for testing

The fastener schedule used in constructing the wall specimens is presented in Table 4. Four types of screws were used: 1) #8 self-drilling screws with low-profile head connected the framing where sheathing was to be installed, 2) #8 self-drilling screws with hex heads were used to connect the framing otherwise, 3) #8 self-drilling screws with bugle-heads attached sheathing to the framing and 4) #12 self-drilling screws with hex heads were used to attach the wall channel to test fixture in some cases. Sheathing screws were spaced 152 mm (6 in.) on the perimeter and 305 mm (12 in.) in the field to attach OSB sheathing and 178 mm (7 in.) on the perimeter and 254 mm (10 in.) in the field - for gypsum wallboard. A minimum edge distance of 10 mm (3/8 in.) was maintained in all tests. Tie-down anchors were attached to the double end-studs using #8 self-drilling screws with hex heads, one located in each of the 32 pre-punched holes in the metal anchor.

Test Setup

Tests were performed with the shear walls in a horizontal position as shown in Figure 4. with OSB sheathing on top (except for the wall with the dry wall - Configuration **A,** where in the dry wall was on the top). The wall was raised 410 mm (16 in.) above the ground to allow sufficient clearance for instruments and the load cell to be attached to the wall.

Table 4 - Fastener schedule

Connection Description	No. and Type of Connector	Connector Spacing
Framing	Screws:	
Top / Bottom Plate to Stud	2 - #8, self-drilling, low-profile head[1]	per stud at each end
Stud to Stud	#8, self-drilling, hex head[2]	24 in. o.c.
Stud to Header	2 - #8, self-drilling, low-profile head[1]	per stud at each end
Header to Header	#8, self-drilling, hex head[2]	16 in. o.c.
Tie-down Anchor/ Shear Bolts		
Tie-down Anchor to Stud	32 - #8, self-drilling, hex head screws[2]	per tie-down
Tie-down to Foundation	1 - A307 ∅5/8-in. bolt	per tie-down
Shear bolts	1 - A307 ∅5/8-in. bolt with 1½-in. steel washers	24 in. o.c.
Screws to transmit shear to foundation	2-#12*, self-drilling, hex head screws[3]	12in. o.c
Sheathing:		
OSB	#8, self-drilling, bugle-head screws[4]	6 in. edge / 12 in. field (2 rows for end stud)
Gypsum wallboard	#8, self-drilling, bugle-head screws[4]	7 in. edge / 10 in. field

Note: 1ft. = 304.8 mm, 1in. = 25.4 mm

1. Grabber item # 2347, 8 x 1/2 Pan head
2. Grabber item # 10075H3, 10 x 3/4 Hex head
3. Grabber item # V12075H, 12x 3/4 Hex hed
4. Grabber item # P81516F3, 8 x 1 15/16 Bugle head

In this setup, no dead load was applied in the plane of the wall, which conservatively represented walls parallel to floor joists. Racking load was applied to the top right corner of the wall (for the configurations shown in Table 2) by a programmable servo-hydraulic actuator with the range of displacement of ±152 mm (6 in.) and capacity of 245 kN (55 Kips). Load was distributed along the length of the wall by means of a 76×127-mm (3×5-in.) steel tube attached to the top track of the wall with 16-mm (5/8-in.) diameter bolts at 610 mm (24 in.) on center. Oversize of boltholes was limited to 0.8 mm (1/32 in.) to minimize slip. Bolts attaching the bottom plate were located a minimum of 305 mm (12 in.) away from the studs adjacent to openings or end of wall. Although, the *Builder's Steel-Stud Guide* (AISI 1996) requires a piece of steel stud underlying the nut to serve as a washer, 38-mm (1.5-in.) round washers were used

instead to ensure the test results were conservative. Eight casters were attached to the distribution beam parallel to loading to allow free horizontal motion.

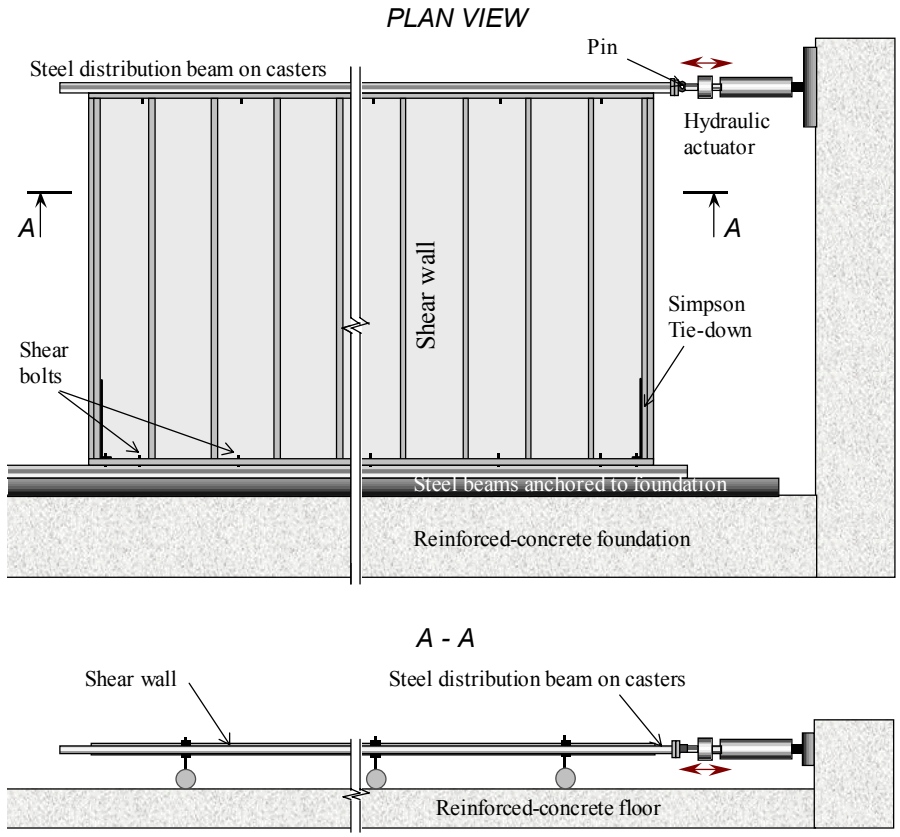

Figure 4 - Test Setup.

Instrumentation and Measurements

The instrumentation locations used in the tests is illustrated in Figure 5. The hydraulic actuator contained the load cell and internal LVDT that supplied information on applied force and displacement. In addition, each specimen accommodated two resistance potentiometers (pots), two instrumented bolts, and two linear variable differential transformers (LVDT's).

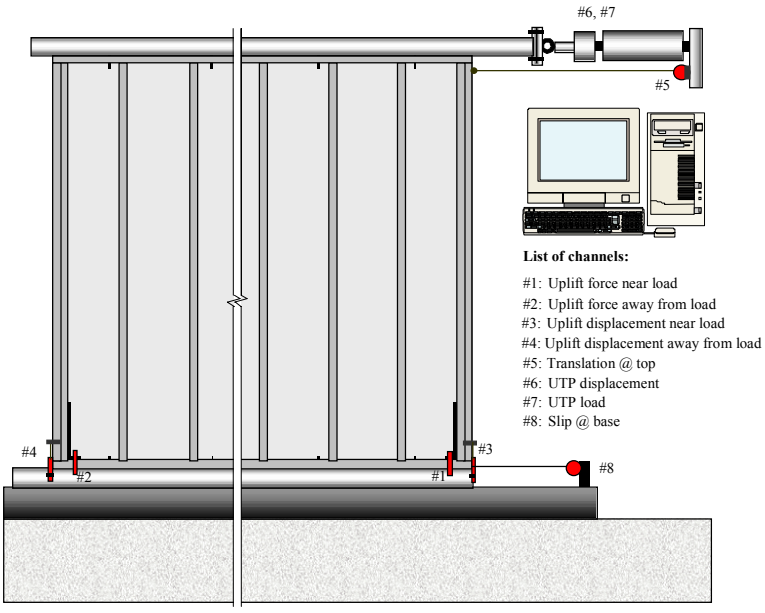

Figure 5 - Data acquisition system

Bolts were instrumented with strain gages and calibrated, thus allowed direct measurment of tension forces resisted in the overturning anchors during loading. LVDT's were mounted on the foundation to measure uplift displacement of the frame. Pots attached to the foundation measured lateral translation of the top and bottom plates, respectively. The difference between the readings of these two instruments produced story drift. Pot readings and the difference between readings of LVDT and pot showed the amount of the bottom and top plate slippage along the foundation and the distribution beam, respectively. Data was recorded at a frequency 10 Hz in monotonic tests and 20 Hz in cyclic tests.

Load Regime

A cyclic load regime was used to test the walls. A sequential phased displacement (SPD) procedure, adopted by Structural Engineers Association of Southern California (SEAOSC) (1997) and described by Porter (1987) was used in this study in order to be consistent with previous tests

conducted by Salenikovich, et al. (1999). The SPD loading consisted of two displacement patterns and is illustrated in Figures 6 and 7

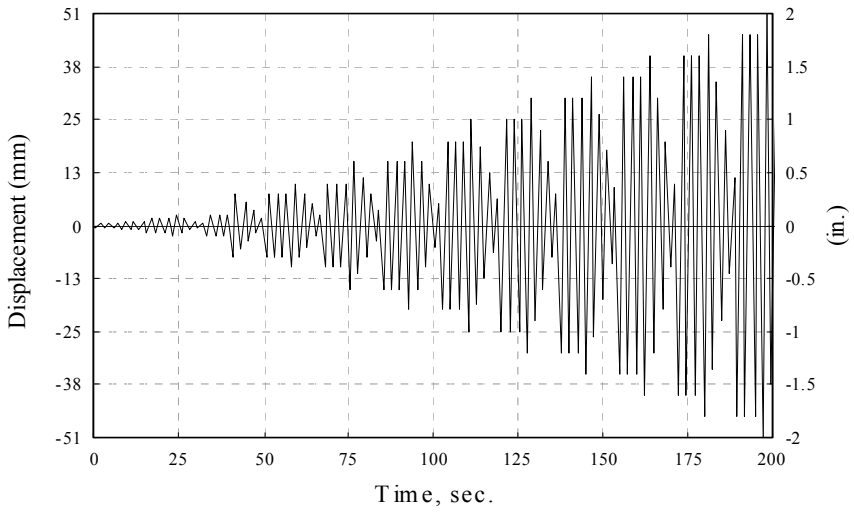

Figure-6 Displacement pattern of SPD procedure

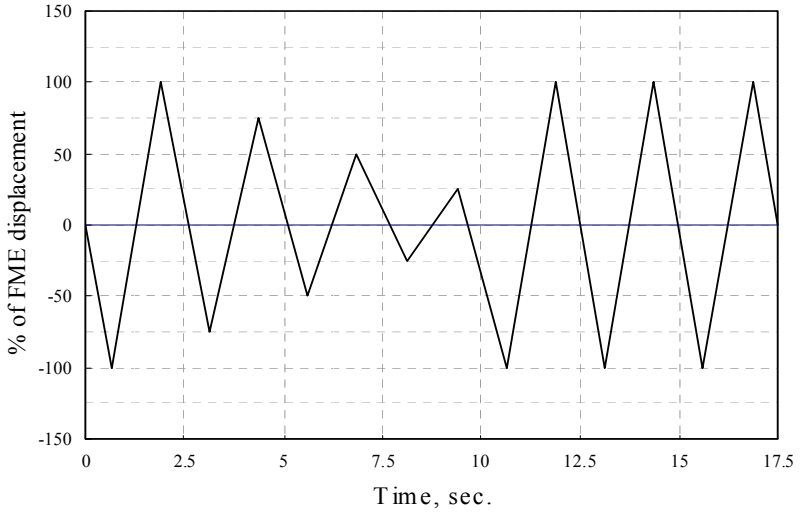

Figure 7 - Single phase of SPD pattern.

The first pattern gradually displaced the wall to its anticipated yield displacement. Elastic behavior of the wall was observed in this part of the test. The second displacement pattern began once the wall had past its anticipated yield displacement (i.e., started inelastic behavior) or first major event (FME). To make results of the cyclic tests compatible with previous tests FME = 2.5 mm (0.1 in.) was used, although in the tests, FME actually occurred at deflections exceeding 5 mm (0.2 in.).

The excitation was a triangular reversing ramp function at a frequency of 0.4 Hz. The cycles started with the negative stroke (i.e., with the ram pushing the specimen).

The first displacement pattern consisted of three phases, each containing three full cycles of equal amplitude. The first set of three cycles displaced the wall at approximately 25% of the FME. The second set displaced the wall 50% of the FME and the final set displaced the wall at 75% of the FME. The next cycle displaced the wall to approximately the FME to begin the second displacement pattern.

One phase of the second displacement pattern in SPD loading is illustrated in Figure 7. The initial cycle was followed by three decay cycles of 75%, 50%, and 25% of the initial amplitude for the phase. The decay cycles were followed by three cycles with the initial amplitude for the phase. Such a pattern was determined to be sufficient in order to obtain a "stabilized" response for nailed shear walls and was found to provide the stabilized response for screws as well. Stabilized response is defined as when the load resistance of the wall displaced to the same amplitude in two successive cycles decreased less than 5%. The amplitude of initial cycle in subsequent phases increased in the following pattern: 200%, 300%, 400%, and so on in 200% increments of the FME displacement until the amplitude reached 102 mm (4 in.).

While the SPD test protocol was used for these tests in order to maintain consistency with prior tests, it has been shown to provide overly conservative results. The International Standards Organization's draft test protocol (ASTM, 1995) or the test protocol developed by the California Universities for research in Earthquake Engineering Wood-Frame Project (Krawinkler, 2000)

would be a better test protocols to follow. The test results would probably show higher capacities for all tests if a similar trend as seen for wood-framed walls were found.

Property Definitions

Data collected during the wall tests was analyzed using guidelines of SEAOSC (1997) and proposed ASTM method (1995). According to these methods, strength, stiffness, and damping characteristics were determined. Definitions of the properties are given in this section.

Story drift was determined as the difference between horizontal movement at the top of the wall and at the bottom plate. However, to perform quantitative analyses and comparisons of wall performance, load-deflection curves were generated for each specimen based on data produced by hydraulic actuator load cell and displacement transducer. In this case, fewer random and systematic errors related to measurements were involved in computation of wall parameters. On one hand, this allowed obtaining more consistent results and more accurate estimation of energy dissipation. On the other hand, the results conservatively ignored the amount of slip at the top and bottom plates, which varied from 0.1 mm (0.005 in.) at proportional limit to 1 mm (0.04 in.) at peak loads. *Envelope response curves* were produced for the analysis of the cyclic tests. Actual response curves by Salenikovich, et al. (1999) were used to analyze the walls subjected to monotonic tests.

A typical response curve of shear walls subjected to SPD loading is shown in Figure 8. It is a series of hysteresis loops corresponding to each cycle of negative and positive deflections of the wall. From the hysteresis loops, complete (negative and positive) envelope, or 'backbone' curves were determined by producing the curve of best fit through the maximum force and associated displacement for each cycle. Two types of envelope curves were obtained. The *'initial' envelope curve* accommodated peak loads from the first cycle of each phase of SPD loading; the *'stabilized' envelope curve* contained peak loads from the last cycle of each phase.

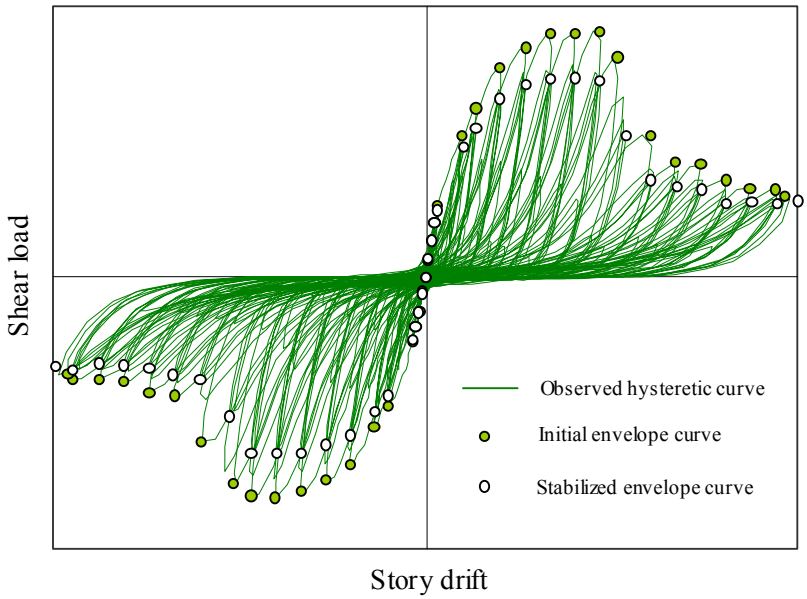

Figure 8 - Typical response curve of a shear wall under SPD loading.

The envelope curves of light-frame shear walls resemble the shape of monotonic response curves. Differences between these curves allow quantifying the strength and stiffness degradation of the structure due to repeated reversed loading. Therefore, all parameters were determined from the three curves: monotonic, initial, and stabilized (monotonic and cyclic test values generated by Salenikovich, et al. (1999) were combined with the cyclic test results generated for the various wall configurations shown in Table 2). Parameters of the negative and positive envelope curves were averaged assuming variability was due to random effects.

Definitions of variables used in this report are those used for similar investigations of the perforated shear wall method with wood-framed wall specimens. They have not been agreed upon as standard definitions, and there are several other definitions being proposed for many of the variables. However, the variables used provide some measure of performance and the ability to compare performance between specimens. The data can be reanalyzed to provide quantitative information once the variable definitions are finalized.

The way which strength and stiffness parameters were defined from a load-deflection or envelope curve is shown in Figure 9. Capacity of a wall, F_{max}, was determined as the extreme load in the corresponding load-deflection curve.

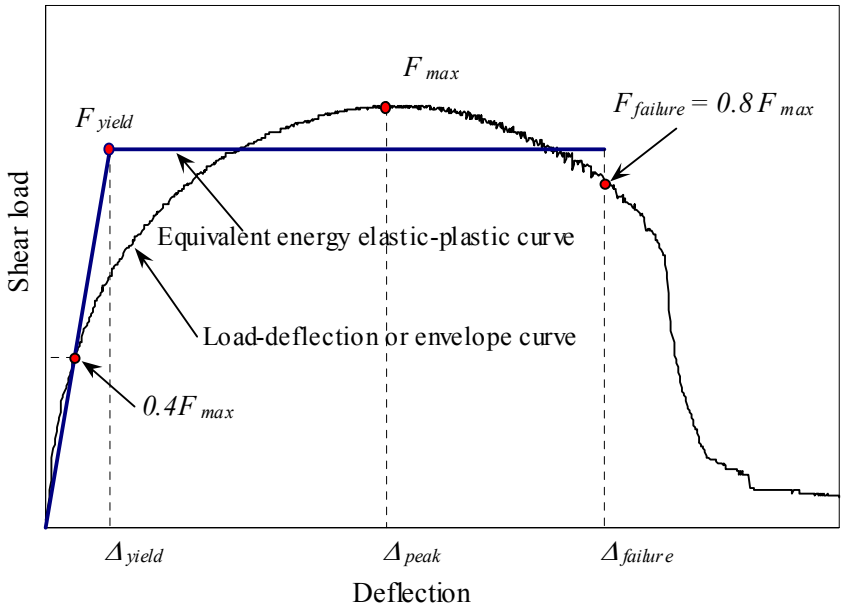

Figure 9 - Performance parameters of shear walls.

Deflection corresponding to the capacity was determined and denoted as Δ_{peak}. Failure load, $F_{failure}$, and corresponding deflection, $\Delta_{failure}$, were found at the point when the resistance dropped to 80% of the wall capacity. In this report, elastic stiffness, k_e, was defined as the slope of the line passing through the origin and the point on the response curve where the load was equal to 40% of F_{max}. *(This is one of the questionable definitions used in this report. The definition is one that was used in the proposed ASTM standard for cyclic tests of mechanical connections, and is a compromise reached in an effort to harmonize the ASTM test standard and the equivalent CEN standard. The definition has been used in other researcher, however, the variable may need to be adjusted once a final definition is reached. This definition also affects the values determined for other variables that used the initial stiffness directly or indirectly such*

as ductility. In cyclic tests, this stiffness represented a good estimate of the stiffness that shear walls would exhibit after being loaded a number of times at low to moderate amplitudes).

For comparison purposes, an equivalent energy elastic-plastic (EEEP) curve was determined for each wall. This artificial curve, shown in Figure 9, depicts how an ideal perfectly elastic-plastic wall would perform and dissipate an equivalent amount of energy as the mototonic or envelope curve. This definition of the EEEP curve was used for both monotonic and cyclic tests.[1)]

The elastic portion of the EEEP curve contains the origin and has a slope equal to the elastic stiffness, k_e. The plastic portion of the EEEP curve is a horizontal line positioned so that the area under the EEEP curve equals the area under the response or envelope curve from zero deflection to $\Delta_{failure}$. Displacement at yield, Δ_{yield}, and load at yield, F_{yield}, are defined at the intersection point of the elastic and plastic lines of the EEEP curve.[2)] Equating the areas under the response curve and the EEEP curve, the yield load can be expressed as:

$$F_{yield} = \frac{-\Delta_{failure} \pm \sqrt{\Delta^2_{failure} - \frac{2A}{k_e}}}{-\frac{1}{k_e}} \tag{5}$$

where: A = area under the response curve between zero and $\Delta_{failure}$.

Information about deformation of walls is an important parameter that indicates the ability to sustain relatively high loads at significant deflections. Useful information about wall deformation capacity is provided by ductility ratio, D, and so-called toughness of failure, D_f, determined from the EEEP curve:

[1)] Total energy dissipated by walls during cyclic tests is significantly greater than determined from the envelope curve because hysteresis loops overlap. This definition is used for comparison purposes only.

[2)] F_{yield} must be greater than or equal to 80% of F_{max}.

$$D = \Delta_{failure} / \Delta_{yield} \tag{6}$$

$$D_f = \Delta_{failure} / \Delta_{peak} \tag{7}$$

Another important characteristic of cyclic performance of structural systems is their ability to dissipate the energy, or damping. Hysteretic energy, W_D, dissipated per cycle of the wall is calculated by integrating the area enclosed by the hysteresis loop at the corresponding displacement (as shown in Figure 10). The strain energy, U_0, equals the area enclosed by the triangle *ABC* in Figure 10. To compare damping properties of the walls, equivalent viscous damping ratio for each initial and stabilized cycle, ζ_{eq}, and work to failure were estimated:

$$\zeta_{eq} = \frac{1}{4\pi} \frac{W_D}{U_0} \tag{8}$$

Because hysteresis loops were not ideally symmetric, the areas of triangles *ABC* and *ADE* in Figure 10 were averaged to approximate the value of the strain energy U_0 in Equation (8).

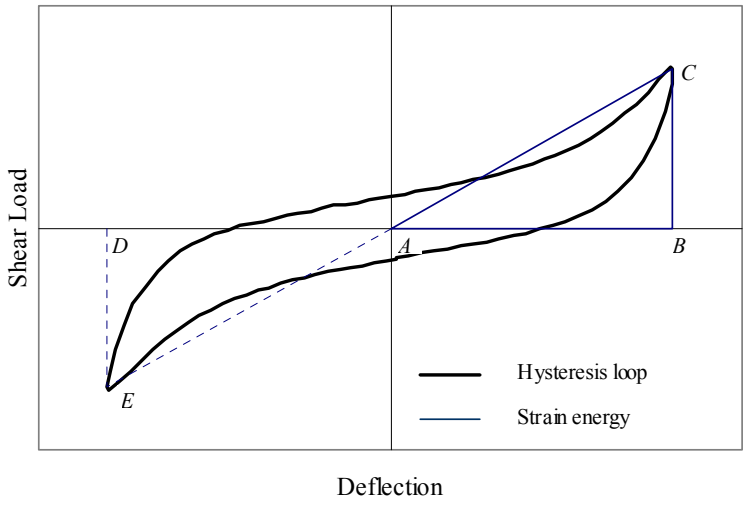

Figure 10 - Damping and strain energy of a cycle.

Work to failure, or energy dissipation, was measured as the total area enclosed by hysteresis loops until failure in cyclic tests, or the area under the load-deflection curve until failure in monotonic tests.

To validate Equations (2) to (4), load resisted by walls at shear angles 1/300, 1/200, 1/100, and 1/60 radian were extracted from the monotonic, and cyclic initial and stabilized envelope data from Salenikovich, et al. (1999) and the walls being tested as part of this study. These angles correspond to deflections of 8 mm (0.32 in.), 12 mm (0.48 in.), 24 mm (0.96 in.), and 41 mm (1.6 in.). To determine the actual shear capacity ratio at a given deflection, the load resisted by a wall with sheathing area ratio *r* was divided by the corresponding load resisted by the fully-sheathed wall with equivalent overturning anchorage.

In addition to the parameters introduced in this section, the discussion of test results includes uplift forces resisted by tie-down anchors, uplift movement of end studs, failure modes, and general observations.

Test Results

A total of 17 specimens were constructed and tested in this study. The number of tests performed in each category and their nomenclature (in bold characters) are displayed in Table 5. **Appendix A** contains summary data for each specimen tested including parameters defined in the previous section. **Appendix B** contains observed load-deflection curves along with graphs of uplift forces and displacements at the wall ends as a function of wall deflection for each specimen. Note that load-deflection curves in Figures 11 to 15 in this section were plotted using reduced data for convenience of display. Graphs in **Appendix B** display the original non-reduced data. While three specimens for configuration C4b were tested and the data specimen C4b1 is included in the Appendices, the data for this specimen was excluded from the comparative data. This is due to the test being stopped before the end of the displacement pattern due to a power surge causing the test machine to reset.

Table 5 - wall nomenclature and number of tests conducted.

Load regime	Wall type [1]											Total
	A2hb[2]	**B2gab**	**C2ab**	**C2gab**	**C2gb**	**C4b**	**C4s**	**D2ab**	**D2gab**	**D4b**	**D4s**	
cyclic	1	1	1	1	1	3	2	2	1	2	2	17

1: Wall nomenclature is explained in Table 2**.**
2: This walls had interior gypsum wallboard sheathing oriented in a horizontal staggered pattern in addition to exterior OSB sheathing.

The wall configurations and the number of tests carried out by Salenikovich, et al. (1999) are shown in Table 6. The table has been included, as the test results are used for the sake of comparison with the cyclic test specimens presented in Table 5. For opening effects, specimen **Amon** (configuration A, loaded monotonically) tested by Salenikovich, et al. (1999) was used as a control trial for all other wall configurations.

Table 6 - wall nomenclature and tests conducted by Salenikovich, et al. (1999)

Load regime	Wall type						Total
	Agyp [1]	**A**	**B**	**C**	**D**	**E**	
monotonic	1	1	1	1	1	1	6
cyclic	-	2	2	2	2	2	10
Total	1	3	3	3	3	3	16

1: These walls had interior gypsum wallboard sheathing in addition to exterior OSB sheathing.

Effects of opening size

To illustrate response of walls with various opening sizes, load-deflection and envelope curves observed in monotonic and cyclic tests are shown in Figure 11, and performance parameters obtained from the analysis of these curves are summarized in Table 7. Each envelope curve represents the average of negative and positive envelopes of individual specimens. All

replications are shown in the graphs to illustrate variation in the cyclic response of walls. Cyclic data in Table 7 represent average values of all specimens for each configuration, which in turn were obtained by averaging parameters determined separately for negative and positive envelopes.

For clarity of graphs and to aid in discussion, the response curves illustrated in Figure 11 are divided by configuration (**A, B, C**, and **D**) and combined with the response curves of the walls tested by Salenikovich, et al. (1999) and plotted in Figures 12 to15.

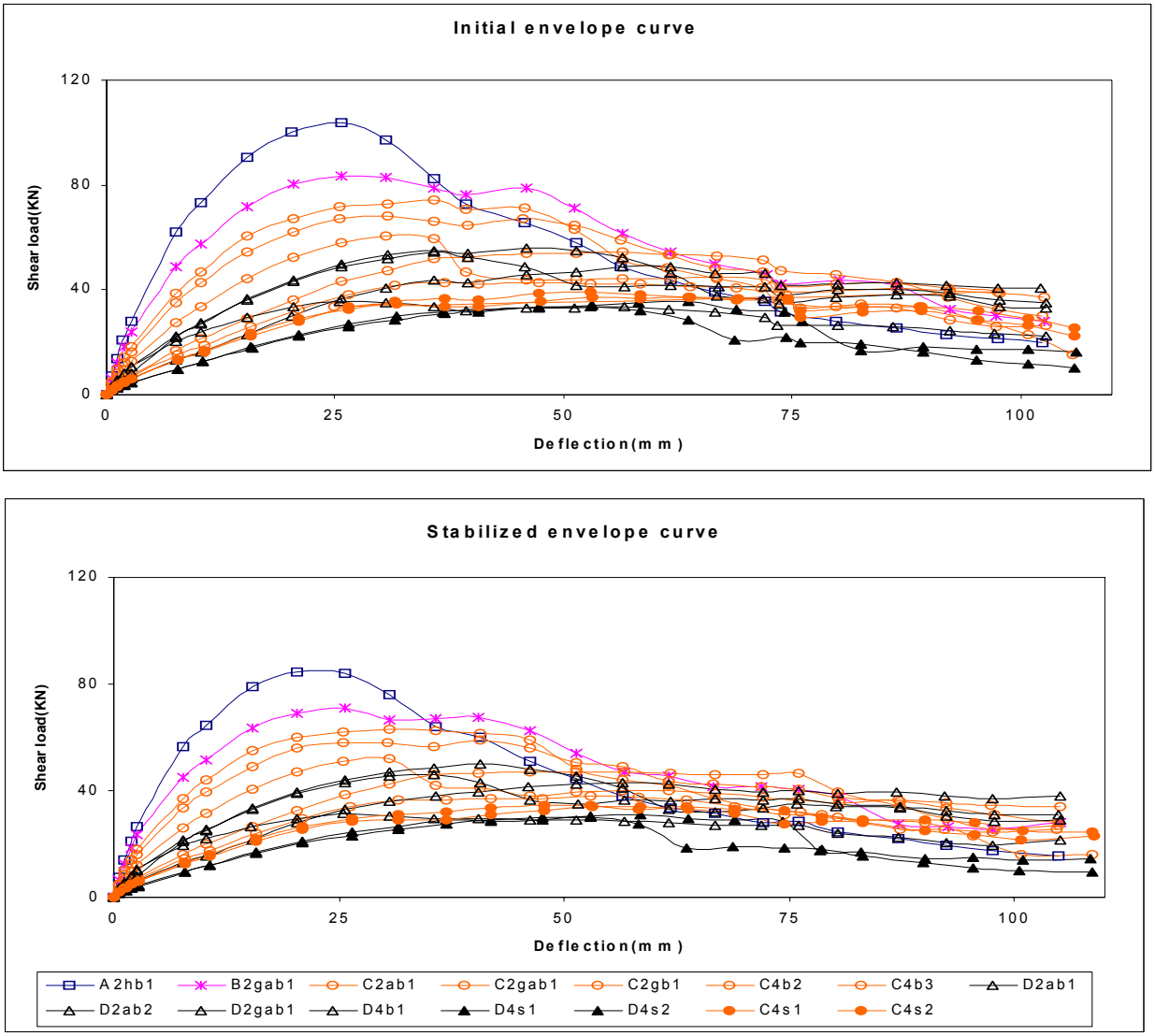

Figure11 - Response of walls with various openings

Table 7 - Performance parameters of walls with various openings

Parameter	Load condition	Units	Wall configuration															
			A	**A2hb**	**B**	**B2gab**	**C**	**C2ab**	**C2gab**	**C2gb**	**C4b**	**C4s**	**D**	**D2ab**	**D2gab**	**D4b**	**D4s**	**E**
F_{peak}	*monotonic*	*Kips*	32.5		20.7		13.9						12.8					7.7
	cyclic initial		26.7	23.3	20.5	18.9	13.3	13.6	16.7	15.5	11.2	8.8	11.6	12.4	8.0	11.0	7.8	6.5
	cyclic stabilized		21.7	19.3	17.5	15.9	11.7	11.7	14.2	13.5	9.8	7.8	10.1	10.8	7.1	9.7	6.9	5.6
Δ_{peak}	*monotonic*	*in.*	1.49		2.19		2.09						1.84					2.85
	cyclic initial		1.31	1.01	1.41	1.11	1.49	1.20	1.31	1.50	1.89	2.08	1.51	1.50	1.01	2.33	2.19	1.66
	cyclic stabilized		1.16	0.90	1.30	1.01	1.46	1.10	1.20	1.41	1.85	1.88	1.46	1.51	1.01	2.13	2.19	1.50
F_{yield}	*monotonic*	*Kips*	28.1		18.5		12.6						11.6					6.7
	cyclic initial		24.1	20.8	18.2	17.09	11.8	12.1	15.2	14.1	10.3	7.78	10.3	11.1	7.3	9.9	7.1	5.7
	cyclic stabilized		19.6	17.2	15.5	14.42	10.3	10.2	13.1	12.1	8.9	6.97	9.0	9.6	6.3	8.8	6.2	4.9
Δ_{yield}	*monotonic*	*in.*	0.41		0.46		0.54						0.76					0.82
	cyclic initial		0.38	0.40	0.54	0.41	0.54	0.56	0.49	0.51	0.94	0.88	0.56	0.68	0.40	1.12	1.05	0.58
	cyclic stabilized		0.30	0.34	0.47	0.34	0.49	0.49	0.42	0.43	0.84	0.79	0.51	0.60	0.35	1.05	0.97	0.51
$\Delta_{failure}$	*monotonic*	*in.*	2.05		2.55		2.44						2.51					4.31
	cyclic initial		1.68	1.40	1.90	2.11	2.43	1.53	2.08	2.37	3.06	3.21	2.37	2.21	2.82	4.03	2.77	2.07
	cyclic stabilized		1.58	1.33	1.75	1.96	2.20	1.49	1.98	2.21	3.08	3.36	2.39	2.03	3.14	4.14	2.67	1.93
k_e	*monotonic*	*Kip/in*	68.4		40.5		23.4						15.3					8.3
	cyclic initial		64.1	51.54	33.7	41.7	21.9	21.5	31.4	27.7	21.8	9.1	18.5	16.41	27.50	8.76	6.72	9.8
	cyclic stabilized		66.7	50.34	33.1	42.5	21.1	20.7	31.6	28.0	10.6	8.8	18.0	15.89	18.23	8.42	6.41	9.6
ζ_{eq} [1]	*cyclic initial*		0.079	0.090	0.076	0.090	0.070	0.081	0.079	0.081	0.072	0.065	0.073	0.076	0.093	0.069	0.065	0.068
	cyclic stabilized		0.059	0.063	0.060	0.069	0.056	0.065	0.063	0.066	0.062	0.055	0.059	0.063	0.073	0.062	0.058	0.052

1: ζ_{eq} at F_{max}
Note: 1Kip = 4.448 kN, 1in. = 25.4 mm.

Table 8 - Normalized Performance parameters of walls with various openings with monotonic response of configuration as basis.

Parameter	Load condition	Wall configuration															
		A	**A2hb**	**B**	**B2gab**	**C**	**C2ab**	**C2gab**	**C2gb**	**C4b**	**C4s**	**D**	**D2ab**	**D2gab**	**D4b**	**D4s**	**E**
F_{peak}	*initial / monotonic*	82%	72%	99%	91%	96%	98%	120%	112%	81%	63%	96%	97%	63%	86%	61%	84%
	stabilized / monotonic	67%	59%	84%	77%	84%	84%	102%	97%	71%	56%	84%	84%	55%	76%	54%	73%
	stabilized / initial	81%	83%	85%	84%	88%	86%	85%	87%	88%	89%	88%	87%	89%	88%	88%	87%
Δ_{peak}	*initial / monotonic*	88%	68%	64%	51%	72%	57%	63%	72%	90%	100%	72%	82%	55%	127%	119%	58%
	stabilized / monotonic	78%	60%	60%	46%	70%	53%	57%	67%	89%	90%	70%	82%	55%	116%	119%	53%
	stabilized / initial	88%	69%	92%	91%	97%	92%	92%	94%	98%	90%	97%	101%	100%	91%	100%	91%
F_{yield}	*initial / monotonic*	86%	74%	98%	92%	93%	96%	121%	112%	82%	62%	93%	96%	63%	85%	61%	84%
	stabilized / monotonic	70%	61%	84%	78%	82%	81%	104%	96%	71%	55%	82%	83%	54%	76%	53%	73%
	stabilized / initial	81%	83%	85%	84%	87%	84%	86%	86%	86%	90%	87%	86%	86%	89%	87%	87%
Δ_{yield}	*initial / monotonic*	92%	98%	118%	89%	101%	104%	91%	94%	174%	163%	101%	89%	53%	147%	138%	71%
	stabilized / monotonic	72%	83%	103%	74%	91%	91%	78%	80%	156%	146%	91%	79%	46%	138%	128%	63%
	stabilized / initial	78%	85%	87%	83%	90%	88%	86%	84%	89%	90%	90%	88%	88%	94%	92%	89%
$\Delta_{failure}$	*initial / monotonic*	82%	68%	75%	83%	100%	63%	85%	97%	125%	132%	100%	88%	112%	161%	110%	48%
	stabilized / monotonic	77%	65%	69%	77%	90%	61%	81%	91%	126%	138%	90%	81%	125%	165%	106%	45%
	stabilized / initial	94%	95%	92%	93%	91%	97%	95%	93%	101%	105%	91%	92%	111%	103%	96%	93%
k_e	*initial / monotonic*	94%	75%	83%	103%	94%	92%	134%	118%	93%	39%	94%	107%	180%	57%	44%	119%
	stabilized / monotonic	98%	74%	82%	105%	90%	88%	135%	120%	45%	38%	90%	104%	119%	55%	42%	116%
	stabilized / initial	104%	98%	98%	102%	96%	96%	101%	101%	49%	97%	96%	97%	66%	96%	95%	98%
ζ_{eq} [1]	*stabilized / initial*	74%	70%	78%	77%	80%	80%	80%	81%	86%	85%	80%	83%	78%	90%	89%	77%

1: ζ_{eq} at F_{max}

The response curves for the walls with Configuration A (fully-sheathed) are shown in Figure 12. It can be seen from the plots and the values from Tables 7 and 8 that there is variation between the different specimens (13%). There is a drop in performance of the wall without the mechanical tie-down anchors but the variation is not significant and can be attributed to typical testing error. However, due to the positive connection in the framing with the use of screws, the

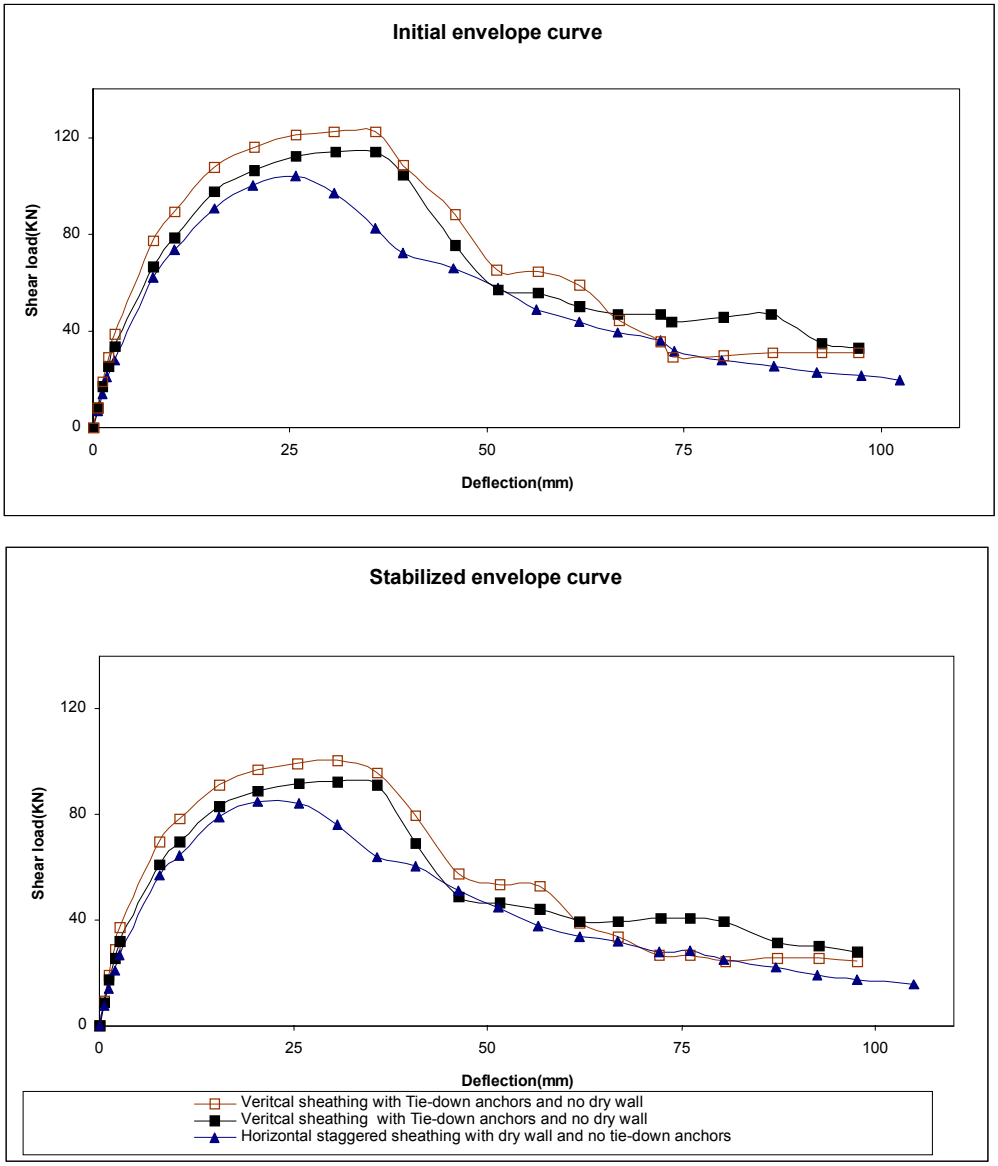

Figure 12- Cyclic Response curves of Configuration A walls

potential increase in stiffness associated with the sheathing being oriented horizontally and any additive effects of the gypsum sheathing used in the specimen without overturning anchors, it is impossible to say that overturning anchors can be eliminated. A series of specimens of similar configurations would have to be tested to quantify the effect of each parameter (horizontal OSB sheathing and Gypsum) under cyclic loading. However, based on these limited tests, combined horizontal oriented OSB and gypsum sheathing provided 90% of the strength expected for walls with OSB sheathing oriented vertically and overturning anchors.

The response curves for the walls with Configuration B are shown in Figure 13. The plot and the values from Tables 7 and 8 show that there is little variation between the different specimens. All the walls tested in this configuration had mechanical tie-down anchors at the ends of the wall specimens and all specimen have similar response. The walls with 0.6 m (2 ft.) end wall segments and gusseted openings had equivalent performance to walls with 1.2 m (4 ft.) end wall segments when overturning anchors were used. Test results for wall Configurations C and D show that the effect of gusseting the corners of openings is not consistent, and therefore, the similar performance in the walls with 0.6 m and 1.2 m (2 ft. and 4 ft.) end wall segments can be assumed to be attributed to the anchorage performance. Therefore, the effect of shortening the end wall segment from 4 to 2 feet can be assumed to be negligible.

The response curves for the walls with Configuration C are shown in Figure 14. The plot and values presented in Tables 7 and 8 show that the wall with 0.6 m (2 ft.) end sheathing, gusseted openings, and mechanical tie-down anchors performs the best for Configuration C. There is a 33% reduction in performance when the anchors and the gusseting is removed. When the results of the test for wall configuration D are considered, the effect of gusseting corners is questionable the effect of overturning anchors is the principle effect on improving wall performance.

Comparing the walls with 1.2 m (4 ft) sheathing on the end wall segments we find that capacity of the walls with the mechanical tie-down anchors is higher (15%) as compared to the performance of those with 1.2 m (4 ft.) end wall segments and no tie-down anchors

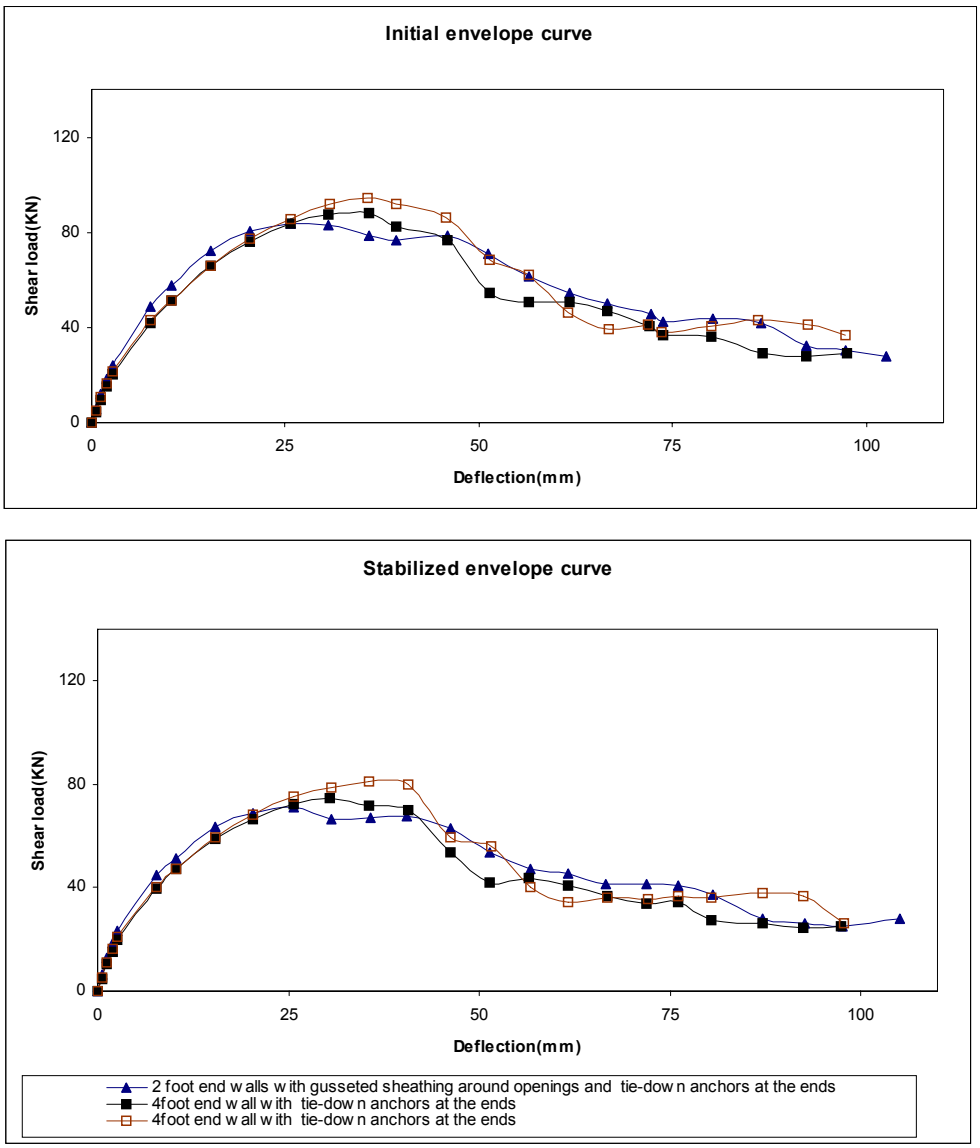

Figurer 13- Cyclic Response curves of **B** configuration walls

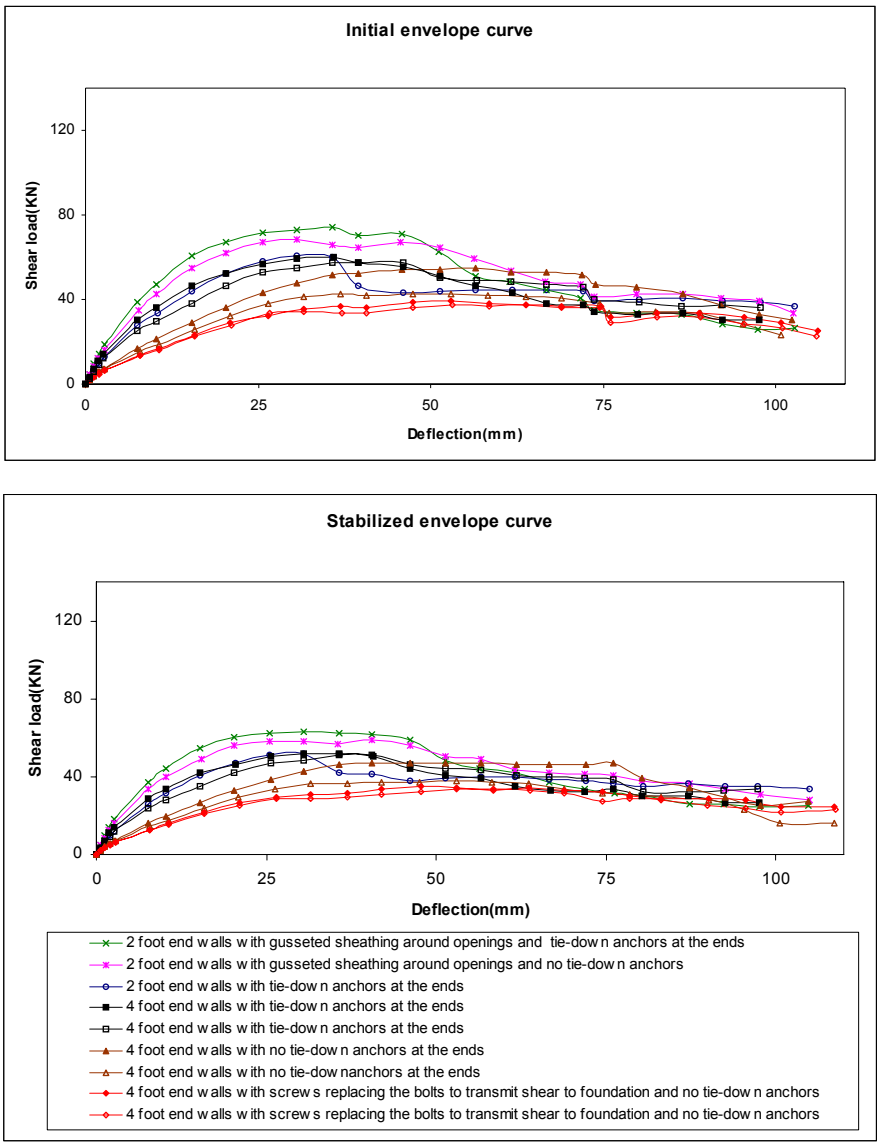

Figure 14 - Cyclic Response curves of **C** configuration walls

Also, it can be seen that the use of screws instead of bolts to transmit shear to the foundation substantially reduces the performance of the wall. Keeping other variables constant (i.e., maintaining 1,2 m (4 ft.) end sheathing, and no mechanical tie-down anchors), we see that there is a 21% reduction in performance of the wall when the shear bolts are replaced by screws to transmit shear to the foundation (e.g., from Table 7, 8.8/11.2 for cyclic initial)

The response curves for the walls with Configuration D are shown in Figure 15. From the plot and the values presented in Tables 7 and 8 we find that with the exception of the effect of tie-down anchors and screws in the foundation there is not significant difference in the performance of the walls with the different variations. The response curves of the wall overlap and the slight variation in the walls can be attributed to standard testing error.

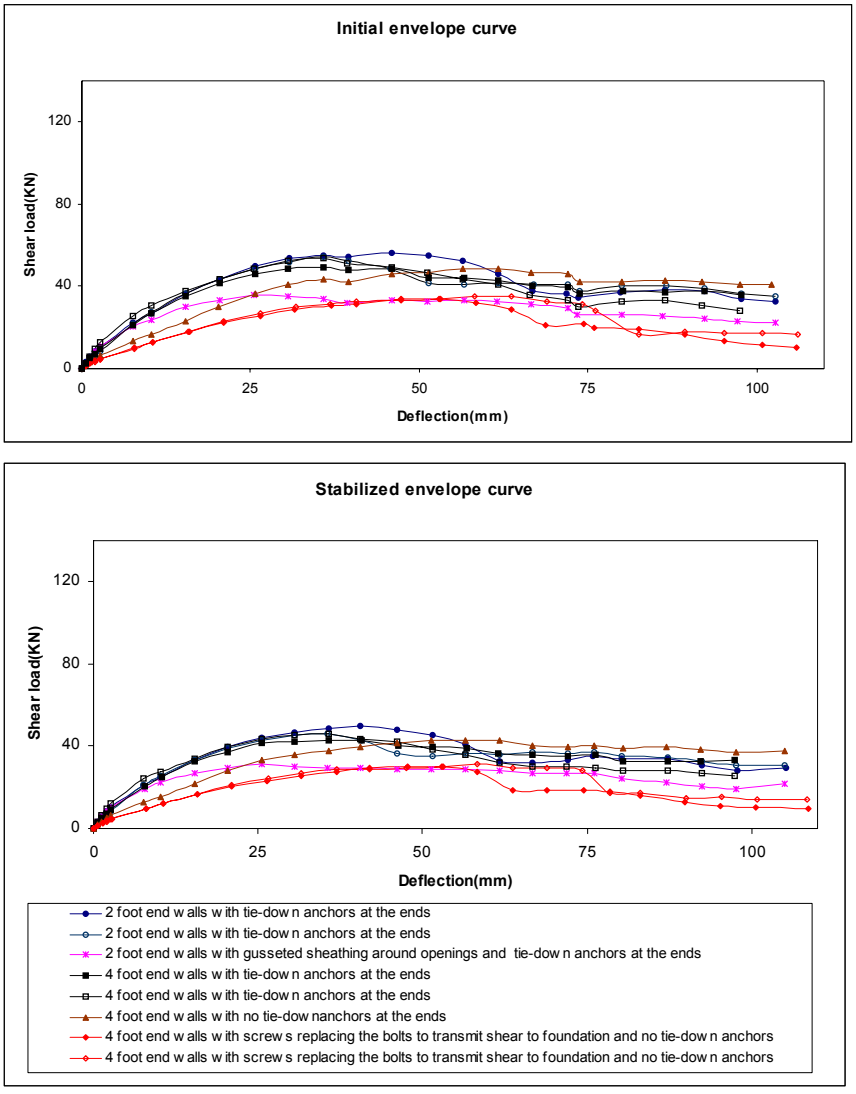

Figurer 15- Cyclic Response curves of **D** configuration walls

Comparing the walls with 1.2 m (4 ft.) end segment sheathing we find that performance of the wall is marginally better (5%) with the mechanical tie-down anchors as compared to the performance of those with 1.2 m (4 ft.) end walls and no tie-down anchors (specimens D and D 4b).

Also, it can be seen that the use of screws instead of bolts to transmit shear to the foundation substantially reduces the performance of the wall as compared to the performance of the rest of the walls. For direct comparison keeping the variables constant (i.e., maintaining 1.2 m (4 ft.) end sheathing, and no mechanical tie-down anchors) we see that there is a 29% reduction in capacity of the wall when the shear bolts are replaced by screws to transmit shear to the foundation (Table 7, 7.8/11.0). This is similar to the results for Configuration B this reduction is substantial.

The gusseted sheathing around the opening corners had no effect on the capacity of the walls. In fact, the strength of the gusseted walls was lower than the ungusseted walls. the inconsistent results for walls with gusseted sheathing indicates that the gusseted sheathing was not effecting performance, but other factors such as tie-down anchors and the method for attaching the framing to the foundation had more significant effects on performance.

A progressive reduction in the resistance of the walls as the sheathing area ratio decreases is shown in Figures 12 to 15. Wall Configuration A with a sheathing area ratio of 1.0 lying on one end of the continuum shows maximum resistance characteristics followed by wall Configurations B, C, and D in the decreasing order of resistance respectively.

Effects of opening size on load resistance of each specimen at various levels of deflection under cyclic loading are illustrated in Figure 16**.** In the graphs, shear load ratio is shown as a function of sheathing area ratio. Lines represent predictions of shear load ratios given by Equations (2), (3), and (4). Numerical support for the graphs is given in Table 9. The data in the table is represented by average values of the walls wherever applicable.

a)

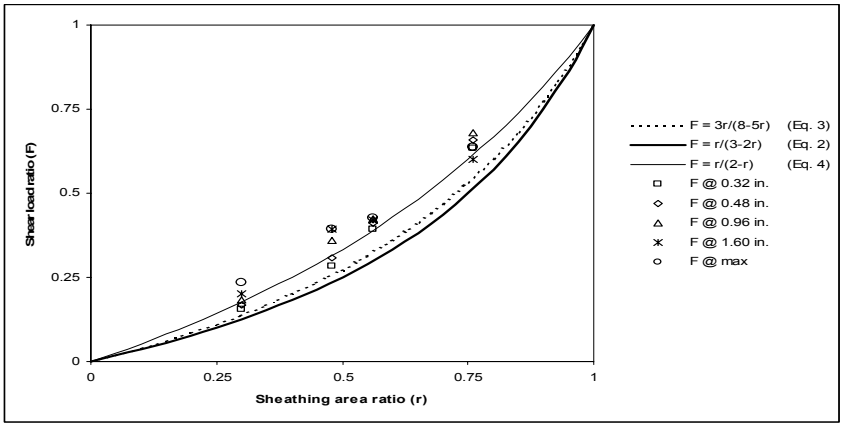

b)

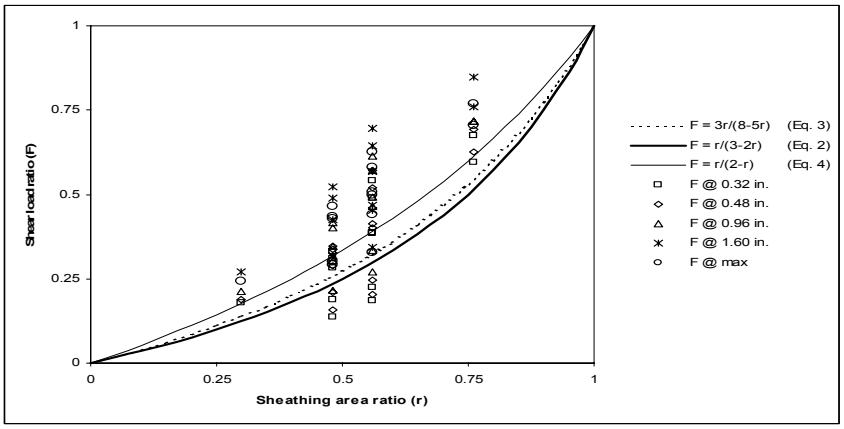

c)

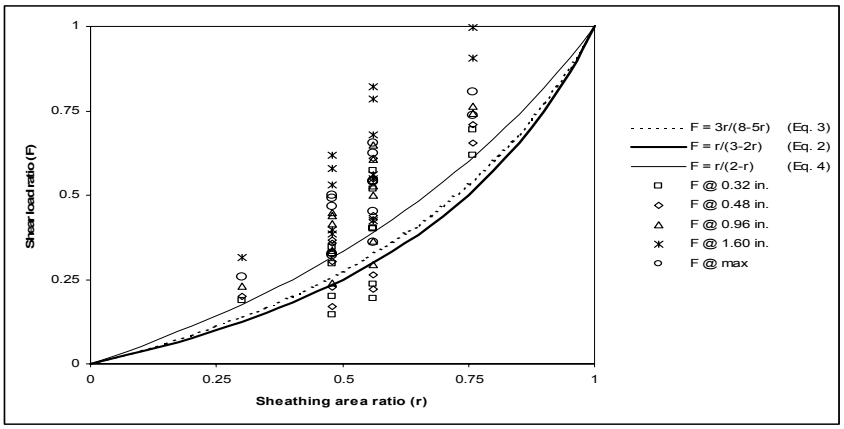

Figure 16 - Shear load ratios:

a) monotonic response, b) initial cyclic response, b) stabilized cyclic response.

Table 9 - Predicted and observed shear load ratio based on fully sheathed anchored condition

Shear load ratio	Load condition	Wall configuration													
		B	**B2gab**	**C**	**C2ab**	**C2gab**	**C2gb**	**C4b**	**C4s**	**D**	**D2ab**	**D2gab**	**D4b**	**D4s**	**E**
Predicted	$F = 3r/(8-5r)$ (Eq. 3)	0.541	0.541	0.320	0.320	0.320	0.320	0.320	0.320	0.257	0.257	0.257	0.257	0.257	0.138
	$F = r/(3-2r)$ (Eq. 2)	0.512	0.512	0.295	0.295	0.295	0.295	0.295	0.295	0.235	0.235	0.235	0.235	0.235	0.125
	$F = r/(2-r)$ (Eq. 4)	0.612	0.612	0.386	0.386	0.386	0.386	0.386	0.386	0.316	0.316	0.316	0.316	0.316	0.176
F @ 0.32 in.	*monotonic*	0.633		0.393						0.283					0.157
	Cyclic initial	0.596	0.676	0.387	0.387	0.541	0.489	0.224	0.184	0.330	0.311	0.284	0.188	0.136	0.178
	Cyclic stabilized	0.619	0.693	0.402	0.400	0.574	0.518	0.235	0.194	0.344	0.328	0.296	0.201	0.146	0.187
F @ 0.48 in.	*monotonic*	0.658		0.412						0.307					0.169
	Cyclic initial	0.625	0.692	0.402	0.414	0.572	0.519	0.247	0.203	0.347	0.338	0.288	0.209	0.158	0.188
	Cyclic stabilized	0.655	0.710	0.426	0.440	0.608	0.548	0.265	0.220	0.366	0.358	0.303	0.227	0.171	0.200
F @ 0.96 in.	*monotonic*	0.680		0.423						0.361					0.182
	Cyclic initial	0.716	0.718	0.465	0.492	0.613	0.571	0.335	0.270	0.402	0.416	0.348	0.303	0.216	0.213
	Cyclic stabilized	0.763	0.742	0.501	0.528	0.650	0.605	0.365	0.294	0.438	0.449	0.415	0.335	0.238	0.229
F @ 1.60 in.	*monotonic*	0.600		0.420						0.392					0.201
	Cyclic initial	0.848	0.759	0.567	0.454	0.697	0.643	0.468	0.344	0.488	0.524	0.319	0.425	0.315	0.269
	Cyclic stabilized	0.997	0.906	0.679	0.548	0.821	0.785	0.560	0.425	0.580	0.619	0.397	0.531	0.384	0.314
$F @ \Delta_{max}$	*monotonic*	0.637		0.426						0.394					0.236
	Cyclic initial	0.768	0.706	0.498	0.509	0.625	0.582	0.440	0.329	0.434	0.466	0.301	0.429	0.291	0.242
	Cyclic stabilized	0.807	0.735	0.539	0.541	0.655	0.623	0.452	0.362	0.468	0.499	0.326	0.492	0.321	0.259

Note: 1in. = 25.4 mm.

Results suggest that Equation (2), used in the design codes to determine shear wall strength and Equation (3) produced conservative estimates for walls with tie-down anchors. At all levels of deflection under monotonic and cyclic loading, the resistance of each specimen with tie-down anchors significantly exceeded values predicted by these equations. As shown in Figure 16 the closest predictions were obtained at the early stages of deflection using Equation (4).

For walls tested without tie-down anchors the equations were non-conservative at deflections below capacity. This is because the walls were compared to a fully sheathed wall (Configuration A) with tie-down anchors. As shown in Figure 17 Equations 3 and 4, are non-conservative at maximum load for walls without tie-down anchors when the ratios are compared to a fully sheathed wall with tie-down anchors.

If the strength of specimen A2hb (fully-sheathed wall without tie-down anchors) is used as the base strength rather than the fully-sheathed anchored results, the predicted equations are conservative at the maximum load as shown in Figure 18. The recalculated shear load ratios for the various wall configurations without the tie-down anchors and using the fully sheathed wall without tie-down anchors as the base value for the equations are shown in Table 10. While

specimen A2hb had similar anchorage conditions to the unanchored walls, it also had gypsum sheathing. The fact that using this specimen as the basis for application of the perforated shear wall method to unanchored walls provides good predictions. This also indicates that gypsum probably does not contribute significantly to strength under cyclic loading. This change in apparent conservatism illustrates that the fully sheathed configuration strength used as the base strength for the perforated shear wall method must have the same end restraint as the perforated shear wall being designed. Otherwise the perforated shear wall method may provide unconservative results.

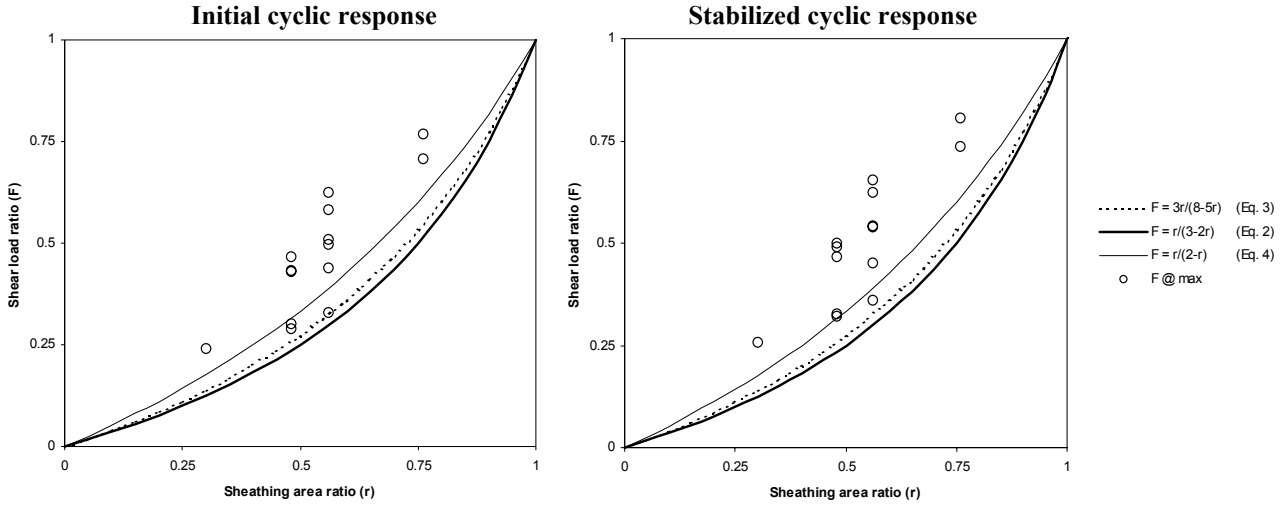

Figure 17-Shear load ratios at Δ_{max} using wall configuration A with tie-down anchor as the base value.

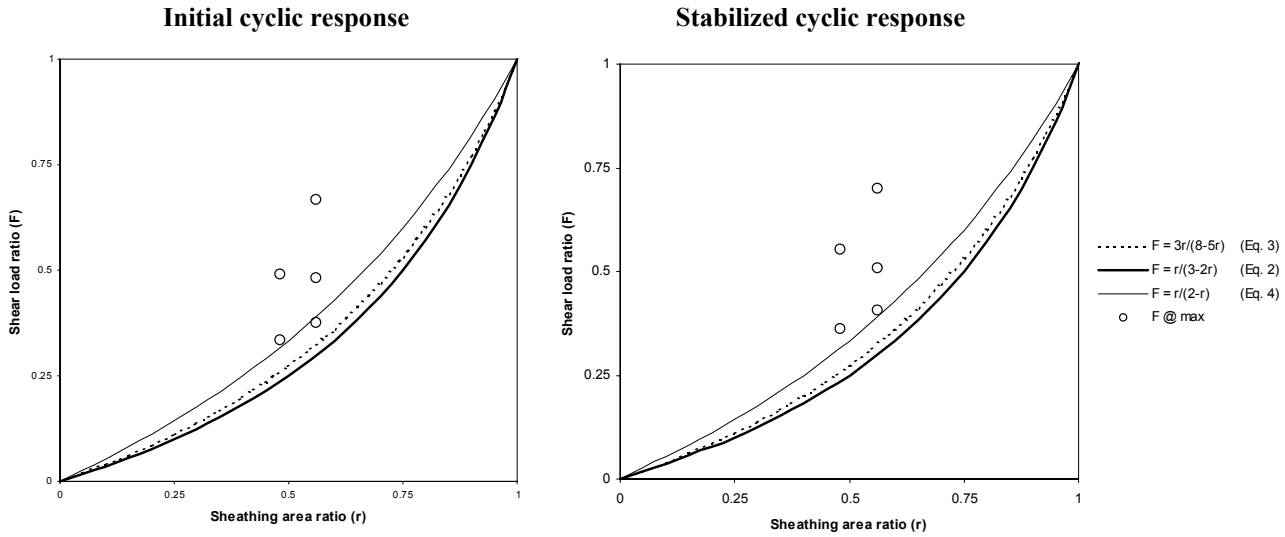

Figure 18- Shear load ratios at Δ_{max} using wall configuration **A** without tie-down anchor as base value

Table 10 - Predicted and observed shear load ratio for walls based on wall Configuration A without tie-down anchors.

Shear load ratio	Load condition	Wall configuration				
		C2gb	**C4b**	**C4s**	**D4b**	**D4s**
Predicted	*F = 3r/(8-5r)* (Eq. 3)	0.320	0.320	0.320	0.320	0.320
	F = r/(3-2r) (Eq. 2)	0.295	0.295	0.295	0.295	0.295
	F = r/(2-r) (Eq. 4)	0.386	0.386	0.386	0.386	0.386
F @ 0.32 in.	*Cyclic initial*	0.566	0.259	0.214	0.218	0.158
	Cyclic stabilized	0.596	0.271	0.223	0.231	0.168
F @ 0.48 in.	*Cyclic initial*	0.592	0.282	0.232	0.238	0.180
	Cyclic stabilized	0.619	0.299	0.248	0.256	0.193
F @ 0.96 in.	*Cyclic initial*	0.640	0.375	0.302	0.339	0.242
	Cyclic stabilized	0.682	0.411	0.331	0.377	0.268
F @ 1.60 in.	*Cyclic initial*	0.915	0.666	0.490	0.605	0.449
	Cyclic stabilized	0.979	0.699	0.530	0.662	0.479
F @ Δ_{max}	*Cyclic initial*	0.667	0.481	0.377	0.492	0.335
	Cyclic stabilized	0.702	0.509	0.408	0.554	0.361

Note: 1in. = 25.4 mm.

The reasons for obtaining high shear load ratios can be found by looking at Tables 7 and 9. Although fully-sheathed walls (A) were significantly stiffer than walls with openings, they were also less ductile. Configuration A walls reached capacity and degraded earlier than other walls. Wall Configuration A is a fully-engineered wall configuration with full overturning restraint, while all other configurations are partially restrained. Comparisons of elastic stiffness and yield points in Tables 7 and 9 indicate that walls with larger openings were less stiff under both monotonic and cyclic load conditions. This is why these walls have higher displacement capability.

Mechanism of Failure

The steel frames for all the walls tested were assembled in the same way as they are constructed in buildings. This allowed their racking without separation of studs from the tracks due to pivoting of the stud ends around framing screws. Such an assembly was relatively stiff because it engaged all sheathing screws and panel edges into load resistance. The predominant failure of sheathing was due to screw head pull through. Deflection demand on the sheathing connections increased until screws tore through the edge of the sheathing or the screw heads pulled through the sheathing panel. Dry wall screws simply tore a path through the relatively weak gypsum wallboard, due to the cyclic motion of the wall. Typical failure due to unzipping of the sheathing along the edges is shown in Figure 19. Elimination of the tear out of the sheathing edge or screw head pull through would significantly increase the stiffness and capacity of the walls. For instance, the use of screws with pan heads rather than bugle heads would improve performance significantly.

While framing connections of steel-frame walls proved to be strong, the framing elements suffered from low bending rigidity. As shown in Figure 20, the framing tracks and the studs experienced significant bending / buckling especially at the wall ends and after the peak load was reached, which lead to severe damage of sheathing connections leading to ultimate failure of sheathing connections. However, the predominant failure mode of steel-frame walls subjected to cyclic loading was head pull-through of sheathing screws and bending of frame elements. Due to pivoting and local buckling in the light-gage steel studs and track (Figure 21), very few screws failed in fatigue and the fatigue failure of the screws that occurred was primarily near wall corners where the steel framing had multiple layers holding the screw. Failure of sheathing screws due to fatigue is illustrated in Figure 22.

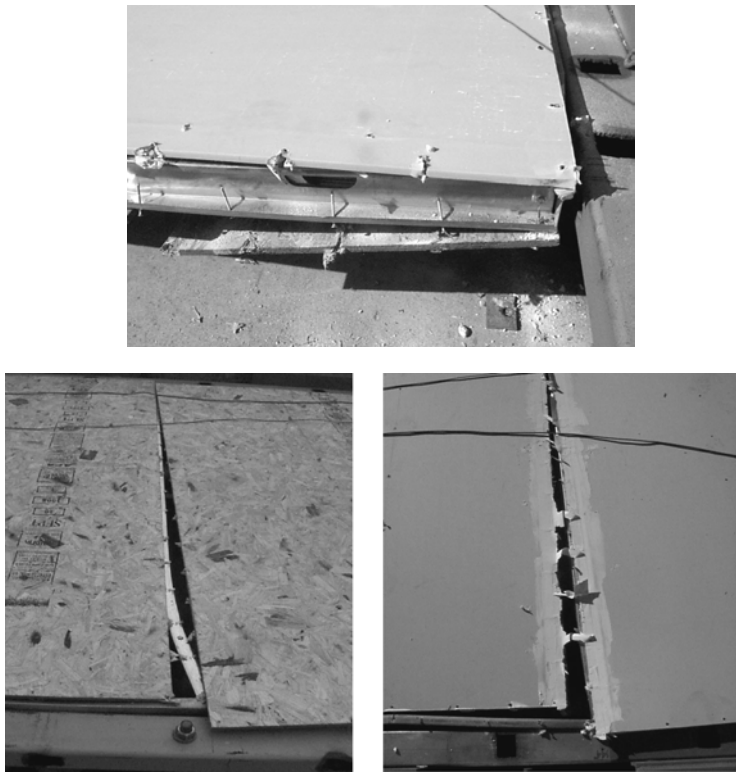

Figure 19- Sheathing and screw head pull-through along the panel edges.

Tie-down anchors improve overall performance of the wall by contributing significantly to the stiffness of the walls and providing overturning resistance to the wall. As shown in Figure 23 little damage is sustained by the wall track incorporating tie-down anchors at the end studs. Without the anchorage the end studs have a tendency to lift from the test frame causing damage to the wall bottom track. As shown in Figure 24 damage sustained by the wall track in the form of localized buckling and bending, due to absence of tie-down anchors is significant.

a) b)

Figure 20 - buckling of wall elements past ultimate load: a) wall track, b) studs

Figure 21- flaring of steel track

Figure 22- Fatigue failure of sheathing

Figure 23- walls showing tie-down anchors attached to the end studs

Figure 24 -Damage caused to tracks due to absence of tie-down anchors on end studs

A general observation made on all the walls was that tearing of the tabs predominantly caused failure of the wall headers and track around openings as illustrated in Figure 25. In many cases at or beyond maximum load, the entire panel below openings was separated from the wall causing it to hinge on the wall bottom track severely stressing the track as shown in Figure 26 Wall performance might be improved by strengthening the tabs.

Figure 25- Tab tear failure of wall headers and track below openings.

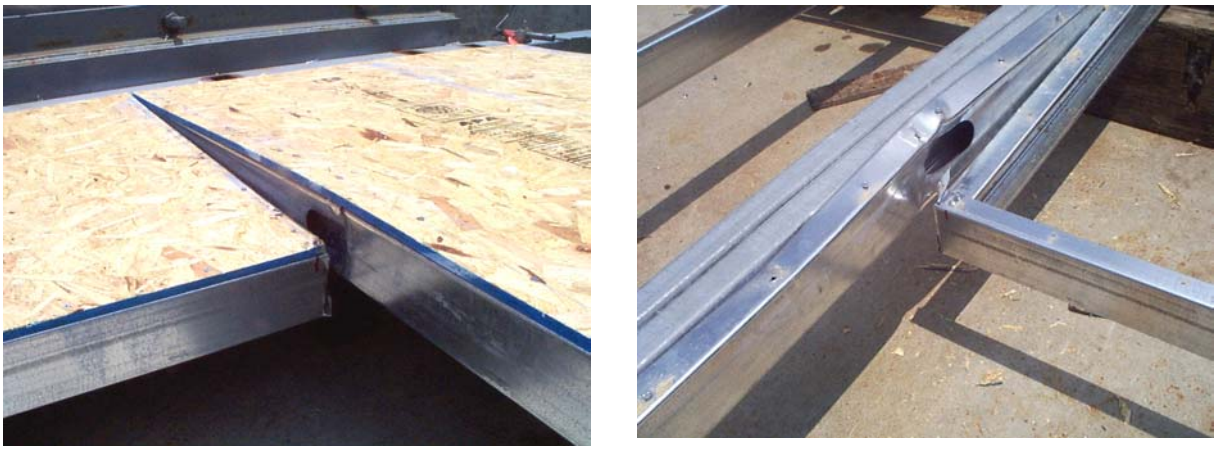

Figure 26 - Hinging of the panel below openings on wall track due to failure of tabs.

In the cases of the walls tested with screws to transmit the shear to the foundation instead of the bolts, the track failed near the maximum load. A typical track failure due to separation of the screws from the steel distribution beam anchored to the foundation is shown in Figure 27. Failure in the walls with gusseting was initiated by the tearing of gussets at the corners. The initial tear happened in the very early stages of the test cycle. A typical failure of walls with gusseting around openings and the propagation of the tear at the corners is shown in Figure 28.

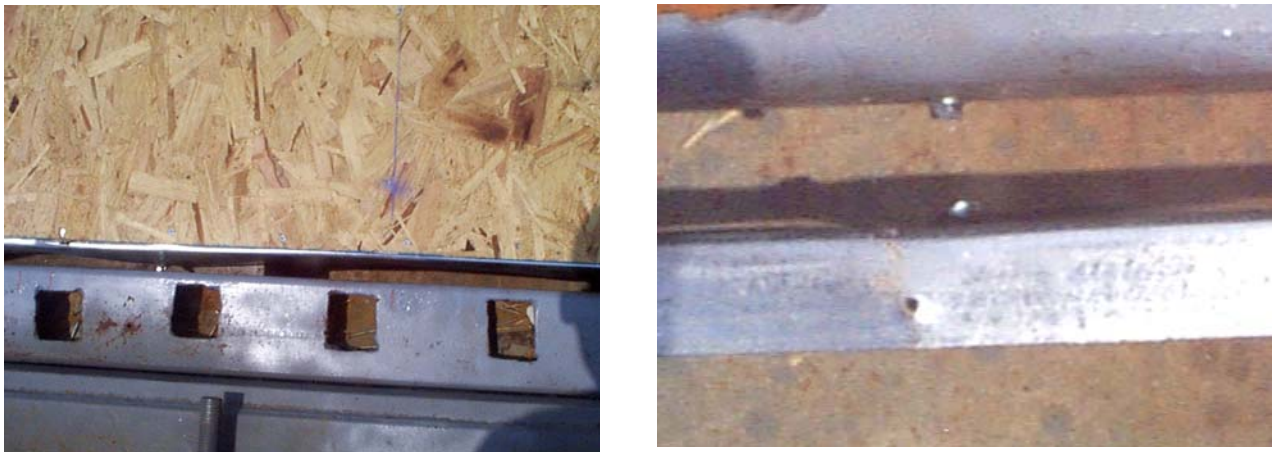

Fgure 27- Seperation of wall track from steel distribution beam.

Figure 28- Failure of walls with gusseting around openings.

Conclusions

Performance for each wall configuration, based on capacity, is illustrated in Table 11. Performance of each configuration is compared to the fully-sheathed wall configuration with equivalent anchorage conditions, except for wall specimen A2hb, which is compared to the fully sheathed condition with full overturning anchorage.

Table 11- various wall configurations tested for the study.

Wall Specimen	Notes
C2ab 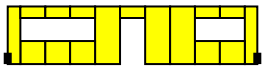	Tested to provide benchmark for performance of walls with 2 ft end wall segments, with full overturning anchorage. Initial Cyclic Performance (Capacity) is essentially equal to performance with 4 ft end wall segments and 50% of fully-sheathed walls with overturning anchors. Stabilized Cyclic Performance (Capacity) is essentially equal to performance with 4 ft end wall segments and 54% of fully-sheathed walls with overturning anchors.
D2ab 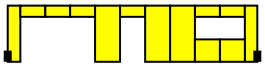	Tested to provide benchmark for performance of walls with 2 ft end wall segments, with full overturning anchorage. Initial Cyclic Performance (Capacity) is essentially equal to performance with 4 ft end wall segments and 46% of fully-sheathed walls with overturning anchors. Stabilized Cyclic Performance (Capacity) is essentially equal to performance with 4 ft end wall segments and 50% of fully-sheathed walls with overturning anchors.
B2gab 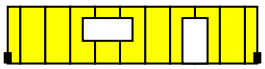	Tested to provide benchmark for performance of gusseting openings with sheathing, with full overturning anchorage Initial Cyclic Performance (Capacity) is essentially equal to performance without gusseted openings and 71% of fully-sheathed walls with overturning anchors. Stabilized Cyclic Performance (Capacity) is essentially equal to performance without gusseted openings and 73% of fully-sheathed walls with overturning anchors.
C2gab 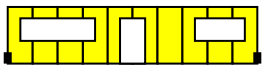	Tested to provide benchmark for performance of gusseting openings with sheathing, with full overturning anchorage Initial Cyclic Performance (Capacity) is essentially equal to performance without gusseted openings with overturning anchors. (62% of full-sheathed) Stabilized Cyclic Performance (Capacity) is essentially equal to performance without gusseted openings with overturning anchors. (65% of fully-sheathed)
D2gab 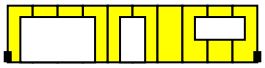	Tested to provide benchmark for performance of gusseting openings with sheathing,2 ft end wall segments, with full overturning anchorage. Initial Cyclic Performance (Capacity) is essentially equal to performance without gusseted openings and with overturning anchors. (30% of full-sheathed) Stabilized Cyclic Performance (Capacity) has not improvement in performance compared to walls without gusseted openings and with overturning anchors. (33% of full-sheathed)
A2hb 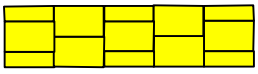	Tested to provide basis for unanchored wall design and check effect of horizontal sheathing. Initial cyclic capacity is 87% of anchored wall with vertical sheathing Stabilized cyclic capacity is 89% of anchored wall with vertical sheathing No shear failure in any horizontal plane
C4b 	Provide benchmark for performance of walls with bolted channels, without overturning anchors. Initial cyclic capacity reduced compared to anchored condition. (84% of anchored condition, 48% of fully-anchored, fully-sheathed condition). Stabilized cyclic capacity reduced compared to anchored condition. (84% of anchored condition and 51% of fully-sheathed, unanchored condition.)
C2gb 	Tested to provide benchmark for performance of gusseting openings with sheathing and 2 ft end wall segments. Small increase in initial capacity compared to standard anchored configuration (16% increase), small reduction compared to anchored and gusseted condition (98%, 67% of fully-sheathed, unanchored condition). Small increase in stabilized capacity compared to standard anchored configuration (15% increase), small reduction compared to anchored and gusseted condition (95%, 51% of fully-sheathed, unanchored condition).

Table 11 (continued) - various wall configurations tested for the study.

Wall Specimen	Notes
D4b 	Provide benchmark for performance of walls with bolted channels, without overturning anchors. Initial cycle performance essentially equal to anchored condition (95%, 47% of fully-sheathed, unanchored condition.) Stabilized cycle performance essentially equal to anchored condition (96%, 50% of fully-sheathed, unanchored condition.)
C4s 	Provide benchmark for performance of walls with screws in channels, without overturning anchors. Significant reduction in initial cycle capacity compared to bolted tracks (79% of bolted tracks) and 66% of standard configuration with overturning anchors, 38% of fully sheathed, unanchored configuration, and 33% of fully-sheathed, anchored configuration. Significant reduction in stabilized cycle capacity compared to bolted tracks (80% of bolted tracks) and 67% of standard configuration with overturning anchors, 40% of fully sheathed, unanchored configuration, and 36% of fully-sheathed, anchored configuration.
D4s 	Provide benchmark for performance of walls with screws in channels, without overturning anchors. Significant reduction in initial cycle capacity compared to bolted tracks (80% of bolted tracks) and 67% of standard configuration with overturning anchors, 33% of fully sheathed, unanchored configuration, and 29% of fully-sheathed, anchored configuration. Significant reduction in stabilized cycle capacity compared to bolted tracks (71% of bolted tracks) and 68% of standard configuration with overturning anchors, 36% of fully sheathed, unanchored configuration, and 32% of fully-sheathed, anchored configuration.

Based on results of the sixteen cyclic tests of 12 m (40 ft.) long steel-frame shear walls with and without openings, the following conclusions were made:

1) Comparison of steel-frame wall resistance with predictions of perforated shear wall method and Sugiyama's equations revealed conservative nature of the predictions at all levels of cyclic loading. With capacity of 12 m (40 ft.) fully sheathed wall taken as a reference, Equation (4) produced the closest estimates in the elastic range. However, the use of Equation (2), as used in the building codes, is more conservative and will provide acceptable prediction of shear wall strength for cyclic loading in cold-formed steel shear walls.

2) The perforated shear wall method is conservative for provided the fully sheathed wall design value is determined using the same overturning anchorage conditions.
3) The initial cycle capacity was 4% - 18% less than the monotonic values for walls with overturning anchors.
4) With the exception of Configuration C with bolts in the track only, cyclic loading resulted in a 1% - 39% reduction in initial cycle capacity.
5) Stabilized cyclic capacity was 11% - 15% lower than the initial cyclic capacity. With the exception of wall configuration C2gab, the stabilized cyclic capacity was 3% - 46% below the monotonic capacity.
6) The fully-sheathed wall was significantly stiffer and stronger but less ductile than walls with openings. This is due to the increased rocking of wall sections in the middle of the wall specimen that were not restrained against overturning.
7) Strength of fully-sheathed walls was affected by cyclic loading to a greater extent than walls with openings. Similar results were observed by Dolan and Johnson (1996b) for wood-framed walls and Salenikovich, et al. (1999) for steel framed walls.
8) The steel-frame walls degraded in abrupt, stepwise manner due to bending of framing elements and pulling heads of sheathing screws through sheathing arbitrarily along the studs or top and bottom tracks. Sometimes, sheathing screws tore through panel edges. Rare cases of fatigue of mechanical connections were observed at the corners of the walls. The randomness of failure locations indicate that the sheathing fasteners share the load uniformly.
9) Based on one specimen, orienting the sheathing horizontally with OSB and gypsum sheathing provided 90% of the strength of a wall with OSB sheathing and overturning anchors for the fully sheathed condition. The orientation with the staggered joints prevented any shear plane occurring in the height of the wall.

10) The effect on strength of shortening the end wall segments from 1.2 to 0.6 m (4 to 2 ft.) on wall performance is negligible.
11) Gusseted sheathing around openings had no effect on capacity of the walls as compared to non-gusseted walls.
12) A reduction in capacity of up to 31% was observed between walls when overturning anchors are eliminated and only bolts are used in the bottom track.
13) A reduction of capacity of up to 34% was observed when screws were used to anchor the walls. A reduction of capacity of up to 29% was observed between walls anchored with screws rather than bolts in the bottom track.
14) Changing the sheathing orientation from vertical to horizontal did not provide sufficient capacity to equal the performance of fully anchored walls. However there are indications that the strength of walls with horizontal sheathing is significantly higher than walls with vertical sheathing when overturning anchors are omitted.
15) The use of screws instead of shear bolts to transmit shear to the foundation reduces the capacity of the wall by 21% - 29%.
16) The use of mechanical tie-down anchors at the ends of the walls increases the capacity of the walls by almost 15% when compared to use of bolts resisting shear in the bottom track only.
17) Tests revealed that the drywall sheathing (gypsum) does not contribute significantly to the strength of the wall under cyclic loading similar observations were made by Salenikovich, et al. (1999) in an earlier study.
18) The stiffness and strength of the walls would be increased if the tear through of the sheathing material and the pull through of the screw head were eliminated or reduced. Improved performance can be achieved by changing the screw head type, or adding reinforcement to the sheathing along the edges.

19) Stiffness of the perforated shear walls would be increased if the track bending stiffness were increased.

20) Stiffness and strength of the perforated shear walls would be increased if connections between the headers and sections of walls below openings were strengthened.

References

1. American Forest & Paper Association (AF&PA), 1995, *Wood Frame Construction Manual for One- and Two- Family Dwellings - SBC High Wind Edition*, American Forest & Paper Association, Washington, D.C.

2. American Society for Testing and Materials, 1995, *Proposed Standard Method for Dynamic Properties of Connections Assembled with Mechanical Fasteners* (*4th Draft*), ASTM, Philadelphia, PA.

3. American Iron and Steel Institute (AISI), 1996, *Builder's Steel Stud Guide*, Publication RG-9607, AISI, Washington, D.C.

4. Dolan, J.D. and A.C. Johnson, 1996a, *Monotonic Tests of Long Shear Walls with Openings*, Virginia Polytechnic Institute and State University Timber Engineering Report TE-1996-001

6. Dolan, J.D. and A.C. Johnson, 1996b, *Cyclic Tests of Long Shear Walls with Openings*. Virginia Polytechnic Institute and State University Timber Engineering Report TE-1996-002

7. Heine, C.P., 1997, *Effect of Overturning Restraint on the Performance of Fully Sheathed and Perforated Timber Framed Shear Walls*, Thesis submitted in partial fulfillment of Master's of Science Degree in Civil Engineering. Virginia Polytechnic Institute and State University, Blacksburg, VA

8. International Code Council, 2000, *International Building Code 2000*, ICC, Falls Church, VA

9. International Conference of Building Officials (ICBO), 1997, *Uniform Building Code*, ICBO, Whitter, CA

10. Johnson, A.C., 1997, *Monotonic and Cyclic Performance of Full-Scale Timber Shear Walls with Openings*, Thesis submitted in partial fulfillment of Master's of Science Degree in Civil Engineering. Virginia Polytechnic Institute and State University, Blacksburg, VA

11. Karacabeyli, E. and A. Ceccotti, 1998. "Nailed Wood-Framed Shear Walls for Seismic Load: Test Results and Design Considerations." *Proceedings of the Structural Engineers World Congress*. San Francisco, CA T207-6.

12. Krawinkler, Helmut, Francisco Parisi, Luis Ibarra, Ashraf Ayoub, Ricardo Medina, 2000. *Development of a Testing Protocol for Wood Frame Structures*, Report submitted to the California Universities for Research in Earthquake Engineering. 74 pp.

13. Patton-Mallory, M., Gutkowski, R.M., and Soltis, L.A., 1984, *Racking Performance of Light-Frame Walls Sheathed on Two Sides,* Research paper FPL 448, USDA Forest Service, Forest Products Laboratory, Madison, WI

14. Porter, M.L., 1987, "Sequential Phased Displacement (SPD) Procedure for TCCMAR Testing." *Proceedings of the Third Meeting of the Joint Technical Coordinating Committee on Masonry Research*, U.S. - Japan Coordinated Earthquake Research Program, Tomamu, Japan.

15. Salenikovich, A.J., Dolan, J.D. and Easterling, W.S., 1999, *Monotonic and CyclicTests of Long Shear Walls with Openings*, Virginia Polytechnic Institute and State University Timber Engineering Report TE-1999-001.

16. Serrette, R., G. Hall, and J. Ngyen, 1996, *Shear Wall Values for Light-Weight Steel Framing*. Research Report prepared for American Iron and Steel Institute, Washington, D.C. 56pp.

17. Serrette, R., 1997, *Additional Shear Wall Values for Light Weight Steel Framing*. Research Report No. LGSRG-1-97 Research Report prepared for American Iron and Steel Institute, Washington, D.C. 78pp.

18. *Standard Building Code*, 1994 with 1996 Revisions, Southern Building Code Congress International, Birmingham, AL

19. Structural Engineers Association of Southern California (SEAOSC), 1997, *Standard Method of Cyclic (Reversed) Load Tests for Shear Resistance of Framed Walls for Buildings*, SEAOSC, Whitter, CA.

20. Sugiyama, H. and T. Matsumoto, 1993, "A Simplified Method of Calculating the Shear Strength of a Plywood-Sheathed Wall with Openings II. Analysis of the Shear Resistance and Deformation of a Shear Wall with Openings", *Mokuzai Gakkaishi*, 39(8): 924-929.

21. Sugiyiama, H. and T. Matsumoto, 1994, "Empirical Equations for the Estimation of Racking Strength of a Plywood-Sheathed Shear Wall with Openings." *Transactions of the Architectural Institute of Japan*.

22. Yasumura, M. and H. Sugiyama, 1984, "Shear properties of plywood-sheathed wall panels with opening." *Transactions of the Architectural Institute of Japan*, 338(4), 88-98

APPENDIX A

Table A1. - Specimen **A2hb1**

Specimen	**A2hb1**	For total length		
Ratio	1.00	**cyclic**		
Full-height length		**40 ft.**	**12.19 m**	
		units	**initial**	**stabilized**
Peak load, F_{peak}		Kips	23.324	19.256
		KN	103.745	85.648
Drift at peak load, Δ_{peak}		in.	1.009	0.904
		mm	25.64	22.96
Yield load, F_{yield}		Kips	20.834	17.205
		KN	92.671	76.527
Drift at yield load, Δ_{yield}		in.	0.404	0.341
		mm	10.25	8.66
Proportional limit, $0.4F_{max}$		Kips	9.330	7.702
		KN	41.498	34.259
Drift at prop. limit, $\Delta@0.4F_{max}$		in.	0.181	0.153
		mm	4.59	3.88
Failure load or $0.8F_{max}$		Kips	18.659	15.404
		KN	82.996	68.519
Drift at failure, $\Delta_{failure}$		in.	1.399	1.326
		mm	35.53	33.67
Elastic stiffness, E $@0.4F_{max}$		Kip/in.	51.623	50.471
		KN/mm	9.040	8.838
Work until failure		Kip·ft.	16.449	19.285
		KN·m	22.301	26.146
Load @ .32 in.		Kips	14.463	13.069
Load @ .48 in.		Kips	17.910	15.736
Load @ .96 in.		Kips	23.141	18.936
Load @ 1.6 in.		Kips	15.998	13.466
$D = \Delta_{failure}/\Delta_{yield}$			3.465	3.888
$C_d^* = \Delta_{peak}/\Delta_{elastic}$			1.892	1.695
$R_d = \Delta_{peak}/\Delta_{yield}$			2.501	2.656
$R_d^* = \Delta_{design}/\Delta_{yield}$			2.501	2.656
$\Delta_{failure}/\Delta_{peak}$			1.386	1.487
$\zeta_{eq} = W_D/U_0/4\pi$			0.090	0.063

Note: ζ_{eq} at F_{max}

Code	***Schematic***	*Wall type*
A2hb1	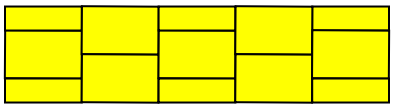	Horizontal staggered-sheathing with dry wall, shear bolts at 2 feet, no tie-down anchors

Table A2. - Specimen **B2gab1**

Specimen	**B2gab1**	For total length		
Ratio	0.76	**cyclic**		
Full-height length		**28 ft.**	**8.534 m**	
		units	**initial**	**stabilized**
Peak load, F_{peak}		Kips	18.866	15.939
		KN	83.916	70.897
Drift at peak load, Δ_{peak}		in.	1.109	1.008
		mm	28.17	25.60
Yield load, F_{yield}		Kips	17.093	14.420
		KN	76.030	64.141
Drift at yield load, Δ_{yield}		in.	0.410	0.340
		mm	10.41	8.65
Proportional limit, $0.4F_{max}$		Kips	7.546	6.376
		KN	33.566	28.359
Drift at prop. limit, $\Delta@0.4F_{max}$		in.	0.181	0.150
		mm	4.59	3.81
Failure load or $0.8F_{max}$		Kips	15.093	12.751
		KN	67.133	56.717
Drift at failure, $\Delta_{failure}$		in.	2.113	1.955
		mm	53.66	49.66
Elastic stiffness, E $@0.4F_{max}$		Kip/in.	43.173	44.171
		KN/mm	7.560	7.735
Work until failure		Kip·ft.	31.962	30.836
		KN·m	43.332	41.806
Load @ .32 in.		Kips	11.316	10.414
Load @ .48 in.		Kips	14.130	12.620
Load @ .96 in.		Kips	18.606	15.830
Load @ 1.6 in.		Kips	17.281	15.216
$D = \Delta_{failure}/\Delta_{yield}$			5.321	5.961
$C_d^* = \Delta_{peak}/\Delta_{elastic}$			2.079	1.890
$R_d = \Delta_{peak}/\Delta_{yield}$			2.757	3.085
$R_d^* = \Delta_{design}/\Delta_{yield}$			2.757	3.085
$\Delta_{failure}/\Delta_{peak}$			1.917	1.940
$\zeta_{eq} = W_D/U_0/4\pi$			0.090	0.069

Note: ζ_{eq} at F_{max}

Code	***Schematic***	*Wall type*
B2gab1	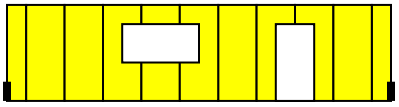	**2** foot end wall , Gusseted sheathing Shear bolts at 2 feet, With tie-down anchor

Table A3 - Specimen **C2ab1**

Specimen	**C2ab1**	For total length		
Ratio	0.56	**cyclic**		
Full-height length		**16 ft.**	**4.876 m**	
		units	**initial**	**stabilized**
Peak load, F_{peak}		Kips	13.602	11.722
		KN	60.504	52.139
Drift at peak load, Δ_{peak}		in.	1.207	1.103
		mm	30.66	28.02
Yield load, F_{yield}		Kips	12.059	10.201
		KN	53.637	45.376
Drift at yield load, Δ_{yield}		in.	0.561	0.491
		mm	14.24	12.48
Proportional limit, $0.4F_{max}$		Kips	5.441	4.689
		KN	24.202	20.856
Drift at prop. limit, $\Delta@0.4F_{max}$		in.	0.253	0.226
		mm	6.43	5.74
Failure load or $0.8F_{max}$		Kips	10.882	9.378
		KN	48.403	41.712
Drift at failure, $\Delta_{failure}$		in.	1.531	1.492
		mm	38.89	37.90
Elastic stiffness, E $@0.4F_{max}$		Kip/in.	21.641	20.983
		KN/mm	3.790	3.674
Work until failure		Kip·ft.	12.163	11.536
		KN·m	16.491	15.640
Load @ .32 in.		Kips	6.493	6.088
Load @ .48 in.		Kips	8.445	7.817
Load @ .96 in.		Kips	12.741	11.239
Load @ 1.6 in.		Kips	10.330	9.207
$D = \Delta_{failure}/\Delta_{yield}$			2.749	3.097
$C_d^* = \Delta_{peak}/\Delta_{elastic}$			2.263	2.068
$R_d = \Delta_{peak}/\Delta_{yield}$			2.167	2.251
$R_d^* = \Delta_{design}/\Delta_{yield}$			2.167	2.251
$\Delta_{failure}/\Delta_{peak}$			1.268	1.371
$\zeta_{eq} = W_D/U_0/4\pi$			0.081	0.065

Note: ζ_{eq} at F_{max}

Code	***Schematic***	*Wall type*
C2ab1	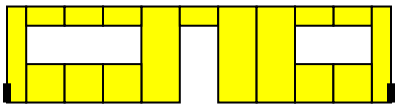	**2** foot end wall , Shear bolts at 2 feet, With tie-down anchor

Table A4 - Specimen **C2gab1**

Specimen	**C2gab1**	For total length		
Ratio	0.56	**cyclic**		
Full-height length		**16 ft.**	**4.876 m**	
		units	**initial**	**stabilized**
Peak load, F_{peak}		Kips	16.717	14.207
		KN	74.359	63.191
Drift at peak load, Δ_{peak}		in.	1.305	1.204
		mm	33.15	30.58
Yield load, F_{yield}		Kips	15.202	13.118
		KN	67.618	58.349
Drift at yield load, Δ_{yield}		in.	0.485	0.415
		mm	12.32	10.54
Proportional limit, $0.4F_{max}$		Kips	6.687	5.683
		KN	29.744	25.276
Drift at prop. limit, $\Delta@0.4F_{max}$		in.	0.213	0.180
		mm	5.42	4.57
Failure load or $0.8F_{max}$		Kips	13.374	11.365
		KN	59.488	50.552
Drift at failure, $\Delta_{failure}$		in.	2.077	1.976
		mm	52.77	50.19
Elastic stiffness, E $@0.4F_{max}$		Kip/in.	31.367	31.619
		KN/mm	5.493	5.537
Work until failure		Kip·ft.	27.623	26.669
		KN·m	37.450	36.156
Load @ .32 in.		Kips	9.055	8.605
Load @ .48 in.		Kips	11.681	10.800
Load @ .96 in.		Kips	15.897	13.875
Load @ 1.6 in.		Kips	15.871	13.800
$D = \Delta_{failure}/\Delta_{yield}$			4.285	4.763
$C_d^* = \Delta_{peak}/\Delta_{elastic}$			2.447	2.258
$R_d = \Delta_{peak}/\Delta_{yield}$			2.690	2.902
$R_d^* = \Delta_{design}/\Delta_{yield}$			2.690	2.902
$\Delta_{failure}/\Delta_{peak}$			1.601	1.641
$\zeta_{eq} = W_D/U_0/4\pi$			0.079	0.063

Note: ζ_{eq} at F_{max}

Code	***Schematic***	***Wall type***
C2gab1	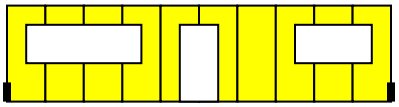	**2** foot end wall , Gusseted sheathing Shear bolts at 2 feet, With tie-down anchor

Table A5 - Specimen **C2gb1**

Specimen	**C2gb1**	For total length		
Ratio	0.56	**cyclic**		
Full-height length		**16 ft.**	**4.876 m**	
		units	**initial**	**stabilized**
Peak load, F_{peak}		Kips	15.549	13.508
		KN	69.164	60.084
Drift at peak load, Δ_{peak}		in.	1.504	1.405
		mm	38.21	35.68
Yield load, F_{yield}		Kips	14.112	12.148
		KN	62.771	54.033
Drift at yield load, Δ_{yield}		in.	0.509	0.435
		mm	12.92	11.05
Proportional limit, $0.4F_{max}$		Kips	6.220	5.403
		KN	27.666	24.033
Drift at prop. limit, $\Delta@0.4F_{max}$		in.	0.224	0.193
		mm	5.69	4.91
Failure load or $0.8F_{max}$		Kips	12.440	10.806
		KN	55.331	48.067
Drift at failure, $\Delta_{failure}$		in.	2.370	2.214
		mm	60.19	56.24
Elastic stiffness, E $@0.4F_{max}$		Kip/in.	28.033	28.297
		KN/mm	4.909	4.955
Work until failure		Kip·ft.	35.860	34.807
		KN·m	48.618	47.190
Load @ .32 in.		Kips	8.181	7.794
Load @ .48 in.		Kips	10.606	9.735
Load @ .96 in.		Kips	14.800	12.912
Load @ 1.6 in.		Kips	14.641	13.185
$D = \Delta_{failure}/\Delta_{yield}$			4.674	5.106
$C_d^* = \Delta_{peak}/\Delta_{elastic}$			2.821	2.634
$R_d = \Delta_{peak}/\Delta_{yield}$			2.930	3.215
$R_d^* = \Delta_{design}/\Delta_{yield}$			2.930	3.215
$\Delta_{failure}/\Delta_{peak}$			1.623	1.595
$\zeta_{eq} = W_D/U_0/4\pi$			0.081	0.066

Note: ζ_{eq} at F_{max}

Code	***Schematic***	*Wall type*
C2gb1	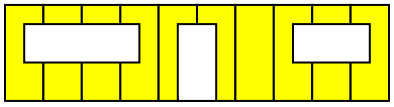	**2** foot end wall , Gusseted sheathing Shear bolts at 2 feet, No tie-down anchor

Table A6 - Specimen **C4b1**

Specimen	**C4b1**	For total length		
Ratio	0.56	**cyclic**		
Full-height length		**16 ft.**	**4.876 m**	
		units	**initial**	**stabilized**
Peak load, F_{peak}		Kips	10.984	9.789
		KN	48.857	43.541
Drift at peak load, Δ_{peak}		in.	1.412	1.600
		mm	35.87	40.63
Yield load, F_{yield}		Kips	9.436	8.319
		KN	41.970	37.002
Drift at yield load, Δ_{yield}		in.	0.822	0.747
		mm	20.89	18.99
Proportional limit, $0.4F_{max}$		Kips	4.394	3.916
		KN	19.543	17.417
Drift at prop. limit, $\Delta@0.4F_{max}$		in.	0.383	0.353
		mm	9.72	8.95
Failure load or $0.8F_{max}$		Kips	10.003	9.789
		KN	44.496	43.541
Drift at failure, $\Delta_{failure}$		in.	1.551	1.600
		mm	39.40	40.63
Elastic stiffness, E $@0.4F_{max}$		Kip/in.	11.478	11.289
		KN/mm	2.010	1.977
Work until failure		Kip·ft.	8.537	10.608
		KN·m	11.574	14.382
Load @ .32 in.		Kips	3.883	3.661
Load @ .48 in.		Kips	5.195	4.880
Load @ .96 in.		Kips	8.699	7.821
Load @ 1.6 in.		Kips	10.319	9.805
$D = \Delta_{failure}/\Delta_{yield}$			1.887	2.157
$C_d^* = \Delta_{peak}/\Delta_{elastic}$			2.648	2.999
$R_d = \Delta_{peak}/\Delta_{yield}$			1.717	2.157
$R_d^* = \Delta_{design}/\Delta_{yield}$			1.717	2.157
$\Delta_{failure}/\Delta_{peak}$			1.099	1.000
$\zeta_{eq} = W_D/U_0/4\pi$			0.074	0.064

NOTE: There was machine failure during test (but critical value had been passed) all data not utilized for tabulating test results.

Note: ζ_{eq} at F_{max}

Code	***Schematic***	*Wall type*
C4b1	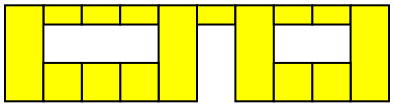	4 foot end wall , 2 shear bolts at 2 feet , No tie-down anchor

Table A7 - Specimen **C4b2**

Specimen	**C4b2**	For total length		
Ratio	0.56	**cyclic**		
Full-height length		**16 ft.**	**4.876 m**	
		units	**initial**	**stabilized**
Peak load, F_{peak}		Kips	12.475	10.931
		KN	55.487	48.619
Drift at peak load, Δ_{peak}		in.	2.017	1.819
		mm	51.23	46.21
Yield load, F_{yield}		Kips	11.357	9.962
		KN	50.516	44.311
Drift at yield load, Δ_{yield}		in.	0.982	0.891
		mm	24.95	22.64
Proportional limit, $0.4F_{max}$		Kips	4.990	4.372
		KN	22.195	19.448
Drift at prop. limit, $\Delta@0.4F_{max}$		in.	0.432	0.391
		mm	10.97	9.94
Failure load or $0.8F_{max}$		Kips	9.980	8.744
		KN	44.389	38.895
Drift at failure, $\Delta_{failure}$		in.	3.170	3.179
		mm	80.53	80.75
Elastic stiffness, E $@0.4F_{max}$		Kip/in.	11.567	11.178
		KN/mm	2.026	1.957
Work until failure		Kip·ft.	41.195	49.753
		KN·m	55.851	67.453
Load @ .32 in.		Kips	3.958	3.760
Load @ .48 in.		Kips	5.419	5.049
Load @ .96 in.		Kips	9.321	8.314
Load @ 1.6 in.		Kips	11.836	10.485
$D = \Delta_{failure}/\Delta_{yield}$			3.225	3.567
$C_d^* = \Delta_{peak}/\Delta_{elastic}$			3.782	3.411
$R_d = \Delta_{peak}/\Delta_{yield}$			2.050	2.039
$R_d^* = \Delta_{design}/\Delta_{yield}$			2.050	2.039
$\Delta_{failure}/\Delta_{peak}$			1.580	1.774
$\zeta_{eq} = W_D/U_0/4\pi$			0.071	0.063

Note: ζ_{eq} at F_{max}

Code	***Schematic***	*Wall type*
C4b2	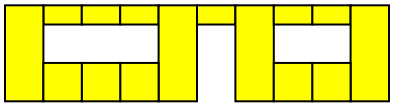	4 foot end wall , 2 shear bolts at 2 feet , No tie-down anchor

Table A8 - Specimen **C4b3**

Specimen	**C4b3**	For total length		
Ratio	0.56	**cyclic**		
Full-height length		**16 ft.**	**4.876 m**	
		units	**initial**	**stabilized**
Peak load, F_{peak}		Kips	9.976	8.688
		KN	44.375	38.642
Drift at peak load, Δ_{peak}		in.	1.771	1.879
		mm	44.98	47.74
Yield load, F_{yield}		Kips	9.152	7.879
		KN	40.706	35.044
Drift at yield load, Δ_{yield}		in.	0.897	0.783
		mm	22.77	19.89
Proportional limit, $0.4F_{max}$		Kips	3.991	3.475
		KN	17.750	15.457
Drift at prop. limit, $\Delta@0.4F_{max}$		in.	0.391	0.346
		mm	9.92	8.78
Failure load or $0.8F_{max}$		Kips	7.981	6.950
		KN	35.500	30.914
Drift at failure, $\Delta_{failure}$		in.	2.948	2.982
		mm	74.89	75.74
Elastic stiffness, E $@0.4F_{max}$		Kip/in.	10.232	10.082
		KN/mm	1.792	1.766
Work until failure		Kip·ft.	26.158	28.720
		KN·m	35.463	38.938
Load @ .32 in.		Kips	3.537	3.312
Load @ .48 in.		Kips	4.667	4.354
Load @ .96 in.		Kips	8.045	7.257
Load @ 1.6 in.		Kips	9.467	8.338
$D = \Delta_{failure}/\Delta_{yield}$			3.305	3.812
$C_d^* = \Delta_{peak}/\Delta_{elastic}$			3.321	3.524
$R_d = \Delta_{peak}/\Delta_{yield}$			1.960	2.372
$R_d^* = \Delta_{design}/\Delta_{yield}$			1.960	2.372
$\Delta_{failure}/\Delta_{peak}$			1.717	1.655
$\zeta_{eq} = W_D/U_0/4\pi$			0.073	0.060

Note: ζ_{eq} at F_{max}

Code	***Schematic***	*Wall type*
C4b3	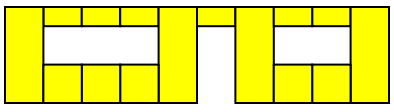	4 foot end wall , 2 shear bolts at 2 feet , No tie-down anchor

Table A9 - Specimen **C4s1**

Specimen	**C4s1**	For total length		
Ratio	0.56	**cyclic**		
Full-height length		**16 ft.**	**4.876 m**	
		units	**initial**	**stabilized**
Peak load, F_{peak}		Kips	8.889	7.855
		KN	39.538	34.939
Drift at peak load, Δ_{peak}		in.	1.976	1.770
		mm	50.19	44.95
Yield load, F_{yield}		Kips	8.096	7.139
		KN	36.011	31.754
Drift at yield load, Δ_{yield}		in.	0.876	0.798
		mm	22.24	20.28
Proportional limit, $0.4F_{max}$		Kips	3.556	3.142
		KN	15.815	13.976
Drift at prop. limit, $\Delta@0.4F_{max}$		in.	0.385	0.351
		mm	9.77	8.92
Failure load or $0.8F_{max}$		Kips	7.111	6.284
		KN	31.631	27.951
Drift at failure, $\Delta_{failure}$		in.	3.436	3.552
		mm	87.27	90.22
Elastic stiffness, E $@0.4F_{max}$		Kip/in.	9.245	8.946
		KN/mm	1.619	1.567
Work until failure		Kip·ft.	25.636	31.201
		KN·m	34.757	42.301
Load @ .32 in.		Kips	3.110	2.936
Load @ .48 in.		Kips	4.226	3.975
Load @ .96 in.		Kips	6.969	6.387
Load @ 1.6 in.		Kips	8.127	7.428
$D = \Delta_{failure}/\Delta_{yield}$			3.937	4.466
$C_d^* = \Delta_{peak}/\Delta_{elastic}$			3.705	3.318
$R_d = \Delta_{peak}/\Delta_{yield}$			2.260	2.223
$R_d^* = \Delta_{design}/\Delta_{yield}$			2.260	2.223
$\Delta_{failure}/\Delta_{peak}$			1.731	2.003
$\zeta_{eq} = W_D/U_0/4\pi$			0.067	0.058

Note: ζ_{eq} at F_{max}

Code	***Schematic***	***Wall type***
C4s1	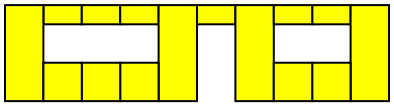	4 foot end wall , 2 screws to transmit shear as every 1 foot No tie- down anchors

Table A10 - Specimen **C4s2**

Specimen	**C4s2**	For total length		
Ratio	0.56	**cyclic**		
Full-height length		**16 ft.**	**4.876 m**	
		units	**initial**	**stabilized**
Peak load, F_{peak}		Kips	8.701	7.842
		KN	38.702	34.881
Drift at peak load, Δ_{peak}		in.	2.194	1.989
		mm	55.74	50.53
Yield load, F_{yield}		Kips	7.859	6.791
		KN	34.957	30.206
Drift at yield load, Δ_{yield}		in.	0.883	0.782
		mm	22.42	19.86
Proportional limit, $0.4F_{max}$		Kips	3.480	3.137
		KN	15.481	13.952
Drift at prop. limit, $\Delta@0.4F_{max}$		in.	0.391	0.361
		mm	9.93	9.18
Failure load or $0.8F_{max}$		Kips	6.961	6.274
		KN	30.962	27.905
Drift at failure, $\Delta_{failure}$		in.	2.979	3.158
		mm	75.67	80.21
Elastic stiffness, E $@0.4F_{max}$		Kip/in.	8.912	8.692
		KN/mm	1.561	1.522
Work until failure		Kip·ft.	23.840	32.400
		KN·m	32.322	43.927
Load @ .32 in.		Kips	3.071	2.905
Load @ .48 in.		Kips	4.074	3.831
Load @ .96 in.		Kips	7.026	6.139
Load @ 1.6 in.		Kips	7.538	6.850
$D = \Delta_{failure}/\Delta_{yield}$			3.381	4.061
$C_d^* = \Delta_{peak}/\Delta_{elastic}$			4.114	3.730
$R_d = \Delta_{peak}/\Delta_{yield}$			2.475	2.530
$R_d^* = \Delta_{design}/\Delta_{yield}$			2.410	2.530
$\Delta_{failure}/\Delta_{peak}$			1.389	1.654
$\zeta_{eq} = W_D/U_0/4\pi$			0.063	0.053

Note: ζ_{eq} at F_{max}

Code	***Schematic***	***Wall type***
C4s2	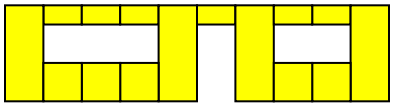	4 foot end wall , 2 screws to transmit shear as every 1 foot No tie- down anchors

Table A11 - Specimen **D2ab1**

Specimen	**D2ab1**	For total length		
Ratio	0.48	**cyclic**		
Full-height length		**16 ft.**	**4.876 m**	
		units	**initial**	**stabilized**
Peak load, F_{peak}		Kips	12.717	11.252
		KN	56.563	50.051
Drift at peak load, Δ_{peak}		in.	1.604	1.718
		mm	40.74	43.64
Yield load, F_{yield}		Kips	11.490	9.986
		KN	51.107	44.416
Drift at yield load, Δ_{yield}		in.	0.698	0.631
		mm	17.72	16.02
Proportional limit, $0.4F_{max}$		Kips	5.087	4.501
		KN	22.625	20.020
Drift at prop. limit, $\Delta@0.4F_{max}$		in.	0.308	0.284
		mm	7.83	7.22
Failure load or $0.8F_{max}$		Kips	10.173	9.002
		KN	45.250	40.041
Drift at failure, $\Delta_{failure}$		in.	2.440	2.238
		mm	61.97	56.84
Elastic stiffness, E $@0.4F_{max}$		Kip/in.	16.727	16.054
		KN/mm	2.929	2.811
Work until failure		Kip·ft.	24.348	23.438
		KN·m	33.010	31.776
Load @ .32 in.		Kips	5.233	4.936
Load @ .48 in.		Kips	6.870	6.330
Load @ .96 in.		Kips	10.897	9.679
Load @ 1.6 in.		Kips	12.235	11.182
$D = \Delta_{failure}/\Delta_{yield}$			3.556	3.602
$C_d^* = \Delta_{peak}/\Delta_{elastic}$			3.007	3.222
$R_d = \Delta_{peak}/\Delta_{yield}$			2.367	2.776
$R_d^* = \Delta_{design}/\Delta_{yield}$			2.367	2.776
$\Delta_{failure}/\Delta_{peak}$			1.541	1.305
$\zeta_{eq} = W_D/U_0/4\pi$			0.077	0.063

Note: ζ_{eq} at F_{max}

Code	***Schematic***	***Wall type***
D2ab1	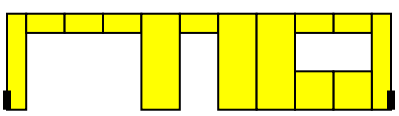	**2** foot end wall , Shear bolts at 2 feet , With tie-down anchor

Table A12- Specimen **D2ab2**

Specimen	**D2ab2**	For total length		
Ratio	0.48	**cyclic**		
Full-height length		**16 ft.**	**4.876 m**	
		units	**initial**	**stabilized**
Peak load, F_{peak}		Kips	12.193	10.393
		KN	54.232	46.228
Drift at peak load, Δ_{peak}		in.	1.409	1.298
		mm	35.79	32.97
Yield load, F_{yield}		Kips	10.719	9.174
		KN	47.677	40.807
Drift at yield load, Δ_{yield}		in.	0.656	0.576
		mm	16.66	14.64
Proportional limit, $0.4F_{max}$		Kips	4.877	4.157
		KN	21.693	18.491
Drift at prop. limit, $\Delta@0.4F_{max}$		in.	0.299	0.261
		mm	7.58	6.64
Failure load or $0.8F_{max}$		Kips	9.754	8.314
		KN	43.386	36.982
Drift at failure, $\Delta_{failure}$		in.	1.973	1.818
		mm	50.12	46.17
Elastic stiffness, E $@0.4F_{max}$		Kip/in.	16.398	15.978
		KN/mm	2.872	2.798
Work until failure		Kip·ft.	16.008	18.087
		KN·m	21.703	24.521
Load @ .32 in.		Kips	5.184	4.938
Load @ .48 in.		Kips	6.921	6.383
Load @ .96 in.		Kips	10.641	9.465
Load @ 1.6 in.		Kips	11.619	9.608
$D = \Delta_{failure}/\Delta_{yield}$			3.012	3.159
$C_d^* = \Delta_{peak}/\Delta_{elastic}$			2.642	2.433
$R_d = \Delta_{peak}/\Delta_{yield}$			2.152	2.249
$R_d^* = \Delta_{design}/\Delta_{yield}$			2.152	2.249
$\Delta_{failure}/\Delta_{peak}$			1.400	1.407
$\zeta_{eq} = W_D/U_0/4\pi$			0.076	0.063

Note: ζ_{eq} at F_{max}

Code	***Schematic***	***Wall type***
D2ab2	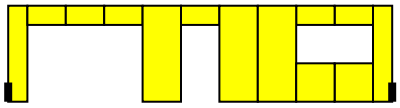	**2** foot end wall , Shear bolts at 2 feet , With tie-down anchor

Table A13 - Specimen **D2gab1**

Specimen	**D2gab1**	For total length		
Ratio	0.48	**cyclic**		
Full-height length		**16 ft.**	**4.876 m**	
		units	**initial**	**stabilized**
Peak load, F_{peak}		Kips	8.043	7.063
		KN	35.777	31.416
Drift at peak load, Δ_{peak}		in.	1.006	1.006
		mm	25.56	25.56
Yield load, F_{yield}		Kips	7.251	6.319
		KN	32.253	28.106
Drift at yield load, Δ_{yield}		in.	0.398	0.346
		mm	10.10	8.79
Proportional limit, $0.4F_{max}$		Kips	3.217	2.825
		KN	14.311	12.566
Drift at prop. limit, $\Delta@0.4F_{max}$		in.	0.177	0.155
		mm	4.48	3.93
Failure load or $0.8F_{max}$		Kips	6.435	5.650
		KN	28.622	25.133
Drift at failure, $\Delta_{failure}$		in.	2.823	3.136
		mm	71.71	79.65
Elastic stiffness, E $@0.4F_{max}$		Kip/in.	18.316	18.300
		KN/mm	3.207	3.205
Work until failure		Kip·ft.	29.050	38.646
		KN·m	39.385	52.395
Load @ .32 in.		Kips	4.751	4.447
Load @ .48 in.		Kips	5.875	5.374
Load @ .96 in.		Kips	7.926	6.975
Load @ 1.6 in.		Kips	7.260	6.670
$D = \Delta_{failure}/\Delta_{yield}$			7.130	9.085
$C_d^* = \Delta_{peak}/\Delta_{elastic}$			1.887	1.887
$R_d = \Delta_{peak}/\Delta_{yield}$			2.539	2.912
$R_d^* = \Delta_{design}/\Delta_{yield}$			2.539	2.912
$\Delta_{failure}/\Delta_{peak}$			2.805	3.116
$\zeta_{eq} = W_D/U_0/4\pi$			0.093	0.073

Note: ζ_{eq} at F_{max}

Code	***Schematic***	***Wall type***
D2gab1	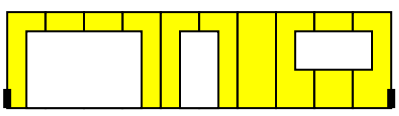	**2** foot end wall , Gusseted sheathing Shear bolts at 2 feet , With tie-down anchor

Table A14 - Specimen **D4b1**

Specimen	**D4b1**	For total length		
Ratio	0.48	**cyclic**		
Full-height length		**16 ft.**	**4.876 m**	
		units	**initial**	**stabilized**
Peak load, F_{peak}		Kips	11.038	9.668
		KN	49.097	43.003
Drift at peak load, Δ_{peak}		in.	2.331	2.128
		mm	59.20	54.06
Yield load, F_{yield}		Kips	9.881	8.835
		KN	43.949	39.299
Drift at yield load, Δ_{yield}		in.	1.124	1.047
		mm	28.56	26.59
Proportional limit, $0.4F_{max}$		Kips	4.415	3.867
		KN	19.639	17.201
Drift at prop. limit, $\Delta@0.4F_{max}$		in.	0.504	0.459
		mm	12.79	11.66
Failure load or $0.8F_{max}$		Kips	9.171	8.540
		KN	40.793	37.986
Drift at failure, $\Delta_{failure}$		in.	4.025	4.135
		mm	102.25	105.04
Elastic stiffness, E $@0.4F_{max}$		Kip/in.	8.834	8.484
		KN/mm	1.547	1.486
Work until failure		Kip·ft.	55.035	59.018
		KN·m	74.613	80.014
Load @ .32 in.		Kips	3.154	3.022
Load @ .48 in.		Kips	4.269	4.033
Load @ .96 in.		Kips	7.849	7.139
Load @ 1.6 in.		Kips	9.686	8.917
$D = \Delta_{failure}/\Delta_{yield}$			3.593	3.970
$C_d^* = \Delta_{peak}/\Delta_{elastic}$			4.370	3.991
$R_d = \Delta_{peak}/\Delta_{yield}$			2.074	2.035
$R_d^* = \Delta_{design}/\Delta_{yield}$			2.057	2.035
$\Delta_{failure}/\Delta_{peak}$			1.731	1.950
$\zeta_{eq} = W_D/U_0/4\pi$			0.069	0.062

Note: ζ_{eq} at F_{max}

Code	***Schematic***	***Wall type***
D4b1	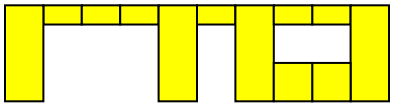	4 foot end wall , 2 shear bolts at 2 feet , No tie-down anchor

Table A15 - Specimen **D4b2**

Specimen	**D4b2**	For total length		
Ratio	0.48	**cyclic**		
Full-height length		**16 ft.**	**4.876 m**	
		units	**initial**	**stabilized**
Peak load, F_{peak}		Kips	10.729	9.427
		KN	47.723	41.929
Drift at peak load, Δ_{peak}		in.	2.013	1.802
		mm	51.12	45.76
Yield load, F_{yield}		Kips	9.807	8.733
		KN	43.623	38.845
Drift at yield load, Δ_{yield}		in.	0.960	0.876
		mm	24.39	22.25
Proportional limit, $0.4F_{max}$		Kips	4.292	3.771
		KN	19.089	16.772
Drift at prop. limit, $\Delta@0.4F_{max}$		in.	0.420	0.378
		mm	10.67	9.60
Failure load or $0.8F_{max}$		Kips	8.623	7.990
		KN	38.356	35.538
Drift at failure, $\Delta_{failure}$		in.	3.973	4.025
		mm	100.93	102.23
Elastic stiffness, E $@0.4F_{max}$		Kip/in.	10.232	9.981
		KN/mm	1.792	1.748
Work until failure		Kip·ft.	52.483	56.085
		KN·m	71.154	76.037
Load @ .32 in.		Kips	3.452	3.299
Load @ .48 in.		Kips	4.871	4.631
Load @ .96 in.		Kips	8.572	7.720
Load @ 1.6 in.		Kips	10.087	9.301
$D = \Delta_{failure}/\Delta_{yield}$			4.154	4.615
$C_d^* = \Delta_{peak}/\Delta_{elastic}$			3.774	3.378
$R_d = \Delta_{peak}/\Delta_{yield}$			2.116	2.073
$R_d^* = \Delta_{design}/\Delta_{yield}$			2.116	2.073
$\Delta_{failure}/\Delta_{peak}$			1.993	2.253
$\zeta_{eq} = W_D/U_0/4\pi$			0.069	0.059

Note: ζ_{eq} at F_{max}

Code	*Schematic*	*Wall type*
D4b2	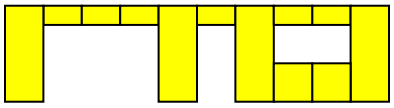	4 foot end wall , 2 shear bolts at 2 feet , No tie-down anchor

Table A16 - Specimen **D4s1**

Specimen	**D4s1**	For total length		
Ratio	0.48	**cyclic**		
Full-height length		**16 ft.**	**4.876 m**	
		units	**initial**	**stabilized**
Peak load, F_{peak}		Kips	7.587	6.848
		KN	33.747	30.460
Drift at peak load, Δ_{peak}		in.	1.976	1.982
		mm	50.19	50.34
Yield load, F_{yield}		Kips	6.868	6.064
		KN	30.548	26.973
Drift at yield load, Δ_{yield}		in.	1.023	0.938
		mm	25.99	23.82
Proportional limit, $0.4F_{max}$		Kips	3.035	2.739
		KN	13.499	12.184
Drift at prop. limit, $\Delta@0.4F_{max}$		in.	0.452	0.424
		mm	11.47	10.77
Failure load or $0.8F_{max}$		Kips	6.070	5.478
		KN	26.998	24.368
Drift at failure, $\Delta_{failure}$		in.	2.555	2.371
		mm	64.90	60.23
Elastic stiffness, E $@0.4F_{max}$		Kip/in.	6.792	6.535
		KN/mm	1.189	1.144
Work until failure		Kip·ft.	15.490	15.074
		KN·m	21.001	20.437
Load @ .32 in.		Kips	2.318	2.195
Load @ .48 in.		Kips	3.204	3.036
Load @ .96 in.		Kips	5.477	4.961
Load @ 1.6 in.		Kips	7.090	6.451
$D = \Delta_{failure}/\Delta_{yield}$			2.545	2.573
$C_d^* = \Delta_{peak}/\Delta_{elastic}$			3.705	3.716
$R_d = \Delta_{peak}/\Delta_{yield}$			1.951	2.159
$R_d^* = \Delta_{design}/\Delta_{yield}$			1.951	2.159
$\Delta_{failure}/\Delta_{peak}$			1.298	1.198
$\zeta_{eq} = W_D/U_0/4\pi$			0.066	0.057

Note: ζ_{eq} at F_{max}

Code	***Schematic***	*Wall type*
D4s1	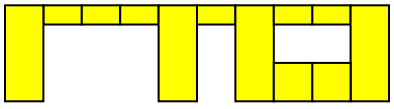	4 foot end wall , 2 screws to transmit shear as every 1 foot No tie- down anchors

Table A17 - Specimen **D4s2**

Specimen	**D4s2**	For total length		
Ratio	0.48	**cyclic**		
Full-height length		**16 ft.**	**4.876 m**	
		units	**initial**	**stabilized**
Peak load, F_{peak}		Kips	8.017	7.049
		KN	35.657	31.356
Drift at peak load, Δ_{peak}		in.	2.407	2.404
		mm	61.13	61.06
Yield load, F_{yield}		Kips	7.244	6.381
		KN	32.221	28.382
Drift at yield load, Δ_{yield}		in.	1.078	1.003
		mm	27.38	25.47
Proportional limit, $0.4F_{max}$		Kips	3.207	2.820
		KN	14.263	12.542
Drift at prop. limit, $\Delta@0.4F_{max}$		in.	0.477	0.443
		mm	12.12	11.25
Failure load or $0.8F_{max}$		Kips	6.413	5.640
		KN	28.526	25.085
Drift at failure, $\Delta_{failure}$		in.	2.992	2.973
		mm	76.00	75.51
Elastic stiffness, E $@0.4F_{max}$		Kip/in.	6.745	6.382
		KN/mm	1.181	1.118
Work until failure		Kip·ft.	21.712	23.351
		KN·m	29.436	31.658
Load @ .32 in.		Kips	2.250	2.204
Load @ .48 in.		Kips	3.247	3.029
Load @ .96 in.		Kips	5.709	5.193
Load @ 1.6 in.		Kips	7.271	6.444
$D = \Delta_{failure}/\Delta_{yield}$			2.781	2.970
$C_d^* = \Delta_{peak}/\Delta_{elastic}$			4.513	4.507
$R_d = \Delta_{peak}/\Delta_{yield}$			2.233	2.397
$R_d^* = \Delta_{design}/\Delta_{yield}$			2.180	2.338
$\Delta_{failure}/\Delta_{peak}$			1.246	1.239
$\zeta_{eq} = W_D/U_0/4\pi$			0.063	0.058

Note: ζ_{eq} at F_{max}

Code	***Schematic***	*Wall type*
D4s2	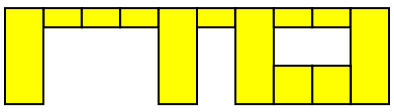	4 foot end wall , 2 screws to transmit shear as every 1 foot No tie- down anchors

APPENDIX B

Figure B1 - Specimen **A2hb1**

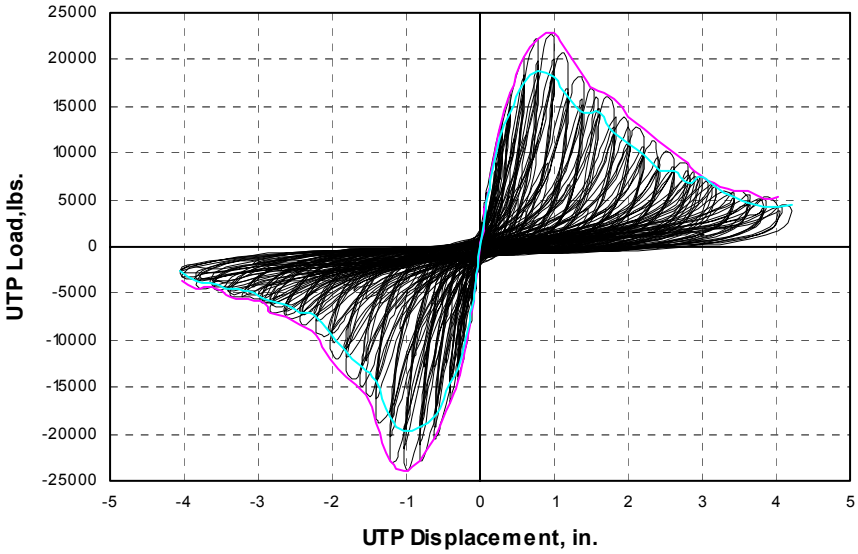

Vertical movement of end studs

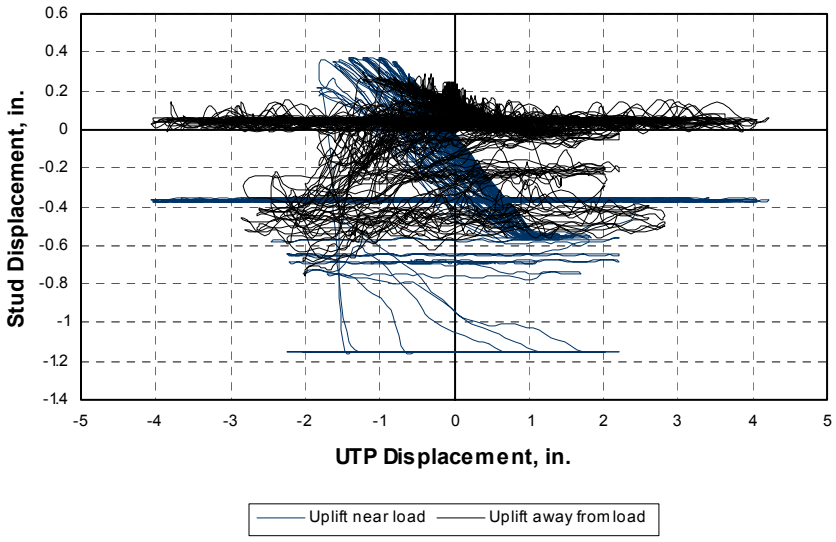

Bolt Load- UTP Displacement

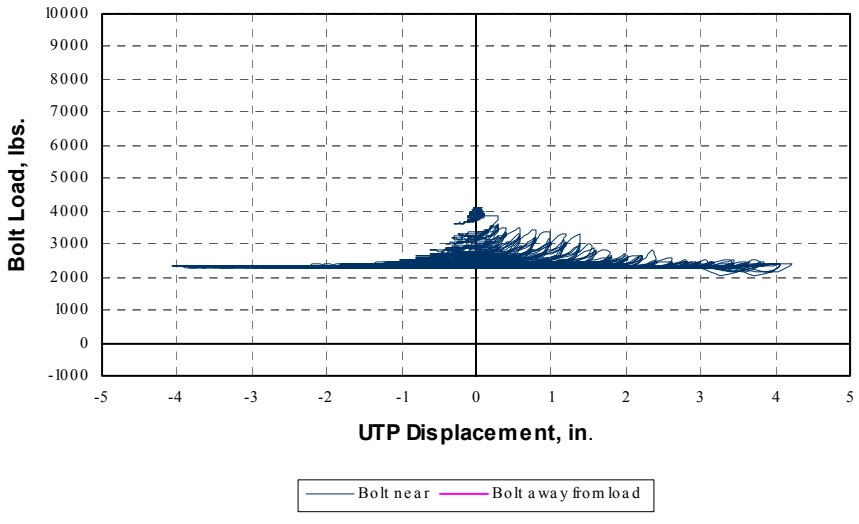

Figure B2 - Specimen **B2gab1**

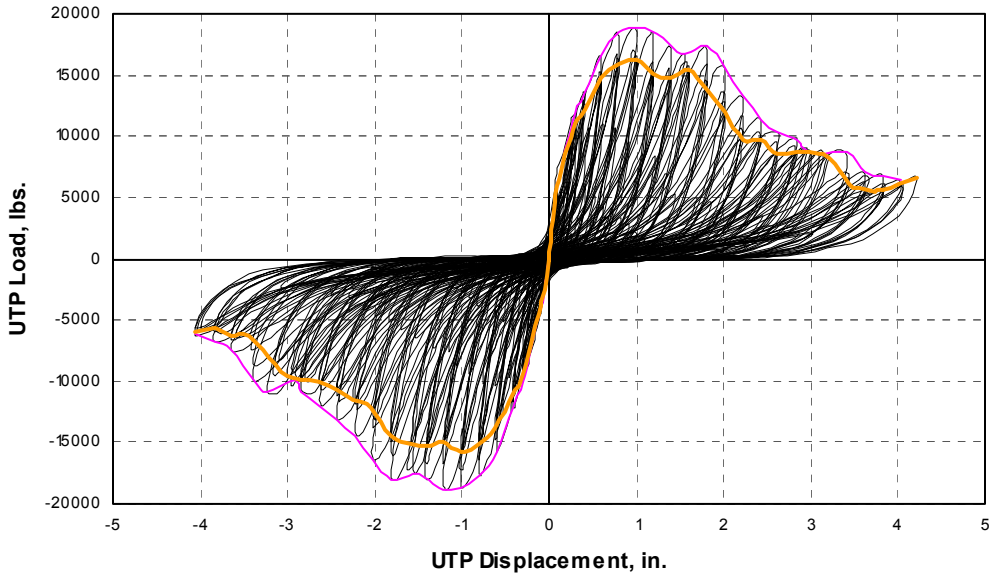

Vertical movement of end studs

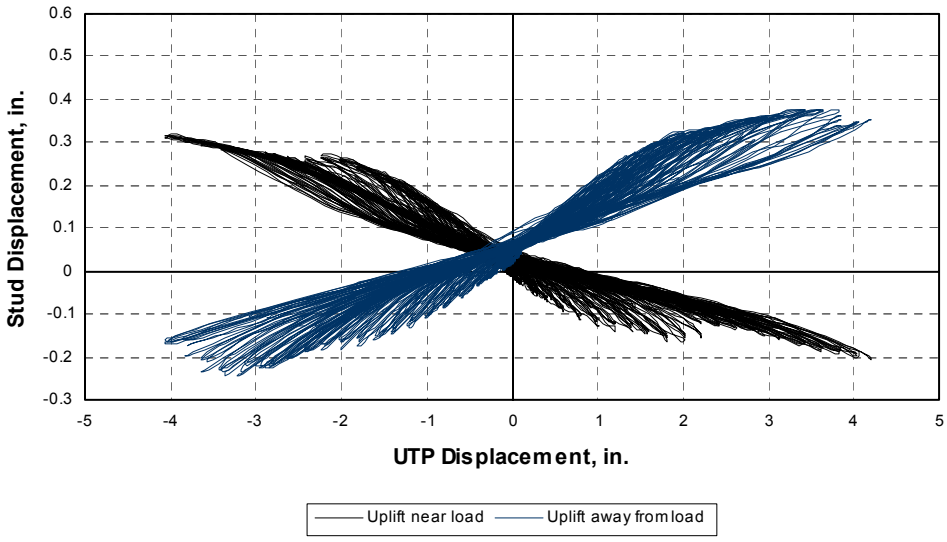

Bolt Load- UTP Displacement

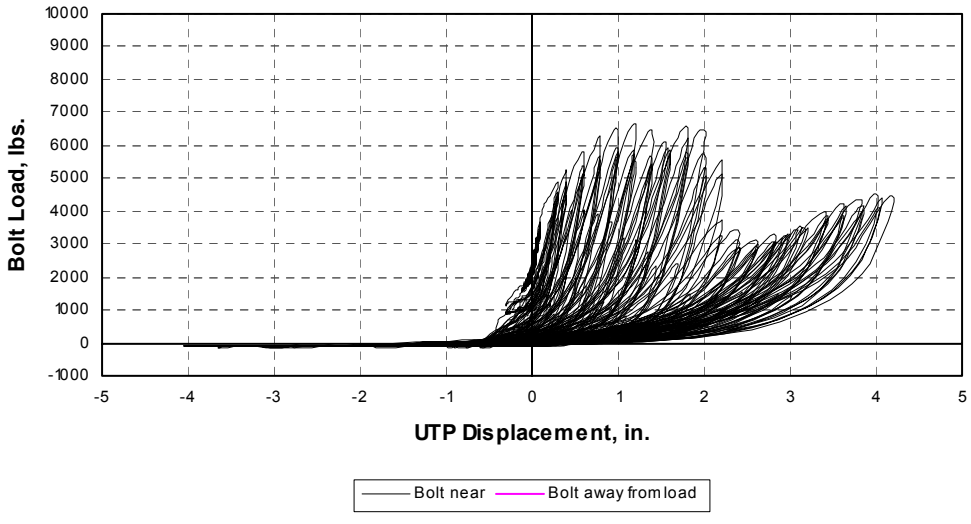

Figure B3 - Specimen **C2ab1**

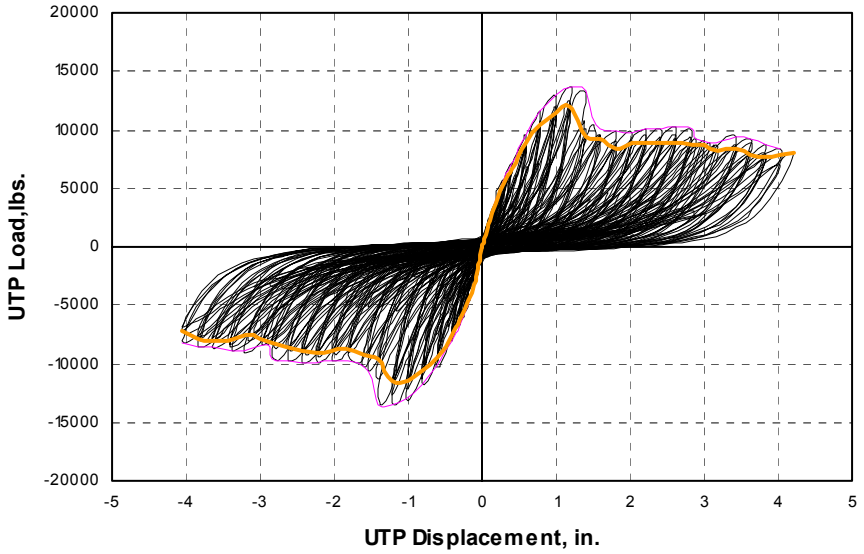

Vertical movement of end studs

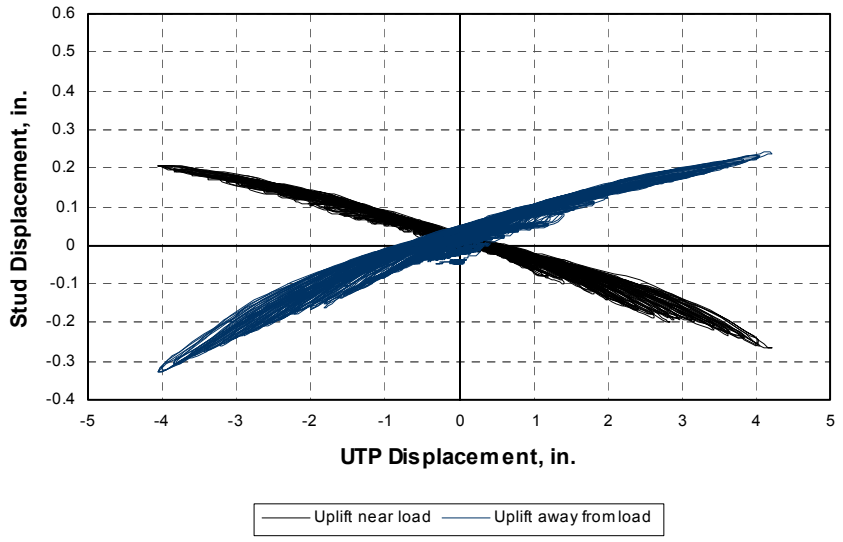

Bolt Load- UTP Displacement

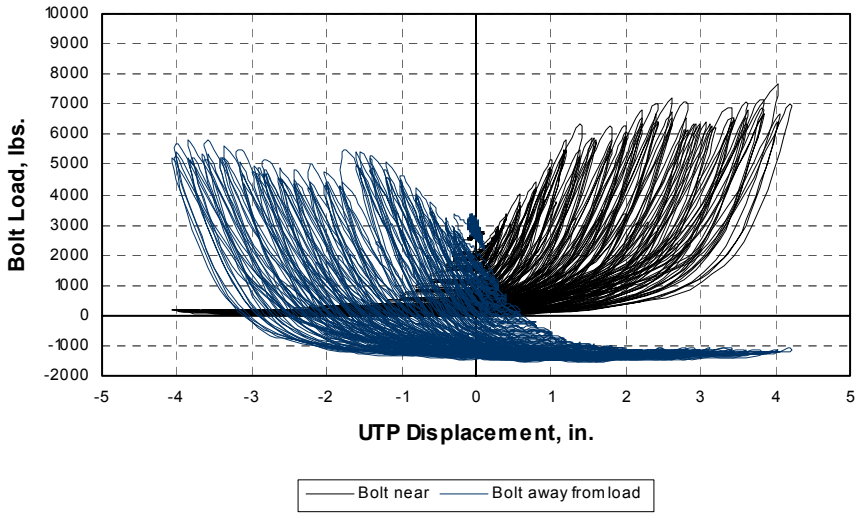

Figure B4 - Specimen **C2gab1**

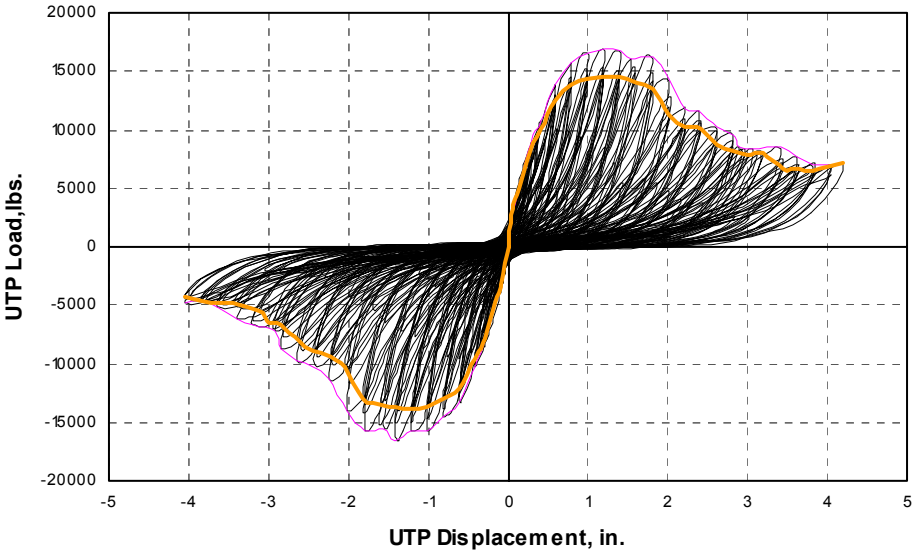

Vertical movement of end studs

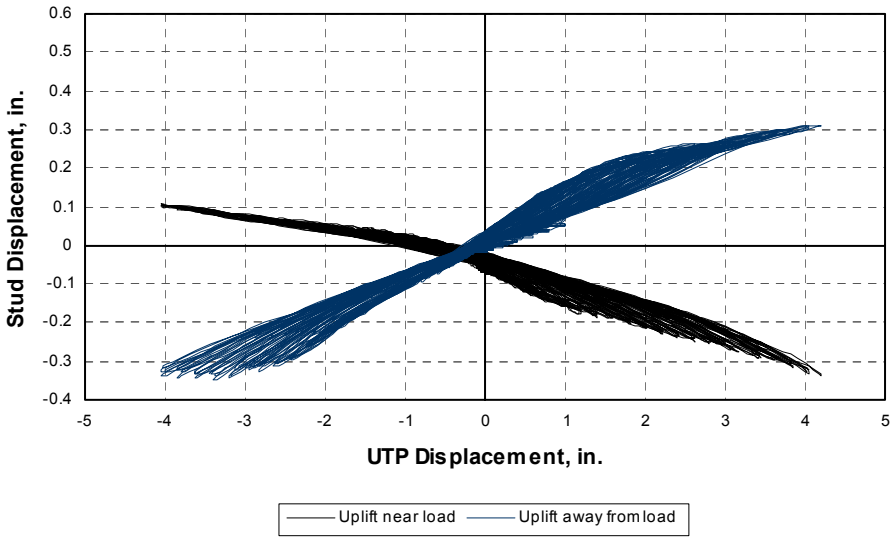

Bolt Load- UTP Displacement

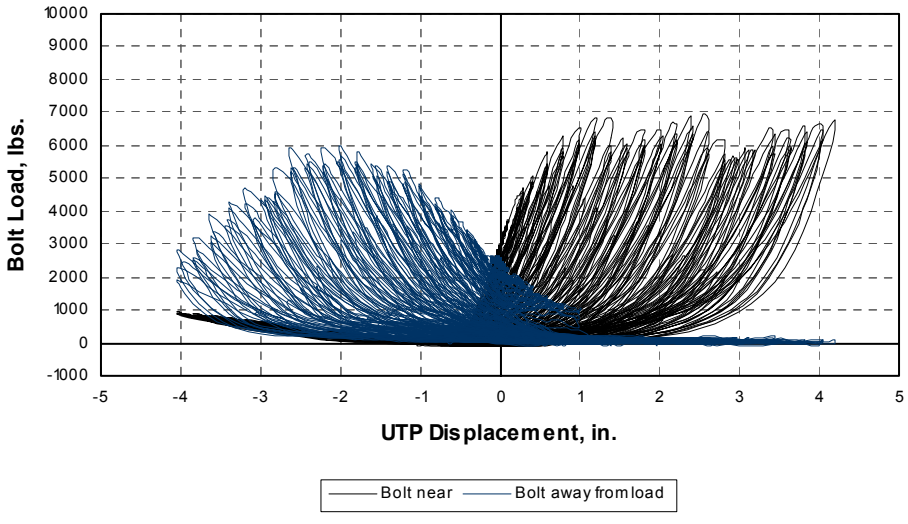

Figure B5 - Specimen **C2gb1**

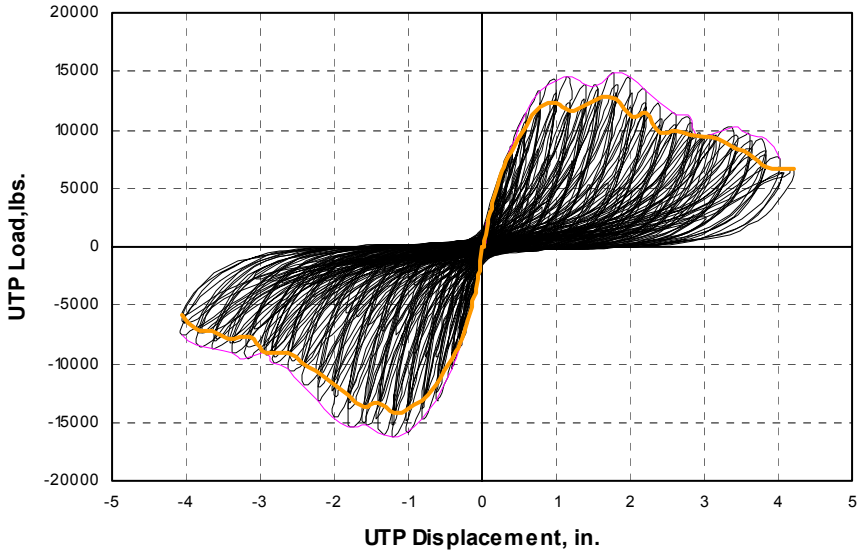

Vertical movement of end studs

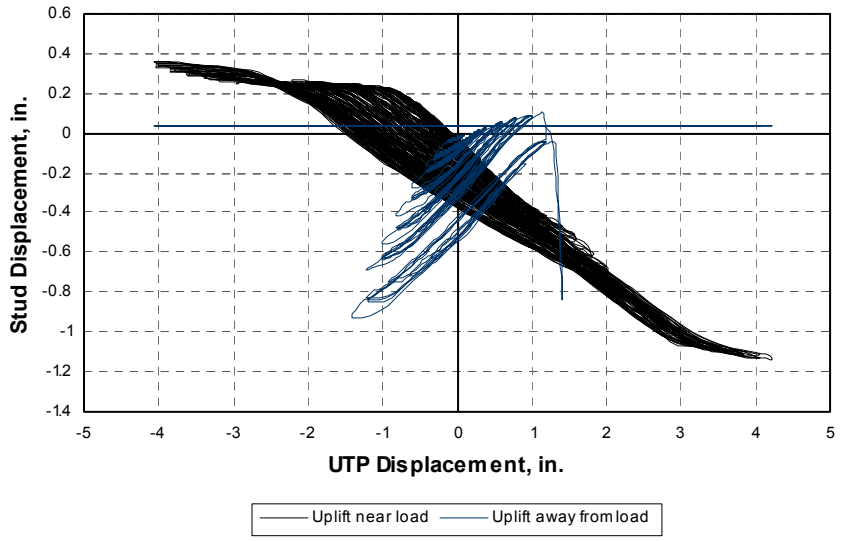

Bolt Load- UTP Displacement

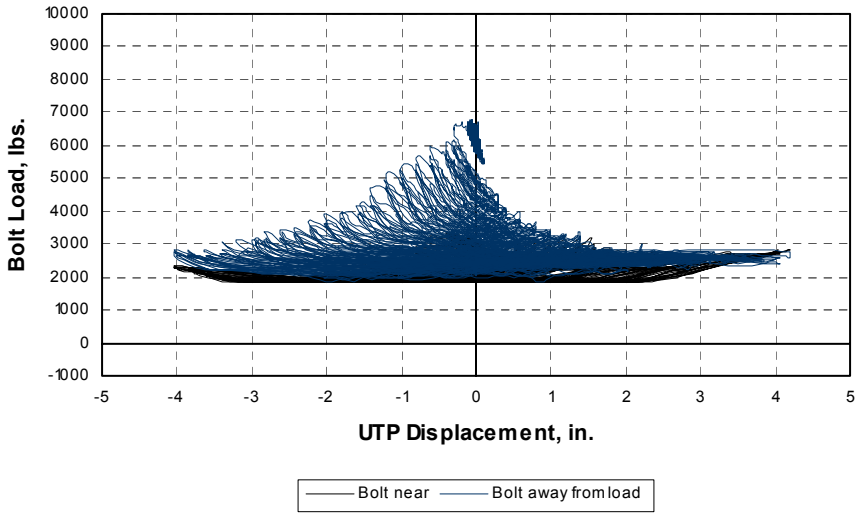

Figure B6 - Specimen **C4b1**

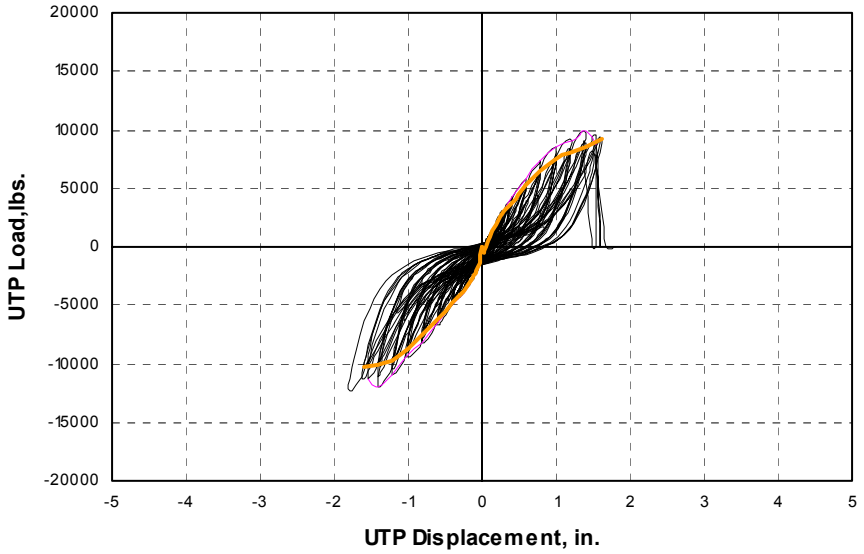

Vertical movement of end studs

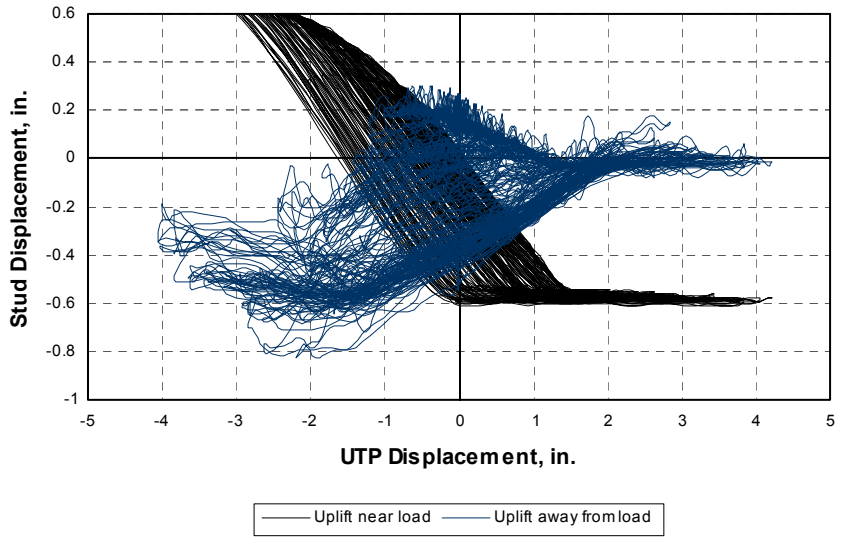

Bolt Load- UTP Displacement

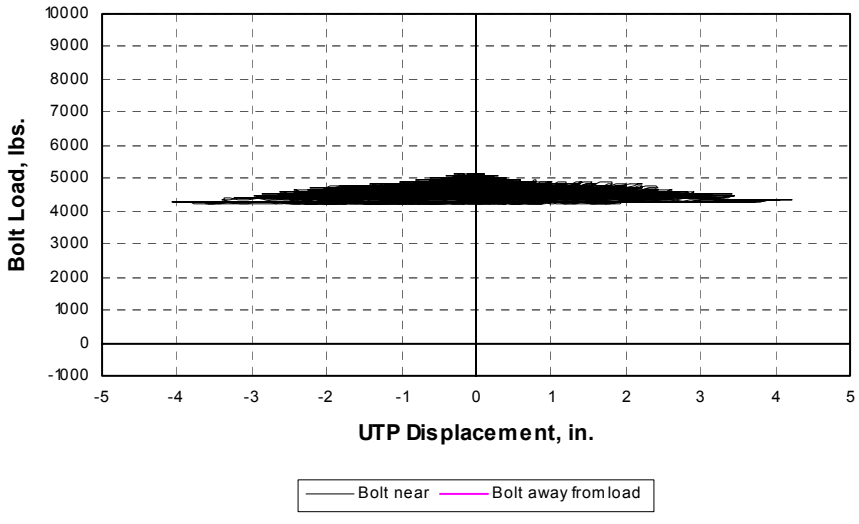

Figure B7 - Specimen **C4b2**

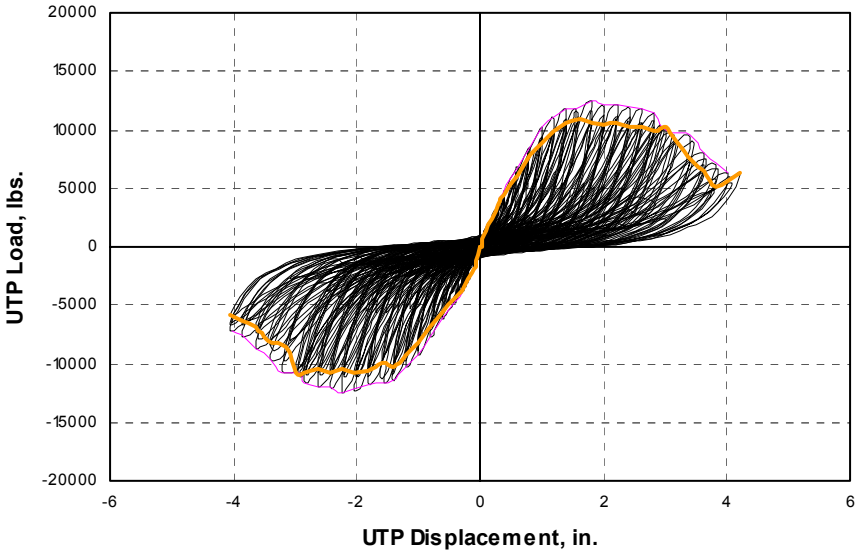

Vertical movement of end studs

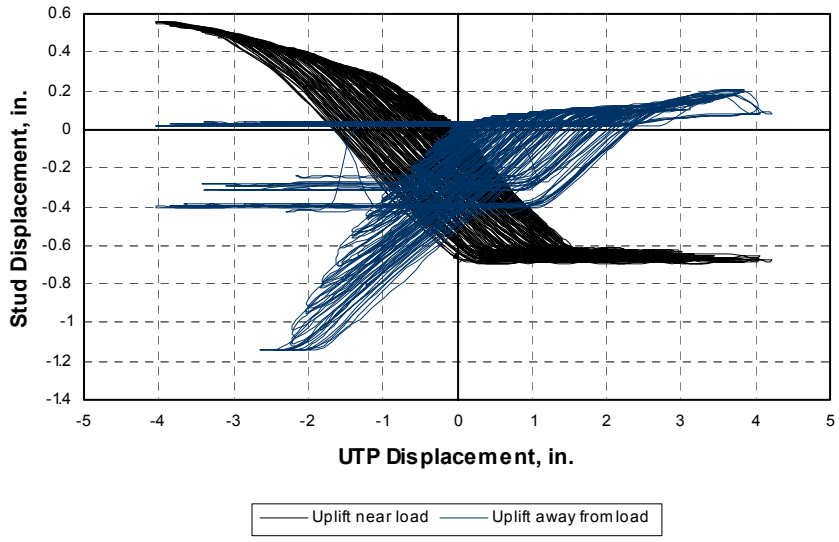

Bolt Load- UTP Displacement

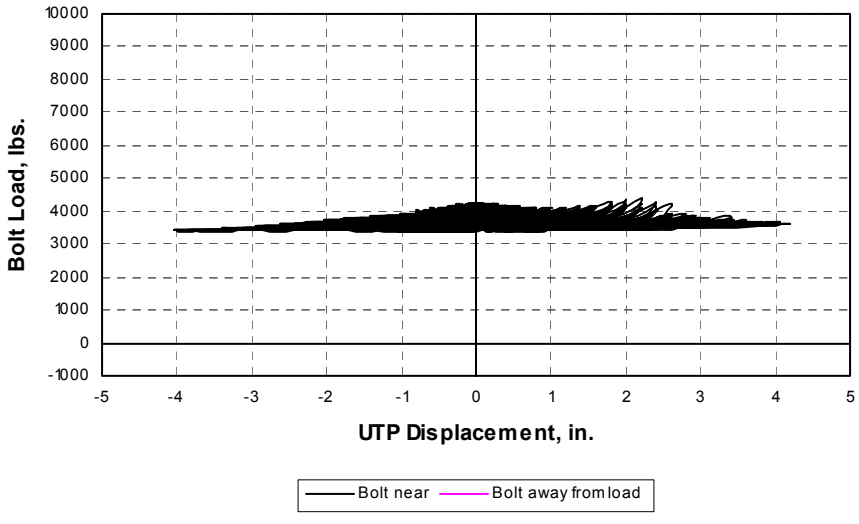

Figure B8 - Specimen **C4b3**

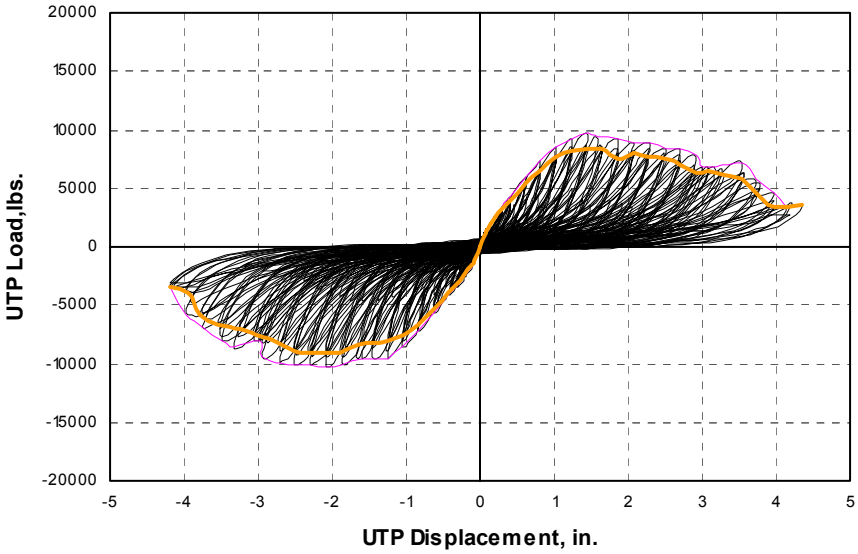

Vertical movement of end studs

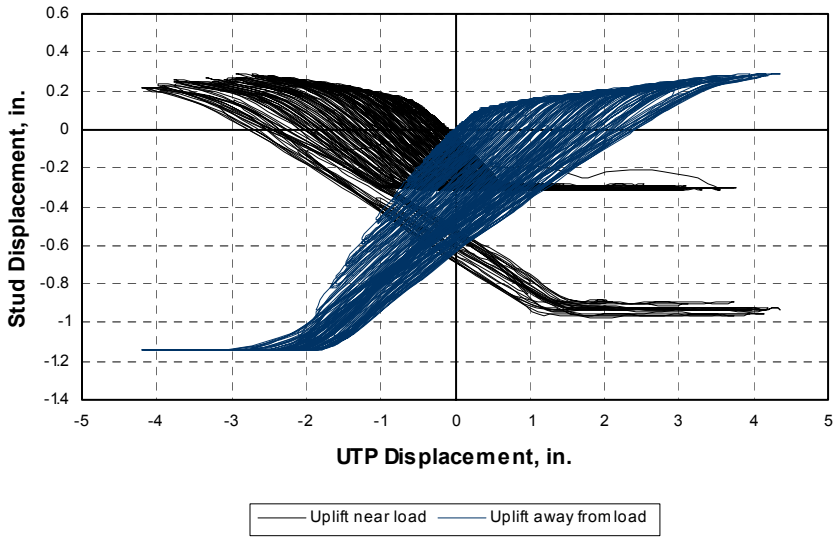

Bolt Load- UTP Displacement

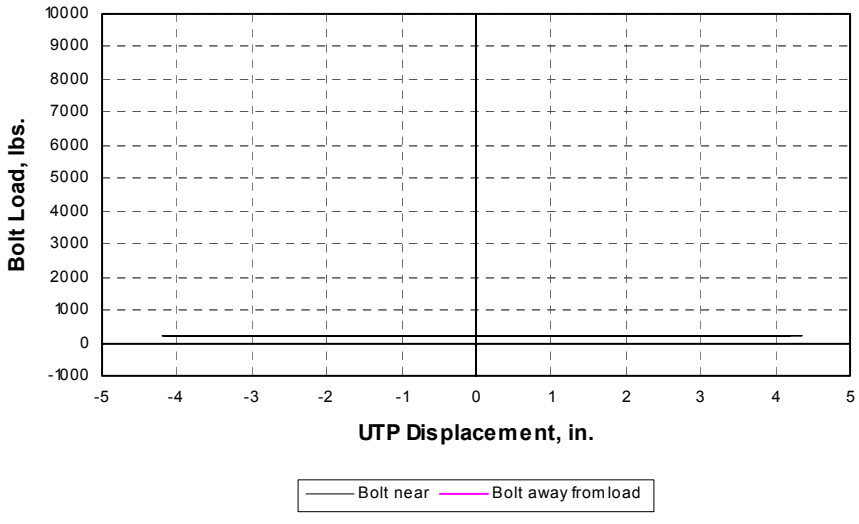

Figure B9 - Specimen **C4s1**

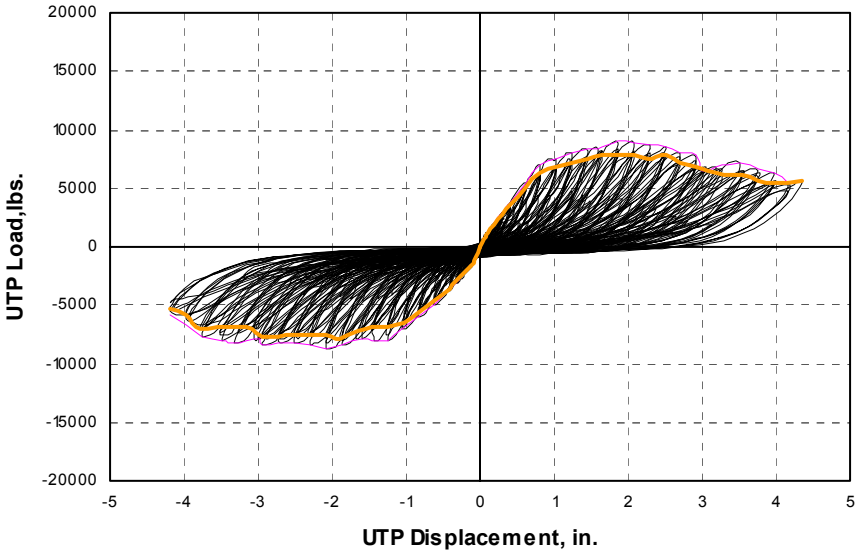

Vertical movement of end studs

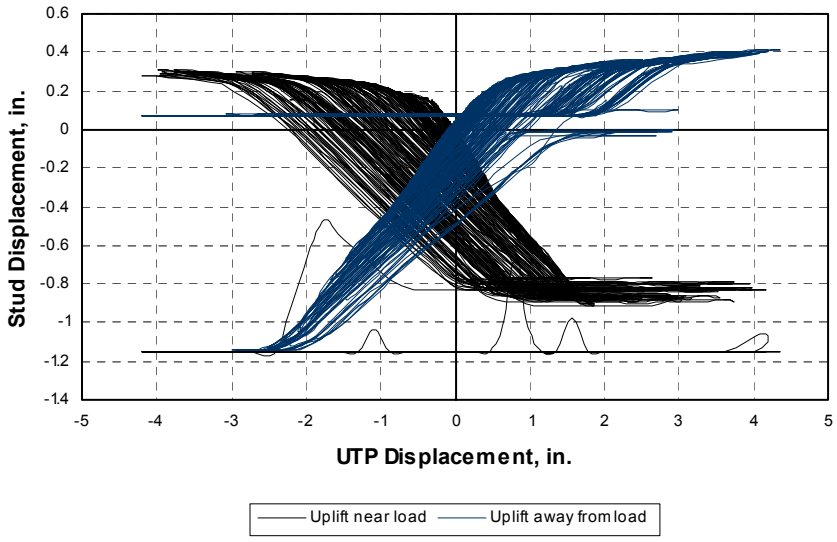

Bolt Load- UTP Displacement

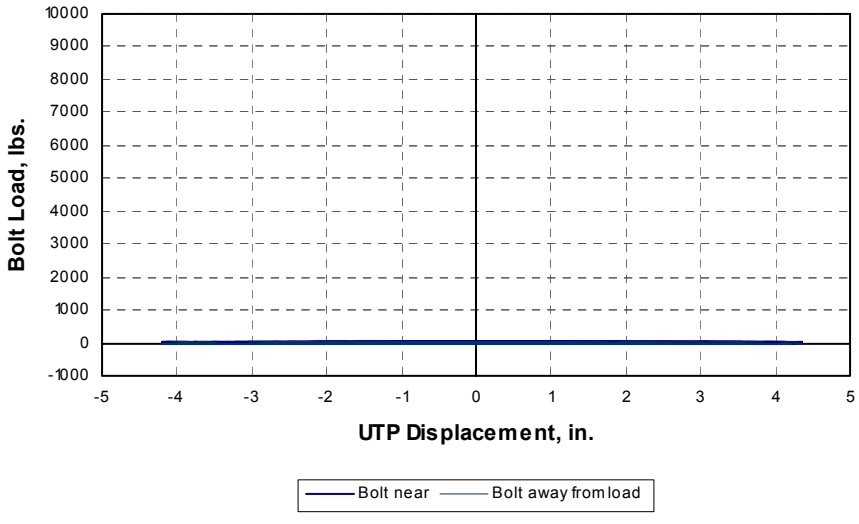

Figure B10 - Specimen **C4s2**

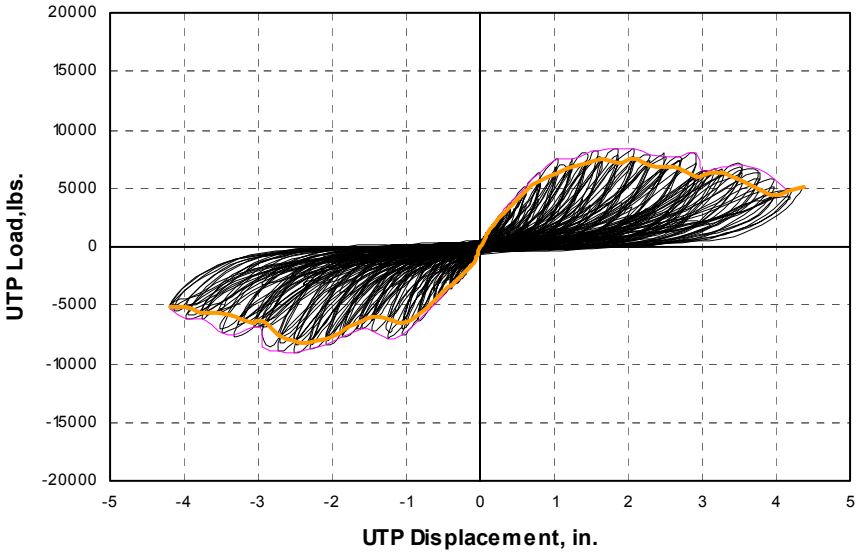

Vertical movement of end studs

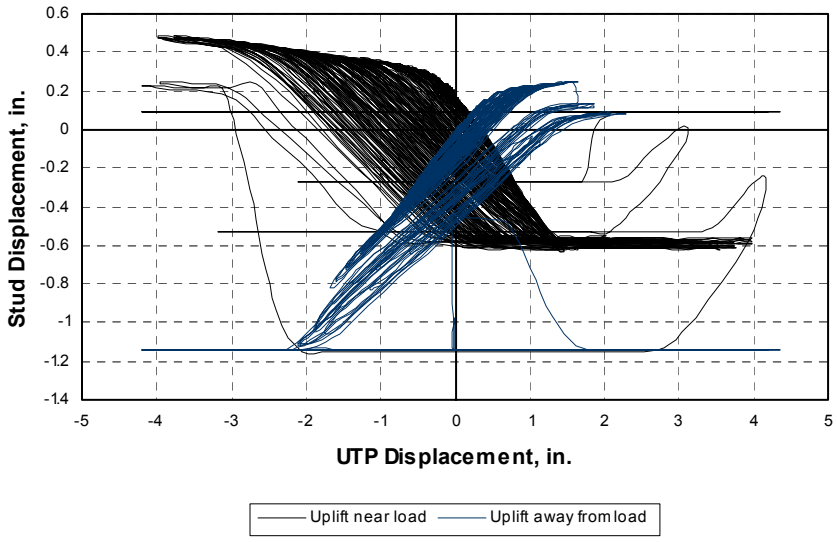

Bolt Load- UTP Displacement

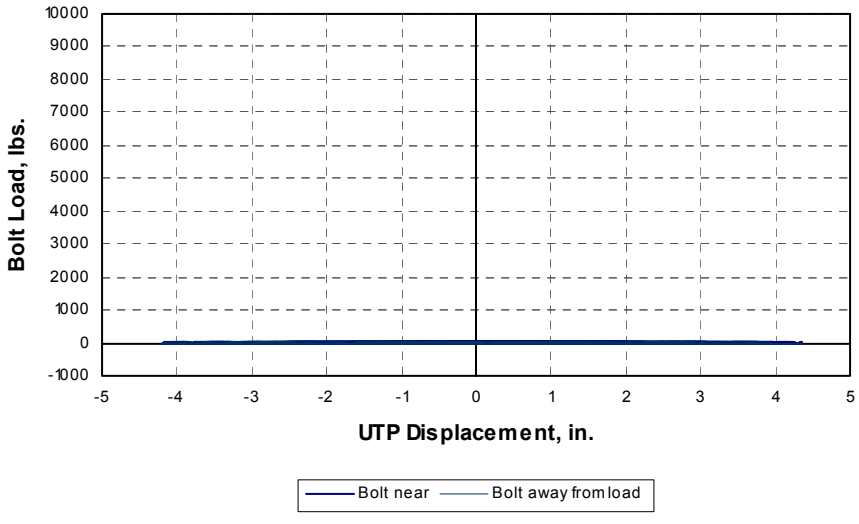

Figure B11 - Specimen **D2ab1**

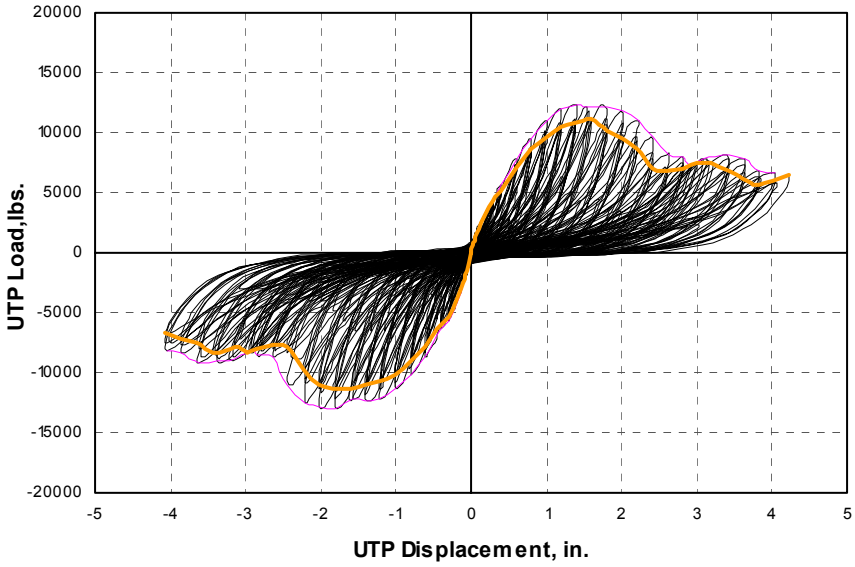

Vertical movement of end studs

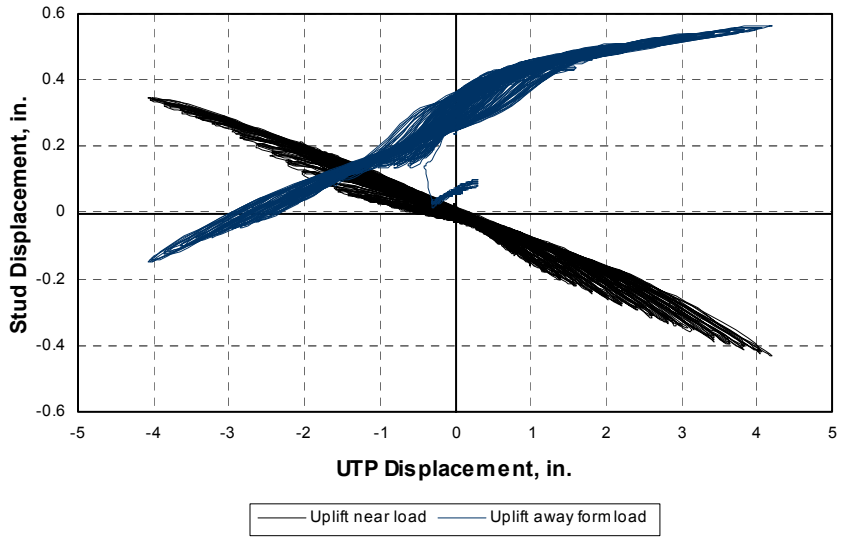

Bolt Load- UTP Displacement

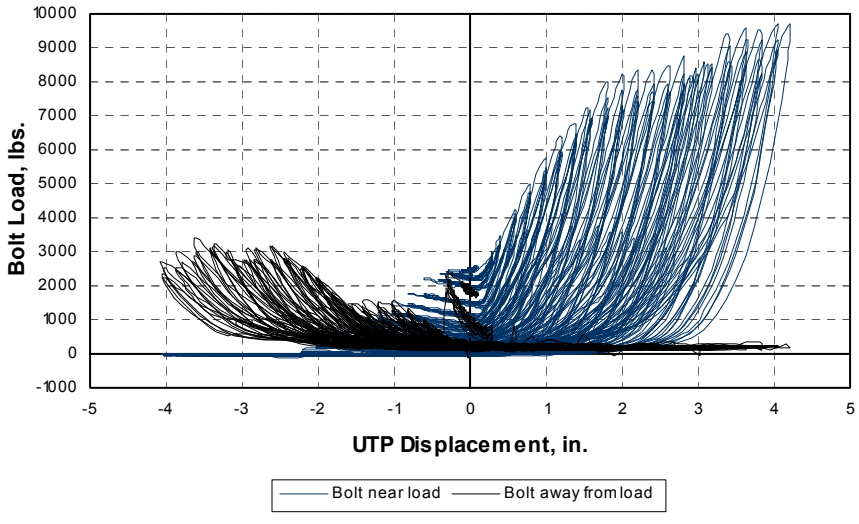

Figure B12 - Specimen **D2ab2**

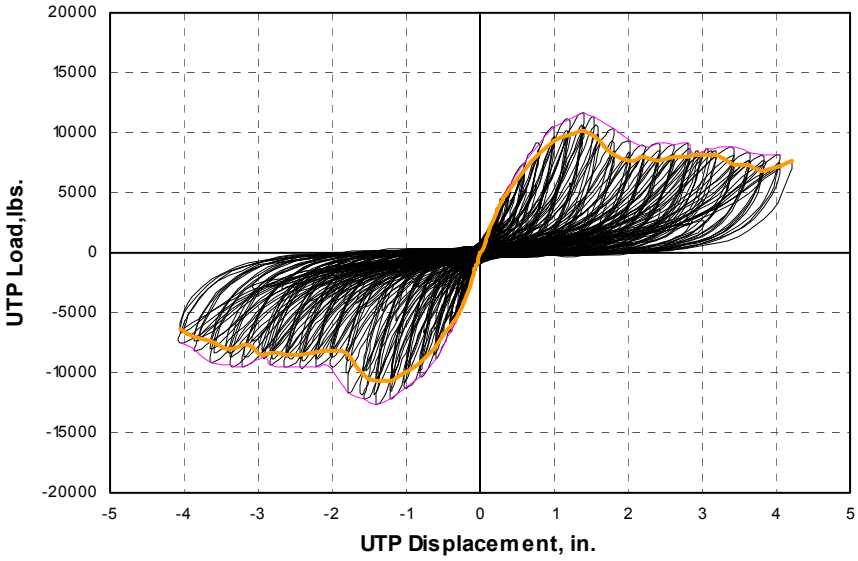

Vertical movement of end studs

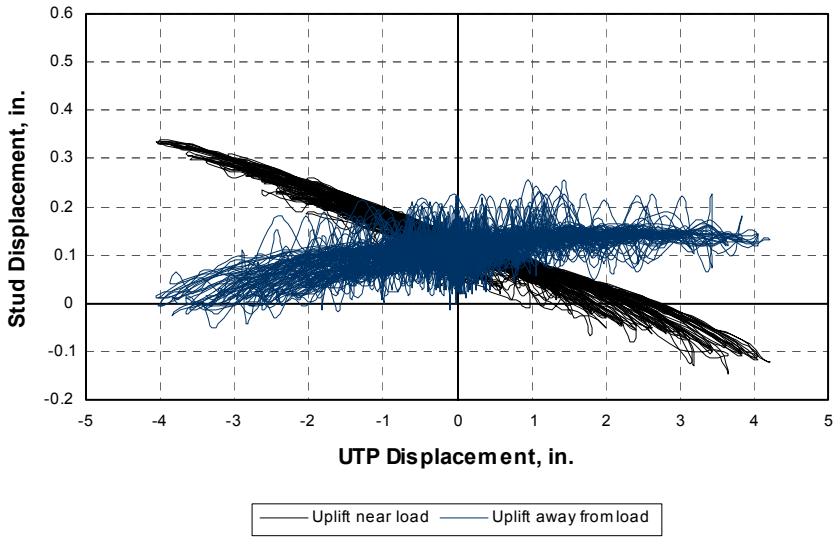

Bolt Load- UTP Displacement

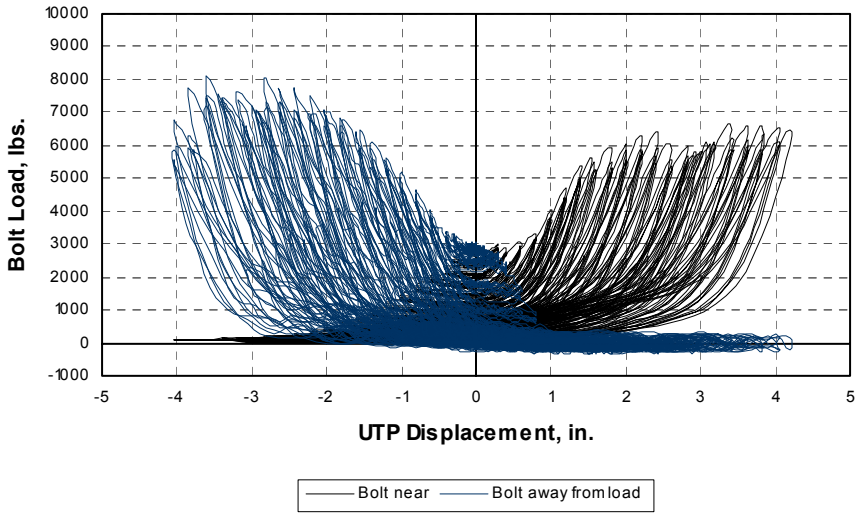

Figure B13 - Specimen **D2gab1**

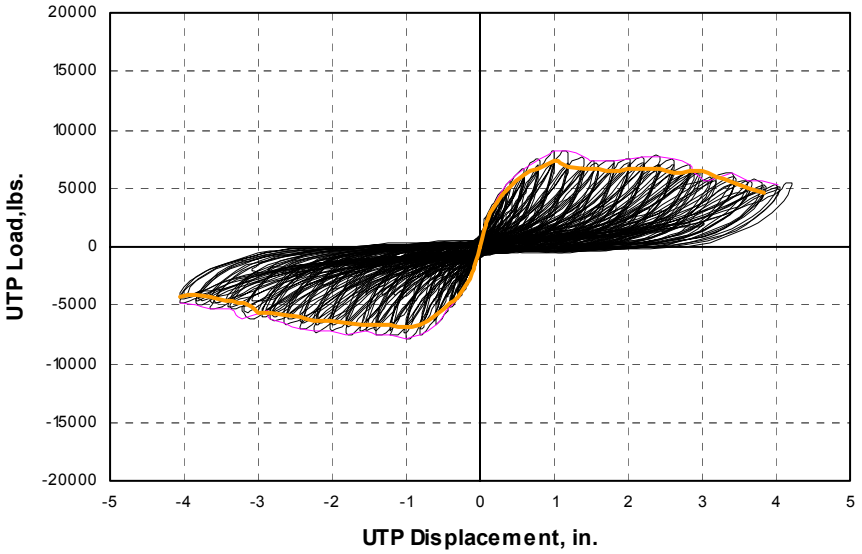

Vertical movement of end studs

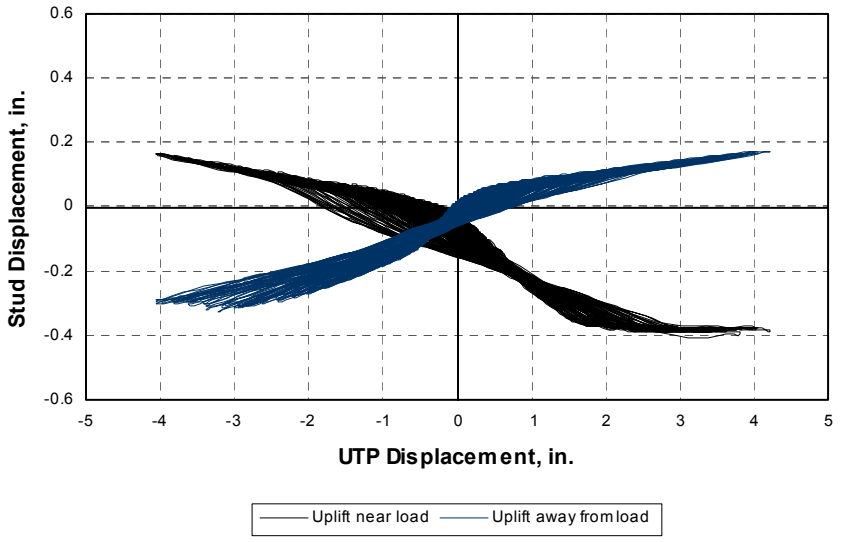

Bolt Load- UTP Displacement

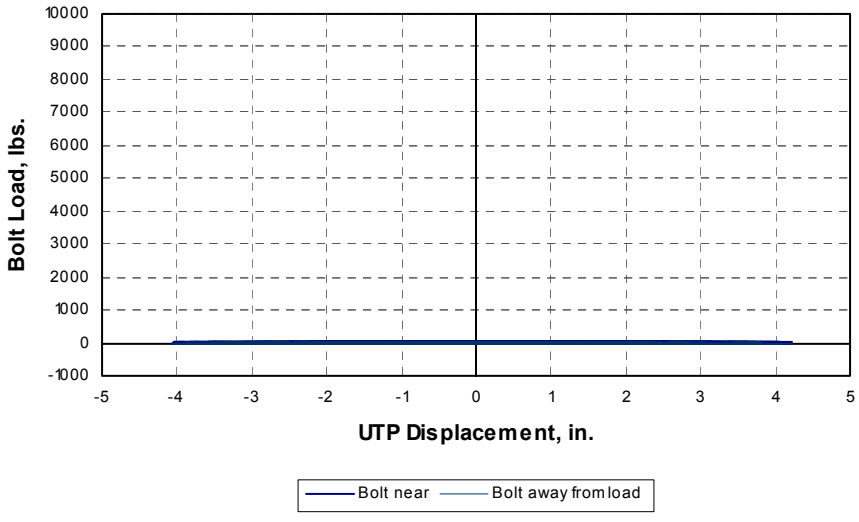

Figure B14 - Specimen **D4b1**

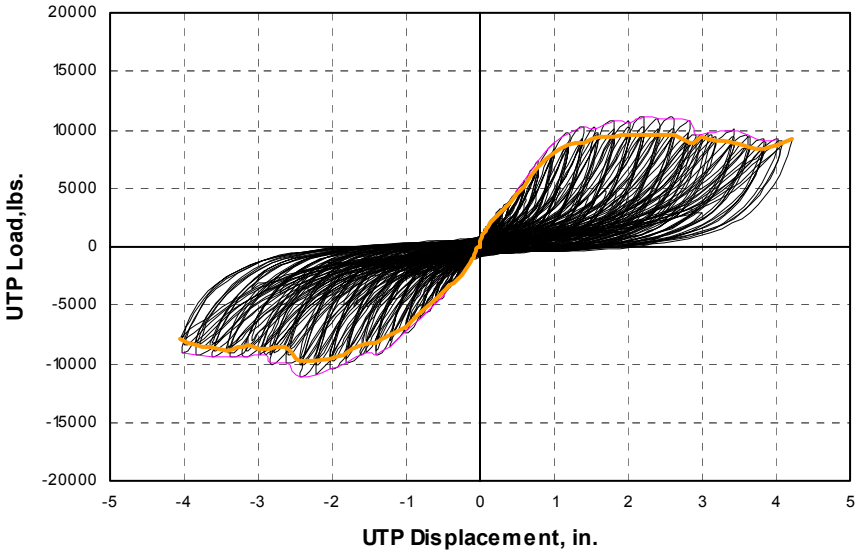

Vertical movement of end studs

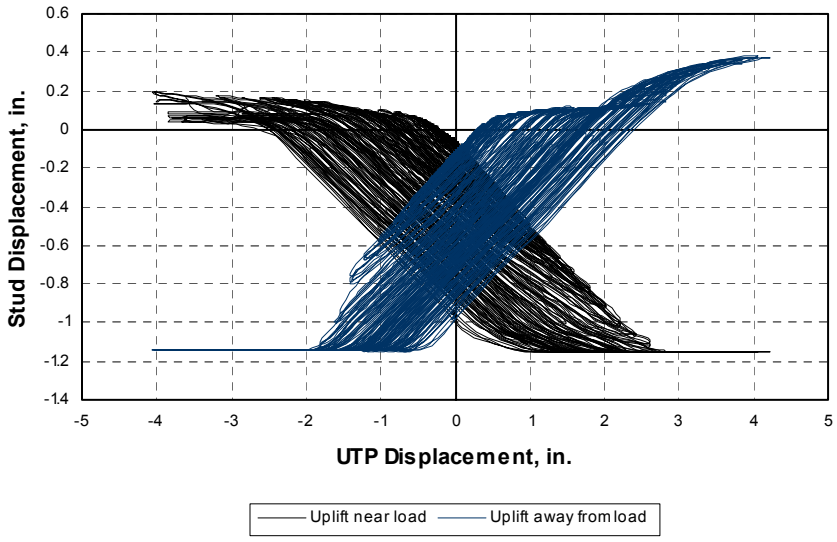

Bolt Load- UTP Displacement

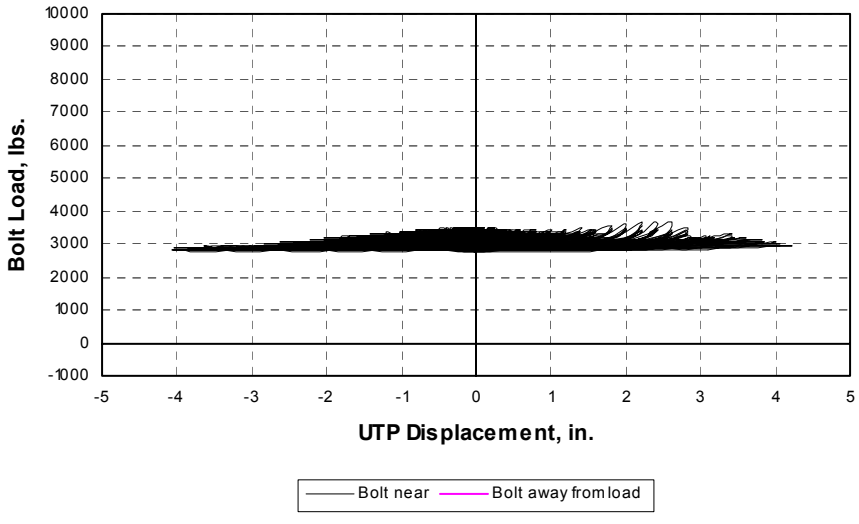

Figure B15 - Specimen **D4b2**

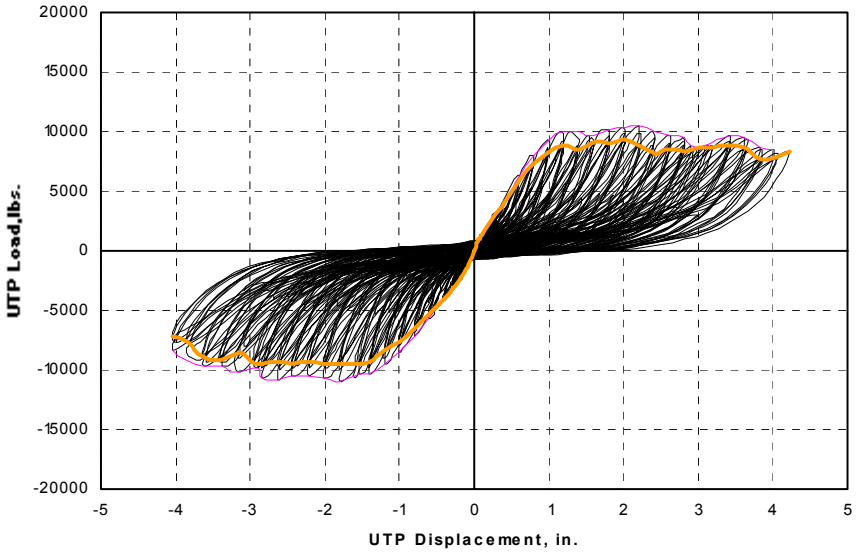

Vertical movement of end studs

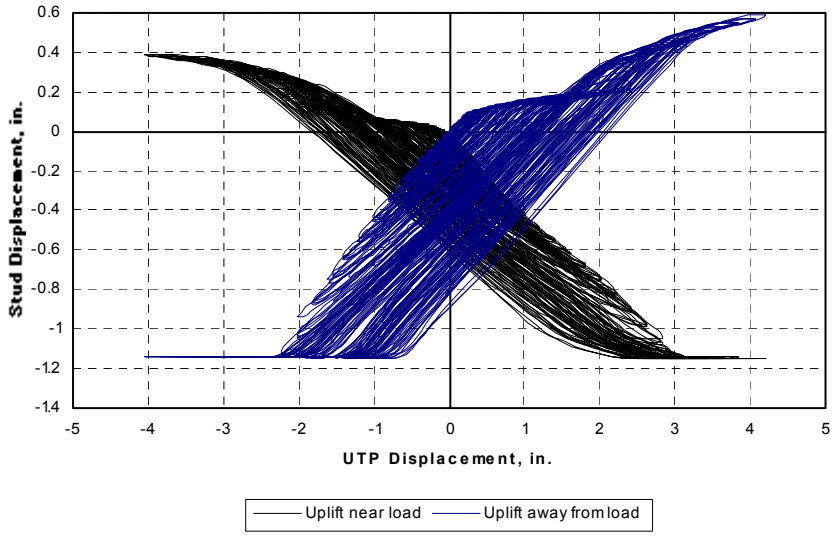

Bolt Load- UTP Displacement

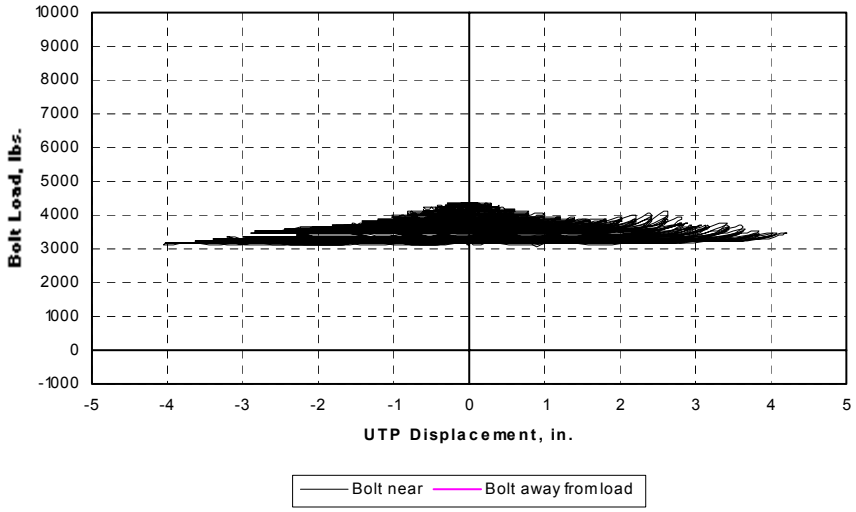

Figure B16 - Specimen **D4s1**

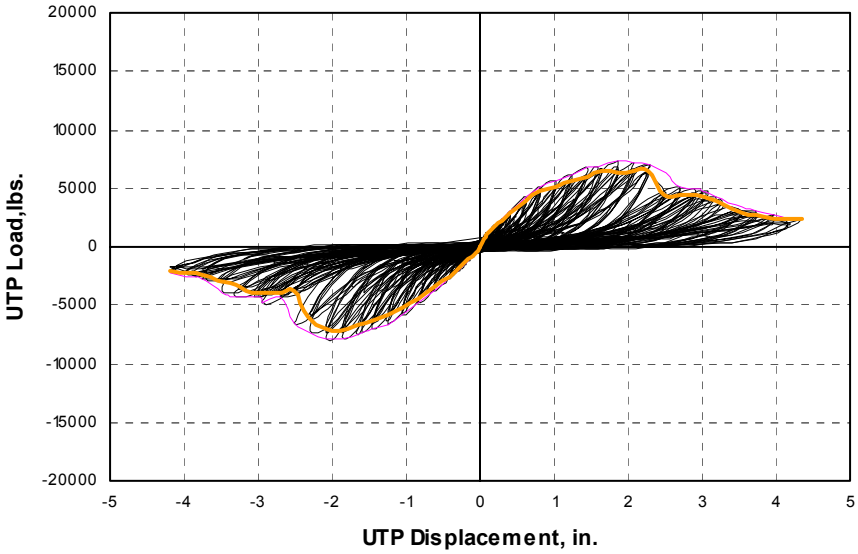

Vertical movement of end studs

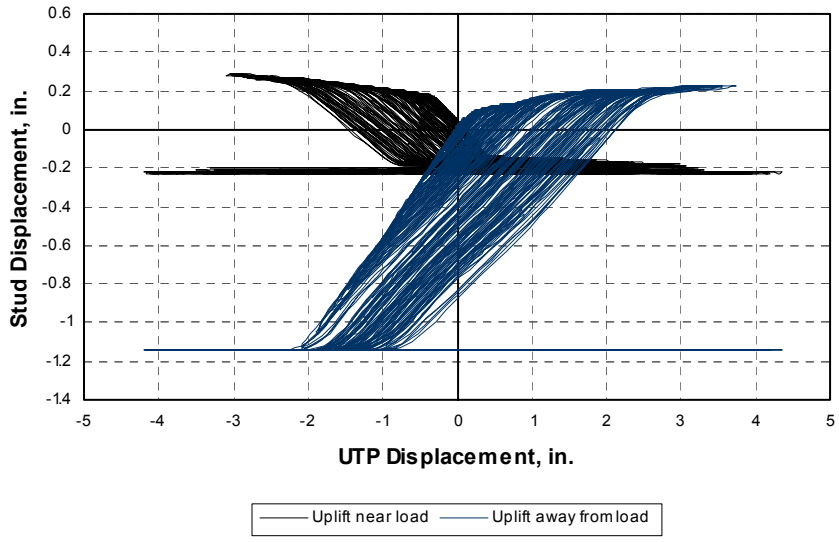

Bolt Load- UTP Displacement

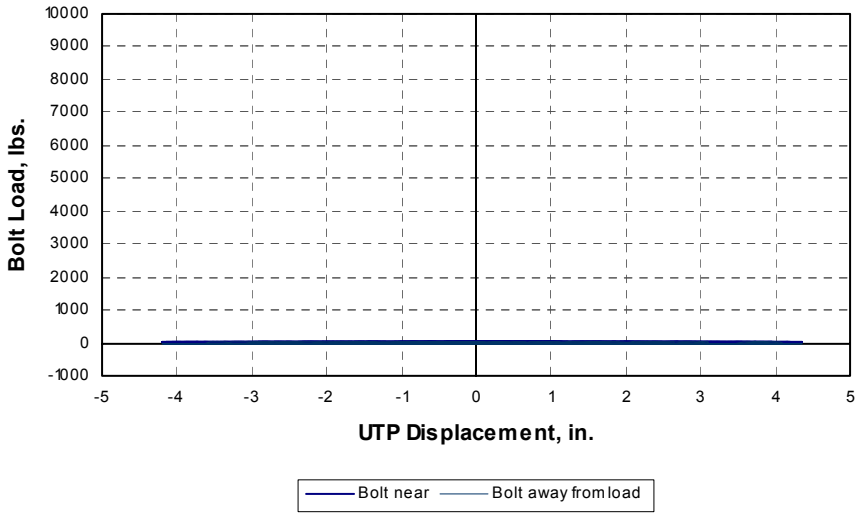

Figure B17 - Specimen **D4s2**

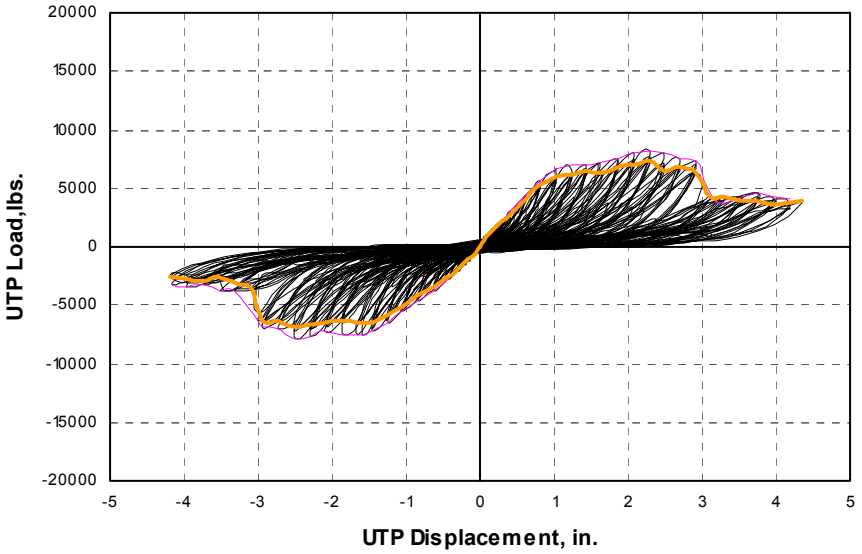

Vertical movement of end studs

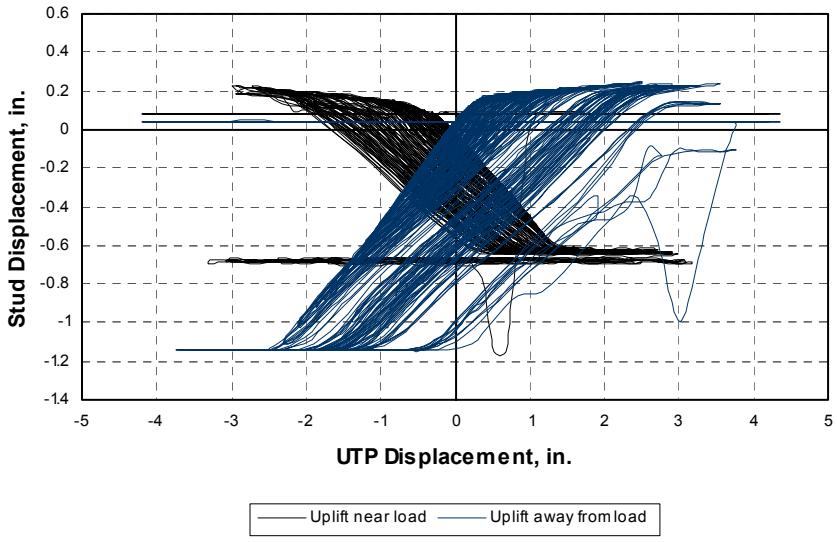

Bolt Load- UTP Displacement

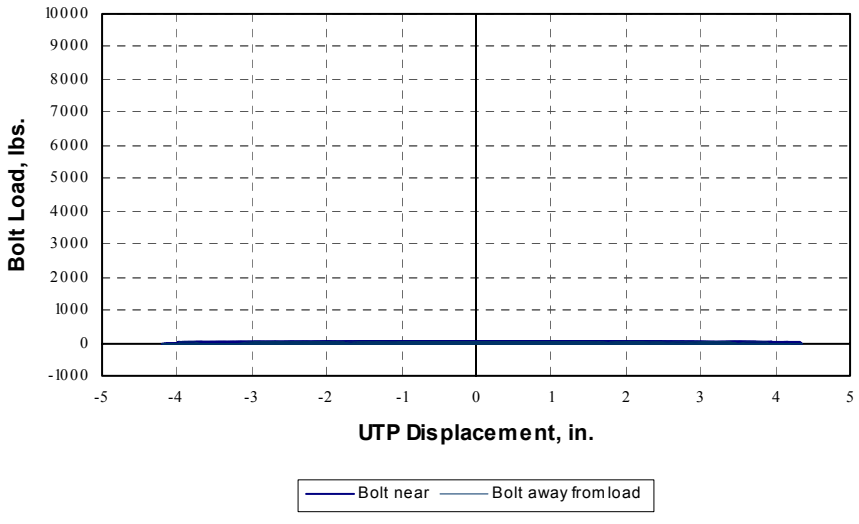

American Iron and Steel Institute

1140 Connecticut Avenue, NW
Suite 705
Washington, DC 20036

www.steel.org

1201 15th Street, NW
Suite 320
Washington, DC 20005

www.steelframing.org

Research Report RP-00-6